

# **A New Metacarpophalangeal Joint Replacement Prosthesis**

**BY  
THEODOROS PYLIOS**



**UNIVERSITY OF  
BIRMINGHAM**

**A thesis submitted to the University of Birmingham  
for the degree of  
DOCTOR OF PHILOSOPHY**

**Biomedical Engineering Research Group  
School of Mechanical Engineering**

**January 2010**

UNIVERSITY OF  
BIRMINGHAM

**University of Birmingham Research Archive**

**e-theses repository**

This unpublished thesis/dissertation is copyright of the author and/or third parties. The intellectual property rights of the author or third parties in respect of this work are as defined by The Copyright Designs and Patents Act 1988 or as modified by any successor legislation.

Any use made of information contained in this thesis/dissertation must be in accordance with that legislation and must be properly acknowledged. Further distribution or reproduction in any format is prohibited without the permission of the copyright holder.

## **Abstract**

The metacarpophalangeal joint is vital for hand function. It is frequently affected by rheumatoid arthritis or osteoarthritis and in some cases the diseased joint is replaced with an implant. The past and current metacarpophalangeal joint replacements can be divided into three main categories: hinge implants, flexible implants and surface replacement implants. There is some frustration among hand surgeons as these implants fail *in vivo* in comparison with the replacement of larger joints such as the hip or knee. The aim of this study was a new design concept for the replacement of the diseased metacarpophalangeal joint.

The biomechanics of the diseased rather than the normal metacarpophalangeal joint have been considered during the design requirements procedure. Retrospective analysis of the past and present designs has been considered. Following selection of the concept of the new metacarpophalangeal joint replacement design well established methods like lubrication analysis and contact stress analysis studies, laboratory wear tests and finite element analysis studies have been used for the evaluation of the final design.

In this study a new metacarpophalangeal joint replacement has been proposed. The new implant is intended to provide a functional range of motion, sustain the forces that a diseased joint experiences and provide pain relief for the patient. The new proposed metacarpophalangeal joint replacement design tries to combine the benefits of a one piece flexible implant with those of a surface replacement implant design that utilises the soft layered concept which has been proposed for larger synovial joints.

## **Acknowledgments**

I would like to thank my supervisor Dr Duncan E.T Shepherd for his valuable guidance, understanding, patience and support throughout this research project.

I would also like to thank Professor David W.L. Hukins for his encouragement and support all these years.

I would also like to thank the School of Mechanical Engineering of the University of Birmingham for the provision of the departmental scholarship that made this research work possible.

I would also like to thank Dr. Stergio Lolas, Dr Aziza Mahomed, Miss Purvi Patel, Miss Farnaz Jabbari Aslani, Dr Daniel Espino, Mr Jugal Parekh, Dr Lei Dang, Dr Laura Leslie and all the other colleagues in the School of Mechanical Engineering of the University of Birmingham for providing a friendly and comfortable academic environment.

I would also like to thank my parents Georgios and Maria and my brother Vasilis for their support and encouragement all these years.

Finally, I would like to thank and dedicate this thesis to my wife Nadia for her continuous encouragement, support and understanding during the last few years and to my new born lovely daughter that comes to my life just before this final draft was submitted.

## Table of Contents

<b>Abstract</b> .....	<b>I</b>
<b>Acknowledgments</b> .....	<b>II</b>
<b>Table of Contents</b> .....	<b>III</b>
<b>List of Figures</b> .....	<b>VIII</b>
<b>List of Tables</b> .....	<b>XII</b>
<b>Chapter 1</b> .....	<b>1</b>
<b>Introduction</b> .....	<b>1</b>
<b>Chapter 2</b> .....	<b>3</b>
<b>Biomechanics of the normal and diseased metacarpo-phalangeal joint</b> .....	<b>3</b>
2.1 Introduction .....	3
2.2 Normal MCP joint biomechanics .....	4
2.2.1 Range of motion .....	4
2.2.2 Centre of rotation.....	6
2.2.3 Forces .....	6
2.2.4 Tendons, muscles and ligaments .....	9
2.3. Diseased MCP joint biomechanics .....	10
2.3.1 Diseases .....	10
2.3.2 Range of motion .....	12
2.3.3 Forces .....	12
2.4 Summary .....	13
<b>Chapter 3</b> .....	<b>14</b>
<b>Metacarpophalangeal Joint Prostheses</b> .....	<b>14</b>
3.1 Introduction .....	14
3.2 Hinge prostheses.....	14
3.2.1 Brannon and Klein prosthesis.....	14
3.2.2 Flatt Prosthesis .....	15
3.2.3 Griffith- Nicolle prosthesis.....	15
3.2.4 Schetrumpf prosthesis .....	16
3.2.5 Schultz prosthesis .....	17
3.2.6 Steffe prosthesis .....	18
3.2.7 St George – Buchholtz prosthesis .....	19
3.2.8 KY Alumina ceramic prosthesis.....	19
3.2.9 Minami Alumina prosthesis .....	20
3.2.10 Strickland Prosthesis .....	21
3.2.11 Walker Prosthesis .....	21
3.2.12. Weightman Prosthesis .....	22
3.2.13 Mathys prosthesis .....	23
3.2.14 Link arthroplasty prosthesis .....	24
3.2.15 WEKO Prosthesis.....	25
3.2.16 Digital Operative Arthroplasty DJOA prosthesis.....	25
3.2.17 Daphne Prosthesis .....	26
3.3 Flexible one-piece prostheses.....	27
3.3.1 Swanson prosthesis.....	27

## Table of contents

3.3.2 Niebauer prosthesis (Cutter).....	31
3.3.3 Soft Skeletal Implant Avanta (previously known as the Sutter) .....	32
3.3.4 Neuflex prosthesis .....	33
3.3.5 Helap Flap prosthesis .....	34
3.3.6 Calnan – Reis prosthesis.....	35
3.3.7 Calnan-Nicolle prosthesis.....	36
3.3.8 Lundborg prosthesis .....	36
3.3.9 Ascension Silicone implant .....	37
3.4 Surface replacement prostheses.....	38
3.4.1 Pyrolytic Carbon MCP implant.....	38
3.4.2 Avanta SR implant .....	39
3.4.3 Moje implant .....	40
3.4.4 Elogenics implant .....	40
3.4.5 Total Metacarpophalangeal Replacement (TMR) implant.....	41
3.4.6. Andigo implant.....	42
3.4.7 Digitale implants .....	42
3.4.8 Hagert prosthesis .....	42
3.4.9 Sibly & Unsworth (Durham) prosthesis .....	43
3.4.10 Kessler prosthesis .....	43
3.5 Discussion .....	44
<b>Chapter 4.....</b>	<b>47</b>
<b>Design considerations for a new metacarpophalangeal prosthesis.....</b>	<b>47</b>
4.1 Introduction .....	47
4.2 Anatomy and conformity of the bearing surfaces .....	48
4.3 Range of motion .....	50
4.4 Centre of rotation.....	50
4.5 Strength of the implant .....	50
4.6 Stability of the implant .....	51
4.7 Wear performance .....	52
4.8 Fatigue .....	52
4.9 Fixation method.....	53
4.9.1 Introduction .....	53
4.9.2 No fixation.....	54
4.9.3 Cement.....	54
4.9.4 Interference or press fit.....	55
4.9.5 Bone in-growth or osseointegration fixation.....	56
4.10 Minimal bone resection .....	57
4.11 Sizing of the prosthesis.....	57
4.12 Allowance of soft tissue reconstruction .....	58
4.13 Patient considerations.....	60
4.13.1 Pain relief, improved cosmetic appearance and function .....	60
4.13.2 Simplicity of surgical procedure and surgical tooling.....	60
4.14 Revision arthroplasty.....	61
4.15 Manufacturing considerations .....	61
4.16 Summary .....	61
<b>Chapter 5.....</b>	<b>63</b>

## Table of contents

<b>Concept design of the new metacarpophalangeal joint replacement .....</b>	<b>63</b>
5.1 Introduction .....	63
5.2 The concept designs .....	63
5.2.1 Design 1 – (Three piece elastomer and surface replacement design) .....	63
5.2.2 Design 2 – (Four piece elastomer and surface replacement design) .....	64
5.2.3 Design 3 – (Two balls and double socket middle part design).....	64
5.2.4 Design 4 – (Two balls and double socket middle part preflex design with internal elastomer part).....	65
5.2.5 Design 5 – (Two socket stems and elastomer ball design).....	66
5.2.6 Design 6 – (Volar plate approach design) .....	67
5.2.7 Design 7 – (Four stem elastomer design) .....	67
5.2.8 Design 8 – (Five part – two elastomer part design).....	68
5.2.9 Design 9 – (Two sockets and middle ball design).....	68
5.2.10 Design 10 – (One piece elastomer design) .....	69
5.2.11 Design 11 – (Surface replacement ball and socket design).....	70
5.2.12 Design 12 – (Surface replacement socket and ball design – reversed design).....	70
5.2.13 Design 13 – (Three piece elastomer hinge design) .....	71
5.13 Evaluation of the concept designs .....	71
<b>Chapter 6.....</b>	<b>77</b>
<b>Risk analysis.....</b>	<b>77</b>
6.1 Introduction .....	77
6.2 Undertaking risk analysis .....	78
6.3 Risk analysis of the novel metacarpophalangeal joint replacement.....	79
6.3.1. Design description and characteristics .....	79
6.3.2 Identification of hazards and estimation of risks.....	80
<b>Chapter 7.....</b>	<b>82</b>
<b>Lubrication analysis of metacarpophalangeal joint replacement.....</b>	<b>82</b>
7.1. Introduction .....	82
7.2. Lubrication theory .....	82
7.3. Materials and Methods .....	84
7.3.1. Model.....	84
7.3.2 Lubrication analysis equations for soft layered joints.....	85
7.3.3 Lubrication analysis equations for ‘conventional’ material combinations.....	87
7.3.4 Parameters .....	88
7.3.5 Lubrication regimes.....	91
7.4 Results .....	91
7.5. Discussion .....	98
<b>Chapter 8.....</b>	<b>101</b>
<b>Wear of medical grade silicone rubber against titanium and ultra high molecular weight polyethylene .....</b>	<b>101</b>
8.1 Introduction .....	101
8.2 Materials and Methods .....	101
8.2.1 Apparatus.....	101
8.2.2 Materials.....	103
8.2.3 Experimental procedure .....	104
8.2.4 Wear evaluation.....	105

Table of contents

8.3. Results .....	106
8.4. Discussion .....	108
<b>Chapter 9.....</b>	<b>111</b>
<b>Finite element analysis of elastomer part.....</b>	<b>111</b>
9.1 Introduction .....	111
9.2 Finite element analysis of elastomer .....	111
9.3 Software for Finite Element Analysis .....	115
9.4 Model for analysis .....	115
9.5 Method of loading .....	116
9.6 Determination of coefficients of Mooney-Rivlin model.....	117
9.7 Determination of mesh density.....	118
9.8 Results .....	119
9.9 Discussion .....	120
<b>Chapter 10.....</b>	<b>122</b>
<b>Contact stress analysis .....</b>	<b>122</b>
10.1 Introduction .....	122
10.2 Materials and Methods .....	122
10.2.1 Model.....	122
10.2.2 Contact stresses .....	123
10.2.2.1 Conventional material combinations.....	123
10.2.2.2 Soft layer material combinations.....	124
10.2.3 Parameters .....	124
10.3 Results .....	126
10.3.1 Contact stresses .....	126
10.4 Discussion .....	131
<b>Chapter 11.....</b>	<b>132</b>
<b>Detailed design process .....</b>	<b>132</b>
11.1. Introduction .....	132
11.2. Selection of model metacarpophalangeal joint for size accommodation .....	133
11.3. Detailed design of the implant parts.....	133
11.3.1 The metacarpal part.....	133
11.3.1.1 The stem of the metacarpal part .....	133
11.3.1.2 The ball of the metacarpal part.....	137
11.3.1.3 Interfaces in the metacarpal part.....	140
11.3.2 The Middle part.....	141
11.3.3 The proximal phalange part.....	143
11.3.3.1 The stem of the proximal phalange part.....	143
11.3.3.2 The ball of the proximal phalange part .....	145
11.3.3.3 Interfaces in the proximal phalange part .....	147
11.3.4 The elastomer part.....	147
11.4. The assembly.....	150
<b>Chapter 12.....</b>	<b>154</b>
<b>Overall discussion and evaluation of metacarpophalangeal joint replacement .....</b>	<b>154</b>
12.1 Introduction .....	154
12.2 General discussion.....	154
12.3 Evaluation of metacarpophalangeal joint replacements .....	157

Table of contents

12.4 Conclusions .....	159
<b>References .....</b>	<b>161</b>
<b>Appendices .....</b>	<b>183</b>
Appendix A .....	183
Appendix B.....	188
Appendix C.....	189
Appendix D .....	190
Appendix E.....	191
Appendix F.....	193
Appendix G .....	195

## List of Figures

<b>Fig 2-1.</b> Metacarpophalangeal joints of human hand .....	3
<b>Fig 2-2.</b> Normal metacarpophalangeal joint anatomy .....	4
<b>Fig 2-3.</b> Axis of rotation of the metacarpophalangeal joint .....	5
<b>Fig 3-1.</b> Brannon Klein design .....	14
<b>Fig 3-2.</b> Flatt design .....	15
<b>Fig 3-3.</b> Griffiths- Nicolle design .....	16
<b>Fig 3-4.</b> Schetrumpf design .....	17
<b>Fig 3-5.</b> Scultz design .....	17
<b>Fig 3-6.</b> Steffee design .....	18
<b>Fig 3-7.</b> St George- Buchholtz design .....	19
<b>Fig 3-8.</b> KY Alumina design .....	20
<b>Fig 3-9.</b> Minami Alumina design .....	21
<b>Fig 3-10.</b> Strickland design .....	21
<b>Fig 3-11.</b> Walker design .....	22
<b>Fig 3-12.</b> Weightman design .....	23
<b>Fig 3-13.</b> Mathys design .....	23
<b>Fig 3-14.</b> Link design .....	24
<b>Fig 3-15.</b> WEKO design .....	25
<b>Fig 3-16.</b> DJOA design .....	26
<b>Fig 3-17.</b> Daphne design .....	27
<b>Fig 3-18.</b> Swanson design with grommets .....	28
<b>Fig 3-19.</b> Neibauer design .....	31
<b>Fig 3-20.</b> Sutter – Avanta design .....	33
<b>Fig 3-21.</b> Neuflex design .....	34
<b>Fig 3-22.</b> Helap Flap design .....	35
<b>Fig 3-23.</b> Calnan- Reis design .....	35
<b>Fig 3-24.</b> Calcan – Nicolle design .....	36
<b>Fig 3-25.</b> Lundborg design .....	37
<b>Fig 3-26.</b> Ascension silicone implant design .....	37
<b>Fig 3-27.</b> Pyrolytic Carbon design .....	38
<b>Fig 3-28.</b> Avanta SR design .....	39
<b>Fig 3-29.</b> Moje design .....	40
<b>Fig 3-30.</b> Elogenics design .....	41
<b>Fig 3-31.</b> Total metacarpophalangeal replacement design .....	41
<b>Fig 3-32.</b> Andigo design .....	42
<b>Fig 3-33.</b> Digitale design .....	42
<b>Fig 3-34.</b> Hagert design .....	43
<b>Fig 3-35.</b> Sibly-Unsworth design .....	43
<b>Fig 3-36.</b> Kesler design .....	44
<b>Fig 4-1.</b> Interrelations of the surgical aspects, patient expectations and engineering challenges in the design of a new prosthesis .....	48

List of Figures

**Fig 4-2.** Sagittal and transverse view of metacarpophalangeal joint and medullary cavities position ..... 54

**Fig 4-3.** Different types of fixation (a) No fixation (b) Press fit fixation (c) Cement fixation (d) Coated prosthesis (e) Osseointegration fixation ..... 55

**Fig 4-4.** Level of resection of the metacarpophalangeal head ..... 57

**Fig 5-1.** Concept design 1 ..... 63

**Fig 5-2.** Concept design 2 ..... 64

**Fig 5-3.** Concept design 3 ..... 65

**Fig 5-4.** Concept design 4 ..... 66

**Fig 5-5.** Concept design 5 ..... 67

**Fig 5-6.** Concept design 6 ..... 67

**Fig 5-7.** Concept design 7 ..... 68

**Fig 5-8.** Concept design 8 ..... 68

**Fig 5-9.** Concept design 9 ..... 69

**Fig 5-10.** Concept design 10 ..... 70

**Fig 5-11.** Concept design 11 ..... 70

**Fig 5-12.** Concept design 12 ..... 71

**Fig 5-13.** Concept design 13 ..... 71

**Fig 5-14.** 3D design of concept selection 4 ..... 76

**Fig 7-1.** Lubrication regimes (a) Fluid film lubrication, (b) Mixed Lubrication, (c) Boundary lubrication ..... 82

**Fig 7-2.** The design concept of the new metacarpophalangeal implant (a) middle part, (b) implant assembly ..... 84

**Fig 7-3.** Model of the design in Figure 7-2 ..... 85

**Fig 7-4.** Simplified model (a) Ball-and-socket model for lubrication analysis, (b) equivalent ball-on-plane model for lubrication analysis ..... 85

**Fig 7-5.** Effect of velocity on predicted lambda ratio for soft layered joints ..... 92

**Fig 7-6.** Effect of load on predicted lambda ratio for soft layered joints ..... 92

**Fig 7-7.** Effect of elastic modulus of soft layered on predicted lambda ratio ..... 93

**Fig 7-8.** Effect of thickness of soft layered on predicted lambda ratio ..... 93

**Fig 7-9.** Effect of clearance on lambda ratio for different Elastic modulus of soft layered ..... 94

**Fig 7-10.** Effect of clearance on lambda ratio according to load ..... 95

**Fig 7-11.** Effect of clearance on Lambda ratio according to material combination ..... 95

**Fig 7-12.** Effect of metacarpal head radius predicted lambda ratio for soft layered joints .. 96

**Fig 7-13.** Effect of radius of metacarpal on Lambda ratio according to clearance ..... 96

**Fig 7-14.** Effect of viscosity on Lambda ratio according to material combination ..... 97

**Fig 7-15.** Effect of viscosity on Lambda ratio for metal on elastomer material combination according to load ..... 97

**Fig 8-1.** The pin-on-disc set up ..... 102

**Fig 8-2.** The experimental set-up of the wear test ..... 102

**Fig 8-3.** Taylor Hobson Form Talysurf Series 120L ..... 103

**Fig 8-4.** Scanning Electron Microscopy JEOL 6060 ..... 107

**Fig 8-5.** SEM image of the wear track on the silicone (Titanium pin). ..... 107

**Fig 8-6.** SEM image of the wear track on the silicone (UHMWPE pin) ..... 108

**Fig 9-1.** (a) Preflexed design elastomer part,(b) Straight design elastomer part,(c) Preflexed model for finite element analysis,(d) Straight model for finite element analysis. .... 116

List of Figures

**Fig 9-2.** Loading of FEA model by deflection: tangential applied displacement loading. 117

**Fig 9-3.** Fit of Mooney-Rivlin model to literature data (Kult and Vavrik 2001) engineering stress-strain curve ..... 118

**Fig 9-4.** Mesh density and computational (CPU) time ..... 119

**Fig 9-5.** Meshing of model used in the analysis..... 119

**Fig 9-6.** Variation of von Mises stress with angle of flexion for the preflexed and straight designs ..... 120

**Fig 9-7.** Stress distribution during deflexion of the FEA Model (Straight design)..... 120

**Fig 10-1.** (a) Ball-and-socket model, (b) equivalent ball-on-plane model..... 122

**Fig 10-2.** Effect of load on contact stresses for all material combinations ..... 127

**Fig 10-3.** Effect of load on contact stress for cobalt chrome on polyethylene and metal on elastomer material combinations ..... 127

**Fig 10-4.** Effect of load on contact stress for metal on elastomer material combinations over a range of elastomer elastic modulus 5-25 MPa ..... 128

**Fig 10-5.** Effect of radius of metacarpal head on contact stress for soft layer material combinations, with variation in elastic modulus ..... 128

**Fig 10-6.** Effect of soft layer thickness on contact stress for different loading conditions 129

**Fig 10-7.** Effect of radial clearance contact stress for soft layer material combinations . 130

**Fig 11-1.** 3D design of Concept selection 4 ..... 132

**Fig 11-2.** Stem shapes for metacarpophalangeal joint selection ..... 134

**Fig 11-3.** Stem of metacarpal ..... 134

**Fig 11-4.** Drawing of the metacarpal stem..... 136

**Fig 11-5.** Ball of metacarpal part ..... 137

**Fig 11-6.** Drawing of the metacarpal head..... 138

**Fig 11-7.** Section view of the assembly in differend position (a) Neutral, (b) flexed, (c) Full flexion (Note: In (b) and (c) the elastomer part has been excluded for better visualisation of the flexed position)..... 140

**Fig 11-8.** The MCP prosthesis design in extreme positions of extension (a), of flexion (b) and (c) in neutral position..... 140

**Fig 11-9.** Cross section of the metacarpal ball stem interface ..... 140

**Fig 11-10.** Middle part 3D design ..... 141

**Fig 11-11.** Drawing of middle part..... 142

**Fig 11-12.** Comparison of central part of our design in comparison with the commercial available implant Neuflex. .... 143

**Fig 11-13.** Proximal phalange stem ..... 143

**Fig 11-14.** Drawing of proximal phalange stem..... 144

**Fig 11-15.** Proximal phalange head..... 145

**Fig 11-16.** Drawing of proximal head..... 146

**Fig 11-17.** Cross section of proximal stem and proximal phalange head interface. .... 147

**Fig 11-18.** Drawing of elastomer part..... 149

**Fig 11-19.** Elastomer part..... 150

**Fig 11-20.** Free rotation of the stems and heads towards the elastomer part ..... 150

**Fig 11-21.** Parts of the assembly ..... 151

**Fig 11-22.** Exploded view of the assembly of the metacarpophalangeal design ..... 151

**Fig 11-23.** Assembly of the metacarpophalangeal design (a)3D view,(b)section view..... 151

**Fig 11-24.** Engineering drawing of the assembly..... 153

List of Figures

**Fig 12-1.**A typical load cycle proposed for testing finger joints in Durham simulator ..... 158  
**Fig 12-2.** Durham finger joint simulator ..... 158  
**Fig ApA-1.** Disk plate of the pin-on-disk apparatus..... 184  
**Fig ApA-2.** Pin holder of the pin-on-disk apparatus..... 185  
**Fig ApA-3.** Security disk plate ring of the pin-on-disk apparatus ..... 186  
**Fig ApA-4.** Test pin holder of the pin-on-disk apparatus ..... 187  
**Fig ApE-1.**Model of stem for stress calculation ..... 191  
**Fig ApF-1.** Maximum stress against shear load for elastomer part. .... 193

## List of Tables

<b>Table 2-1.</b> Hand grip strength for normal and diseased hands. ....	7
<b>Table 4-1.</b> Anatomical dimensions of metacarpal head and proximal phalange .....	59
<b>Table 5-1.</b> Table according to six thinking hats method .....	73
<b>Table 5-2.</b> Concept design criteria scoring table .....	75
<b>Table 6-1.</b> Rating of occurrence, severity and detection for potential hazards .....	79
<b>Table 6-2.</b> Results of risk analysis. ....	81
<b>Table 7-1.</b> Values of the parameters used in the lubrication analysis .....	88
<b>Table 7-2.</b> Materials properties.....	90
<b>Table 7-3.</b> Compound surface roughness of materials combinations.....	91
<b>Table 8-1.</b> Calculated k factors for silicone rubber against Ti and UHMWPE. K factors are a mean of two samples. (RS: Ringer’s solution, BS: Bovine serum).....	108
<b>Table 10-1.</b> Material properties .....	125
<b>Table 10-2.</b> Values of the parameters used in the contact stress analysis .....	126
<b>Table 12-1.</b> Proposed testing parameters for finger joint testing .....	158
<b>Table ApB-1</b> .Materials properties of Medical grade silicone rubber MED-71 and HP-100 Swanson implant silicone rubber.....	188

## **Chapter 1**

### **Introduction**

The metacarpophalangeal (MCP) joint is crucial for hand function, but this joint is frequently affected by arthritis, leading to pain and disability. Metacarpophalangeal joint arthroplasty has been found to provide pain relief and provide a functional range of motion to improve the life of the patient. The overall aim of this study was to develop a new metacarpophalangeal joint replacement prosthesis.

A review of the biomechanics of the normal and diseased metacarpophalangeal joint is presented in Chapter 2. The normal MCP joint enables a large range of motion in flexion/extension and abduction/adduction, as well as a few degrees of rotation. The diseased joint has reduced range of motion and reduced hand strength compared to the normal joint.

An in depth review of the past and current metacarpophalangeal joint replacement implants is presented in Chapter 3 with a retrospective analysis mainly of their failures. The past and current metacarpophalangeal joint replacements can be divided into three main categories: hinge implants, flexible implants and surface replacement implants. Many designs are prone to fracture as they are unable to withstand the conditions of the diseased joint.

## Chapter 1

Following the review of the biomechanics and the past designs, the design requirements of a new metacarpophalangeal joint are set out in Chapter 4 and the concept designs are presented in Chapter 5. A risk analysis of the concept of choice is presented in Chapter 6.

Prior to finalising the selected concept several validation methods to help with the final decisions were used. Lubrication analysis and contact stress analysis studies using well established theoretical methods are presented in Chapters 7 and 10. Laboratory wear test analysis of possible material combinations using pin-on-disk wear tests are presented in Chapter 8. Finite element analysis has been also used for the critical parts of the design in Chapter 9.

The final design is presented in Chapter 11. The general discussion, the findings, work that could be undertaken to further develop the new metacarpophalangeal joint and conclusions of this study are presented and discussed in Chapter 12.

## Chapter 2

# Biomechanics of the normal and diseased metacarpo-phalangeal joint

### 2.1 Introduction

The metacarpophalangeal joint (Fig 2-1) is the articulation between the metacarpal and phalange bones of the hand. It consists (Fig 2-2) of the metacarpal head, the proximal phalanx, the volar plate, the two collateral ligaments, the two accessory collateral ligaments and the sagittal band (Blazar and Bozentka 1997; Tamai *et al.* 1988; Wilson and Carlblom 1989). It has the outward appearance of a ball-and-socket joint with three degrees of freedom, but it actually acts more as a multiaxial condyloid joint, with its primary motion in flexion and extension (Kimball *et al.* 2003). It is also capable of abduction and adduction (radial and ulnar deviation), as well as rotation about its longitudinal axis (Degeorges *et al.* 2004; Stirrat 1996). The MCP joint is critical for finger positioning and hand function (Rosen and Weiland 1998).

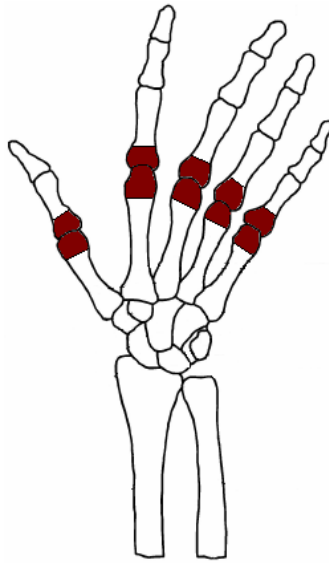


**Fig 2-1.** Metacarpophalangeal joints of human hand

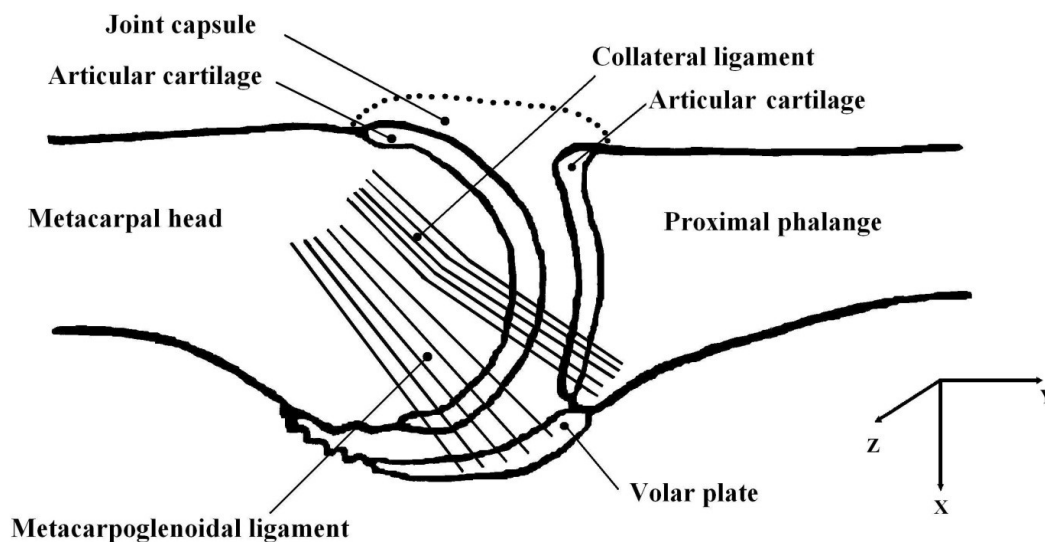


**Fig 2-2.** Normal metacarpophalangeal joint anatomy

The MCP joint is frequently affected by arthritis that leads to great pain and disability. Joint replacement implants are commonly used to replace the diseased MCP joint, but they have had varying success. The aim of this section is to review the biomechanics of the normal and diseased MCP joint in order to help better define the design requirements for the MCP joint replacement implant to be developed in this study.

## **2.2 Normal MCP joint biomechanics**

### **2.2.1 Range of motion**

The passive range of motion of the MCP joint (Fig 2-3) in the sagittal plane is 90° of flexion and 20-30° of extension (hyperextension), 40° arc in the coronal plane for abduction and adduction movement, together with a few degrees of axial rotation of the proximal phalanx towards the metacarpal head (Beevers and Seedhom 1993). There are minor

differences in the range of motion among the individual MCP joints, with increased flexion proceeding from the index to the small finger (Brewerton 1957).

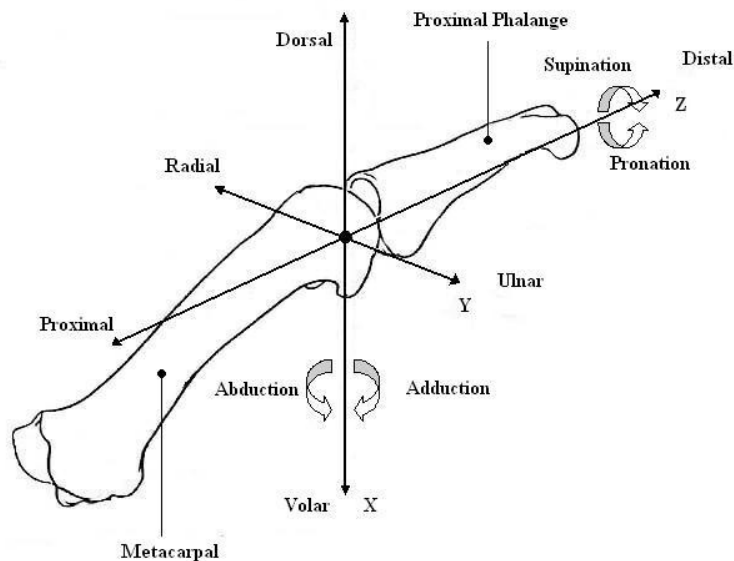


**Fig 2-3.** Axis of rotation of the metacarpophalangeal joint

Monitoring hand function in daily activities as well as specific tasks such as holding a toothbrush, turning a key or typing has revealed that for an individual a smaller range of motion is adequate to perform most of the necessary tasks requiring finger movement. This range of motion is known as a functional range of motion. The functional range of motion of the MCP joint ranges from 33° to 73° of flexion, with an average of 61°. For tasks such as pinch, grasp and grip the flexion of the MCP joint was 58°, 33° and 72°, respectively (Hume *et al.* 1990). The range of motion in flexion/extension for typing was between 0° and 45°, while during various simulated activities of daily living it has been measured to be between 0° and 68° (Rand and Nicol 1993) and 5° to 62° (An *et al.* 1985).

### **2.2.2 Centre of rotation**

The centre of rotation depends not only on the geometry of the joint, but also on the supporting structures of the joint (Ash *et al.* 1996; Tamai *et al.* 1988). Many authors have presented the centre of rotation of the MCP joint to be constant (Flatt and Fischer 1969; Unsworth and Alexander 1979; Youm *et al.* 1978) and in many two- and three-dimensional analyses, it has been considered constant for model and analysis simplification (Berme *et al.* 1977; Chao *et al.* 1976; Storace and Wolf 1979; Weightman and Amis 1982). Also, many MCP joint replacement implants use this assumption in their design (Petrolati *et al.* 1999). On the other hand, some authors support a variable centre of rotation for the MCP joint (Pagowski and Piekarski 1977; Tamai *et al.* 1988; Walker and Erkman 1975; Weiss *et al.* 2004). The constant centre of rotation consideration is based mainly on the necessity for simplification of the modelling of the metacarpophalangeal joint for force analysis. Also the poor results of the hinge metacarpophalangeal joint, described in Chapter 3, in which the centre of rotation is fixed together with the analysis by Weiss *et al.* (2004) that the instantaneous centre of rotation of intact MCP joint varied, support the theory of a variable centre of rotation rather a fixed centre of rotation (Weiss *et al.* 2004).

### **2.2.3 Forces**

The prehensile movements of the human hand can be divided into power grip and precision grip (Napier 1956). A review of hand strength measurement in normal and diseased joints is presented in Table 2-1. The grip strength for normal males has a wide range of values from 81-672 N (Massy-Westropp *et al.* 2004), according to the instrument used, hand dominance, subject occupation and age. The grip strength for normal women ranges from

21-425 N (Massy-Westropp *et al.* 2004). The grip force of women is on average 56 % that of men. Several two- and three-dimensional models have been used to analyse the forces acting on the MCP joint as the direct measurement of them *in vivo* is impossible. According to the published models the MCP joint force is given as a proportion of the external finger force. A wide variation in these forces has been observed due to different assumptions that have been made for modelling, as well as the orientation of the adjacent joints.

**Table 2-1.** Hand grip strength for normal and diseased hands. D – Dominant; F – Female; L – Left; M – Male; N – number; ND - Non dominant; OA - Osteoarthritis; R - Right; RA - Rheumatoid arthritis; ERA – Early Rheumatoid arthritis; SD - Standard deviation.

Reference	Age	Sex	Hand	Normal		Diseased		
				N	Mean (SD)	N	Mean (SD)	Type
(Mathiowetz <i>et al.</i> 1985)	20-94	M	R	310	462 (127)			
		M	L	310	428 (130)			
		F	R	318	280 (75)			
		F	L	318	244 (73)			
(Harkonen <i>et al.</i> 1993)	19-62	M		103	492 (88)			
		F		101	300 (66)			
(Blair <i>et al.</i> 1989)	20-60	M	D	100	467			
		M	ND	100	441			
		F	D	100	241			
		F	ND	100	220			
(Nordenskiöld and Grimby 1993)	20-69	M	R	64	432 (96)			
		M	L	64	393 (85)			
		F	R	105	229 (64)	19	42 (22)	RA
		F	L	105	213 (57)	19	39 (21)	RA
(Fraser <i>et al.</i> 1999)	30-79	M	D	14	322(78)	16	77 (85)	RA
		M	ND	14	302(72)	16	83 (85)	RA
		F	D	67	183 (60)	67	67 (54)	RA
		F	ND	67	165 (56)	67	71 (50)	RA
(Jones <i>et al.</i> 1985)		M	R L	20	355	38	100	RA
(Dellhag and Bjelle 1999)	53.7	M	D			15	194 (115)	ERA
		M	ND			15	194 (109)	ERA
		F	D			28	63 (50)	ERA
		F	ND			28	71 (51)	ERA
(Dominick <i>et al.</i> 2005)	68.9	F	R			700	222 (106)	OA
		F	L			700	208 (107)	OA

A model that has been used concluded that during pinch force the compressive force (Y-axis, see Fig 2-3) ranged between  $3.6P$  to  $5.6P$ , where  $P$  is the external finger force, while their review of previous models has shown the range to be from  $4.1P$  to  $8.8P$  (Weightman and Amis 1982). A review of the literature has estimated and analysed the MCP joint forces during pinch activity to be on average  $6P$  for compressive Y-axis,  $3P$  for subluxing X-axis and  $2P$  for ulnar directed Z-axis, while for power grip analysis it was estimated that the joint forces to be  $12P$ ,  $6P$  and  $4P$  in the Y, X and Z axis, respectively (Beevers and Seedhom 1995a).

The compressive force at pinch has been calculated to be  $5.5P$  and at power grip to be  $12P$  (Berme *et al.* 1977). An estimated MCP force of  $7P$  for compressive and  $3P$  for subluxing has been also calculated (Smith *et al.* 1964). Also it has been proposed an estimated force of  $14P$ ,  $9P$  and  $4P$  for power grip at Y, X, and Z axis, respectively (Chao *et al.* 1976).

Assuming an external pinch force of 70 N for males, it has been shown that the resultant internal joint force acting on the MCP joint is 490 N for a static pinch grip and 980 N for a static power grip (Beevers and Seedhom 1995a). For females, with a smaller external pinch force of 50 N, the calculated values for static pinch and power grips were 350 N and 700 N, respectively. There is a difference in the calculated loads during static pinch and power grips. This difference is mainly due to the fact that during a power grip the whole hand takes part in the movement, whereas only two fingers are used in the pinch action.

In a multidirectional study the index finger generates the maximum force in flexion of 111 N and the forces in extension, abduction and adduction were 38%, 98 % and 79% that of flexion, respectively (Li *et al.* 2003).

The finger, regarding activities such as typing can move at a very high speed under light loading. In a dynamic analysis with an external load of 1 N, the resultant force on the MCP ranged from 5 N to 24 N (Brook *et al.* 1995). Also, with only the muscle force balance the resultant force at 0° flexion is 14 N, while at 45° flexion it is 17.5 N on the MCP joint (Tamai *et al.* 1988; Weightman and Amis 1982).

### **2.2.4 Tendons, muscles and ligaments**

The measurement of finger and hand forces with a dynamometer provides useful data for the overall contribution of the multiple structures of the joint. Specific information can also be extracted for the contribution of each structure within the joint. The position of the other joints of the finger such as the proximal interphalangeal joint and wrist joint affect the forces in the MCP joint (Li 2002). There are a number of muscles and associated tendons divided in two groups namely the extrinsic (extensor digitorum communis, extensor indicis proprius, flexor digitorum superficialis, flexor digitorum profundus) and intrinsic (lubricalm, palmar interosseus, dorsal interosseous) (Li *et al.* 2003). The contribution of the intrinsic and extrinsic finger muscles has been studied with varying results (Knutson *et al.* 2000; Koh *et al.* 2006; Li *et al.* 2000; Li *et al.* 2001). Finger function requires balance of the intrinsic and extrinsic muscles and tendons for stability and strength. The tightening of

the MCP joint in flexion has been connected with decreased laxity of the collateral ligaments (Werner *et al.* 2003).

## **2.3. Diseased MCP joint biomechanics**

### **2.3.1 Diseases**

Arthritis of the hand encompasses a variety of disorders. They can be classified as inflammatory (such as rheumatoid arthritis) and non-inflammatory (such as osteoarthritis and traumatic arthritis). Rheumatoid arthritis is the predominant type of arthritis affecting the human hand joints while osteoarthritis in the MCP joint is less common than in other joints, such as the hip and knee (Linscheid 2000).

Rheumatoid arthritis is a symmetric polyarthritis characterised by synovitis, loss of articular cartilage and bone erosion. The bone in a rheumatoid joint has reduced bone density, strength and stiffness compared with normal or osteoarthritic bone (Bogoch and Moran 1999). There is a selectivity of synovial inflammation for the small joints of the body. Due to the joint anatomy and biomechanical factors in the pathology of the disease in the early stage of rheumatoid arthritis, there is a predominance of the disease on the radial side of the MCP joint; this asymmetry appears the tendency towards symmetry over time (Tan *et al.* 2003; Zangger *et al.* 2005).

Osteoarthritis is a non-inflammatory disease that involves articular cartilage deterioration and new bone formation at the joint edges and mainly affects one joint at a time (Gold *et al.*

## Chapter 2

1988). Osteoarthritis of the metacarpophalangeal joint is very rare and specifically affects the index and middle fingers (Nunez and Citron 2005; Rettig *et al.* 2005).

Traumatic arthritis is a form of arthritis that is caused from penetrating, or repeated trauma, or from forced inappropriate motion of a joint or ligament. Posttraumatic arthritis patients are often young and the limitations imposed by their disease affects their careers and hobbies (Netscher *et al.* 2000).

The metacarpophalangeal joint is more intrinsically unstable than the other joints of the finger and, therefore, more vulnerable to the deforming forces associated with rheumatoid arthritis (Rosen and Weiland 1998). Rheumatoid deformity initiates as painful stretching of the capsule and ligamentous structures by proliferative synovitis (Rosen and Weiland 1998). Rheumatoid arthritis causes an imbalance of static and dynamic forces across the joint and finally leads to destructive changes of the bone and articular cartilage as well as lengthening of the collateral ligaments (Brewerton 1957; Linscheid and Chao 1973; Tan *et al.* 2000). The accessory collateral ligaments and the volar plate are stretched by the synovitic MCP joint and cause the displacement of the flexor sheath from the joint midline (Tan *et al.* 2000). Secondary to pain, instability and muscle disease are the spasm and contracture of the muscles that stabilize the joint (Beckenbaugh 1976). The extensor tendons lose their ability to fully extend the MCP joint and the ulnar collateral ligament may tighten to maintain the ulnar deviated subluxation deformity intrinsically (Stirrat 1996). The rheumatoid tendons have greater rates of stress relaxation and lower strength than healthy tendons (Fowler and Nicol 2002). The periarticular connective tissue that

absorbed the potential destructive forces produced by the muscles, is weakened by the disease progress (Neumann 1999). The combination of volar subluxation and ulnar deviation of the MCP joint is known as ulnar drift.

### **2.3.2 Range of motion**

The range of motion in rheumatoid arthritis is decreased compared to the normal joint. The arc of motion in flexion/extension is moved to a more flexed position, while the proximal phalange is ulnar deviated. The mean preoperative arc of motion in rheumatoid arthritis is 30°, from 57° to 87° of flexion, while the ulnar deviation is 26° on average (Goldfarb and Stern 2003). The range of motion after arthroplasty has been found to deteriorate with time probably due to the stiffness of the joint because of the encapsulation process that takes place around the implant. The maximum average range of motion for patients with rheumatoid arthritis was 6°-58° and the functional range was 52° (Fowler and Nicol 2001b).

### **2.3.3 Forces**

The hand strength of the diseased joint is highly deteriorated, but it is dependent on the type of disease as well as the stage of the disease. Table 2-1 shows the hand grip strength for diseased hands. With rheumatoid arthritis, hand strength deteriorates with time (Joyce and Unsworth 2002b). Loss of hand grip strength and function is a major cause of disability in patients with rheumatoid arthritis. In Table 2-1 it can be seen that the hand strength for hands with rheumatoid arthritis is reduced compared with normal hands. It was stated that the pinch strength is often decreased to a range of 5 to 20 N in late rheumatoid arthritis (Linscheid and Dobyns 1979). Also, the average pulp pinch strength of arthritic patients has

## Chapter 2

been reported as 13 N (Weightman and Amis 1982). Maximum grip strength values of 58 N for active rheumatoid arthritis, 87 N for inactive rheumatoid arthritis and 102 N for osteoarthritis, compared with 238 N for normal have been reported (Helliwell *et al.* 1988). The resultant force acting on the metacarpophalangeal joint of patients with rheumatoid arthritis has been calculated 210 N and 420 N for pinch grip and power grip, respectively (Beevers and Seedhom 1995a). With osteoarthritis, the hand grip strength does not reduce as much compared with rheumatoid arthritis (Table 2-1). The osteoarthritic patients present 15% to 20% decrease in their grip strength, but if the age parameter is taken into account the decrease comes up to 40% (Labi *et al.* 1982).

### **2.4 Summary**

In this chapter the biomechanics of the normal and diseased metacarpophalangeal joint has been described to help understand the performance required by a joint replacement implant for the MCP joint. In the next chapter a review of current and past designs of MCP joint prostheses will be presented.

## Chapter 3

### Metacarpophalangeal Joint Prostheses

#### 3.1 Introduction

Design of finger joint replacements can be divided into three categories: the hinge implants, the flexible one-piece implants and the surface replacement implants. In this section past and current designs of metacarpophalangeal joint prostheses will be reviewed to help understand why they fail and to provide information for the design requirements for a new design of implant.

#### 3.2 Hinge prostheses

##### 3.2.1 Brannon and Klein prosthesis

The Brannon and Klein prosthesis (Fig 3-1) was the first metacarpophalangeal (MCP) joint prosthesis to be implanted in 1953. The device consists of two titanium parts, the metacarpal and the proximal phalange components joined by a half-threaded rivet screw to prevent sinking of the prosthesis into the bone. The arc of motion was 100°. Despite initial enthusiasm as the first follow-up results were encouraging there were later reports of sinking of the prosthesis into the bone and screw loosening (Beevers and Seedhom 1995b; Beevers and Seedhom 1993; Brannon and Klein 1959; Linscheid 2000).

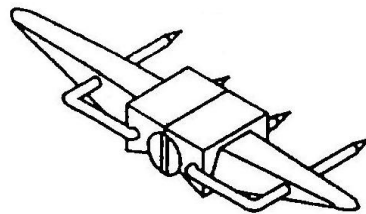


**Fig 3-1.** Brannon Klein design

### 3.2.2 Flatt Prosthesis

The Flatt design (Fig 3-2) is a modified hinge-type Brannon and Klein design. It was introduced in 1961 and was followed by a few modifications in the location of the axis of rotation (Flatt 1973; Flatt and Fischer 1969). It is a three component prosthesis manufactured from 316 stainless-steel. The metacarpal and phalangeal components were inserted separately and then linked together by a screw, which gives a fixed axis and only extension and flexion movement could take place. Its stem consists of two prongs to allow bone ingrowth and prevent rotation of the prosthesis in the medullary canals (Beevers and Seedhom 1993). Reports of bone resorption, subsequent shift of the prosthesis, deposition of metallic debris as well as mechanical failures were major problems of the prosthesis (Blair *et al.* 1984; Flatt and Ellison 1972; Linscheid 2000). On the other hand Flatt emphasized that the prosthesis was designed to withstand the forces of the diseased hand (Flatt 1967; Flatt 1961).

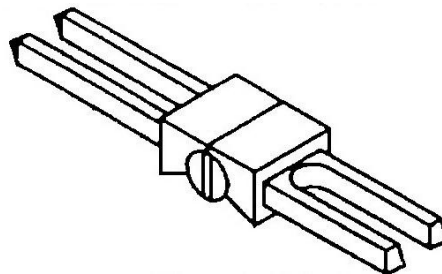


**Fig 3-2.** Flatt design

### 3.2.3 Griffith- Nicolle prosthesis

In 1973 the Griffith-Nicolle prosthesis (Fig 3-3) was introduced as a modification of the Calcan-Nicolle implant described later on in section 3.3.7. It was a roller and socket hinge uncemented design with flanged intramedullary stems. The socket was a polypropylene cup

placed in the metacarpal, while the bearing stainless steel surface was inserted in the proximal phalanx. No fractures have been reported, but the poor range of motion  $38^{\circ}$  and the high recurrence of ulnar drift  $27^{\circ}$  compromised the implant success (Beevers and Seedhom 1995b; Beevers and Seedhom 1993; Griffiths and Nicolle 1975; Nicolle and Gilbert 1979; Varma and Milward 1991).

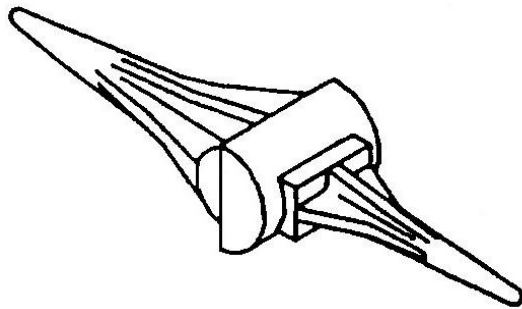


**Fig 3-3.**Griffiths- Nicolle design

### **3.2.4 Schetrumpf prosthesis**

The Schetrumpf implant (Fig 3-4) is a hinge type implant that consists of two components: a roller and a socket. It was introduced in 1975 and the phalangeal roller component was manufactured from polyacetal while the metacarpal socket component was manufactured from polypropylene. Fixation was achieved by three fins on each stem cutting into the cortical bone to prevent rotation of the implant in the medullary canals (Beevers and Seedhom 1993; Hagert 1978). Review of thirteen joint replacements with this implant that appear improvement in power, appearance and pain relief, and no complications (Schetrumpf 1975). Although no other independent survey has been reported.

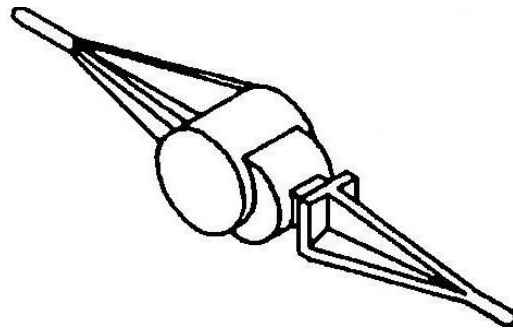


**Fig 3-4.** Schetrumpf design

### **3.2.5 Schultz prosthesis**

The Schultz design (Fig 3-5) is a two-piece semi-constrained implant made of a metal phalangeal component and a plastic metacarpal component. It is a ball and socket articulation with a changing centre of rotation. The axis of rotation changes as the ball could be located in any position in the oblique vertical slot of the metacarpal head for the same angle of flexion. Bone cement is used for fixation into the medullary canals. Biomechanical evaluation of the implant report that the range of motion allowed was from neutral to 90° of flexion and an 8° arc for radial and ulnar deviation (Gillespie *et al.* 1979). It has been stated that in a few clinical cases the Schulz design was effective (Beckenbaugh 1977).

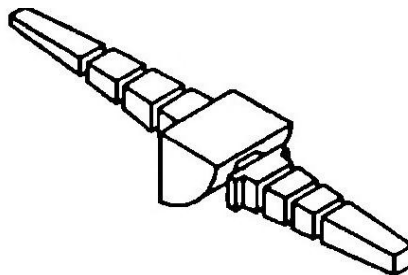


**Fig 3-5.** Scultz design

In a long-term follow-up study after 11 years found a decrease in the active range of motion that finally was 10°, and there was a gradual recurrence towards a more flexed position

(Adams *et al.* 1990). Ulnar deviation deformity recurred in all digits. Although loosening of the components was not presented, plastic deformation of the slot in the metacarpal component and fracture of the metallic neck of the phalangeal component proved that the implant was unable to sustain the forces generated by routine use.

### 3.2.6 Steffee prosthesis

In the late 1960s Steffee developed an Ultra High Molecular Weight Polyethylene (UHMWPE) phalangeal component and cobalt-chrome (CoCr) alloy metacarpal component snap-lock metacarpophalangeal prosthesis (Fig 3-6). Initially the prostheses were implanted without cement, but in 1973 cement fixation was initiated due to fixation problems. The prosthesis allows lateral motion of the finger in extension but achieves stability in flexion simulating the normal joint through a narrow slot.

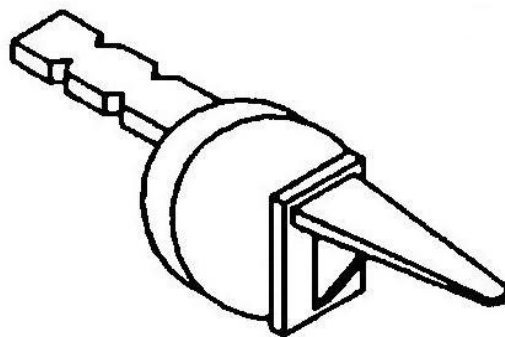


**Fig 3-6.** Steffee design

The original design Type 1 was modified to the Type 2 ball and socket design. Early results showed 80% pain relief and stability among patients. Although limited motion, deformity recurrence and radiographic evidence of loosening with time have been reported in both types of design (Beckenbaugh 1977; Beckenbaugh 1976; Eiken and Hagert 1981; Linscheid

and Dobyns 1979). The Type 3 design has been introduced, but there have not been any clinical trials reported (Beevers and Seedhom 1995b).

### **3.2.7 St George – Buchholtz prosthesis**

The St George-Buchholtz implant (Fig 3-7) is a modification of the Flatt design, but fixation is with bone cement. It consists of a plastic (polyethylene) metacarpal component and a metal (cobalt-chrome-molybdenum) phalangeal part. The two components are assembled by a transverse spindle on the phalangeal part. The range of flexion and extension by the design is 100° while it deviates in radial and ulnar direction in the extended position. A slot in the metacarpal component governed the movement in the sagittal plane while it is laterally stabilized in the flexed position (Hagert 1978). Follow-up examinations showed poor flexion capacity of 30°, recurrence of ulnar drift and in some cases ankylosis was developed (Beevers and Seedhom 1995b; Eiken and Hagert 1981).

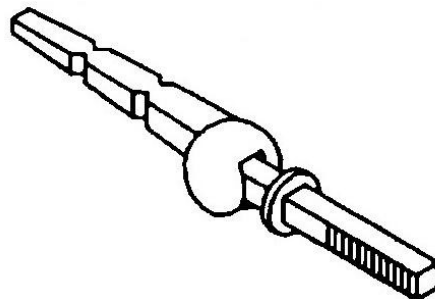


**Fig 3-7.** St George- Buchholtz design

### **3.2.8 KY Alumina ceramic prosthesis**

The KY alumina prosthesis (Fig 3-8) is ceramic hinge-type finger prosthesis. It consists of three components: a polycrystal alumina proximal stem, a proximal part of the hinge joint made of high density polyethylene (HDP) and a distal stem of single crystal alumina. The

fourth design of the implant was commercially available for clinical use. The fourth design allows for 90° to 120° flexion/extension and 20° of abduction and adduction. The stems were fitted uncemented into the intramedullary canals with an interference fit. A preliminary follow-up study (12 to 31 months) has not shown fracture, dislocation or loosening of the implant, but the range of motion was poor as it varied from 10° to 40° (Doi *et al.* 1984).

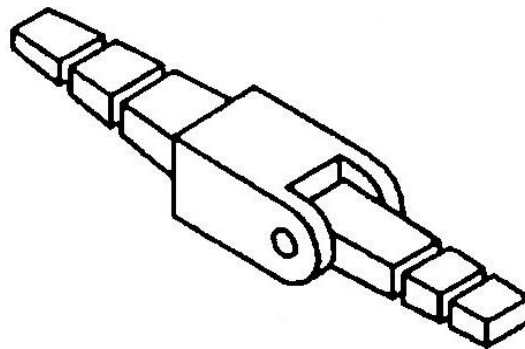


**Fig 3-8.** KY Alumina design

### **3.2.9 Minami Alumina prosthesis**

The Minami alumina ceramic implant (Fig 3-9) consists of three components: a single-crystal alumina proximal phalangeal stem, a polycrystal alumina metacarpal stem and a high-density polyethylene (HDPE) bearing to fix the two stem components together. The prosthesis is designed to provide a range of motion from 0° to 110° flexion and 10° abduction and adduction. The average range of motion 38 months postoperatively for the MCP joint was 36.5°. No dislocation or fracture was found radiographically. The dorsal location of the rotational centre of the prosthesis may be responsible for the limitation in extension movement (Minami *et al.* 1988).

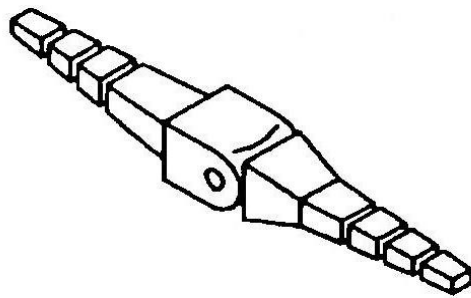


**Fig 3-9.** Minami Alumina design

### **3.2.10 Strickland Prosthesis**

The Strickland design (Fig 3-10) is a two-piece cemented prosthesis which consists of the distal metacarpal metallic component which articulates through a slot on the radial side of the plastic proximal component. A solid shoulder of plastic to prevent ulnar deformation is on the ulnar side of the proximal component. The design allowed 5° of extension, 90° of flexion and 15° of radial and ulnar deviation at zero flexion, but no radial and ulnar deviation at full flexion (Gillespie *et al.* 1979).

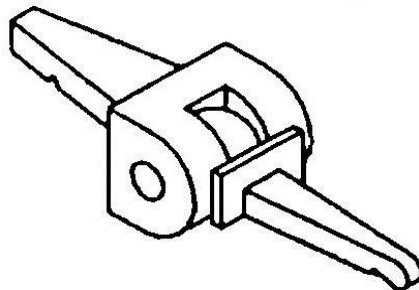


**Fig 3-10.** Strickland design

### **3.2.11 Walker Prosthesis**

The Walker prosthesis (Fig 3-11) consists of a polymer metacarpal component, a metal phalangeal component and a plastic snap-in axle. The stems have a circular shape with slots

to prevent rotation within the medullary canals and cement was used to secure fixation. The polymer axle was protected by transmitting the forces directly from the metacarpophalangeal to the proximal phalangeal components, but the location of the centre of rotation at a fixed line makes flexion difficult (Walker and Erkman 1975).

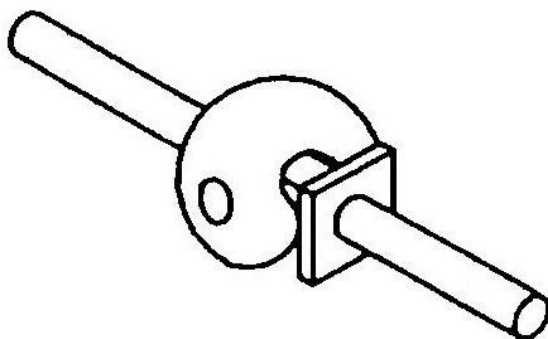


**Fig 3-11.** Walker design

### **3.2.12. Weightman Prosthesis**

The Weightman prosthesis (Fig 3-12) consists of four individual hinge joints in pairs by common hinge-pins, so that forces transmitted on one finger are shared with a neighbouring joint. The phalangeal component was made from metal (Cobalt Chrome alloy) while the metacarpal component was made from UHMWPE. The stems had a saw tooth profile with thin fins that are fixed onto them. The fixation into the intramedullary canals was secured with the insertion of the stems into precision reamed holes of diameter intermediate between the central core and the outer fin diameters (Weightman *et al.* 1983). The necessity of the connection of the two prostheses lengthens the operating time and the design did not allow any abduction or adduction. Also a small torsional force could extract a single prosthesis with this fixation (Beervers and Seedhom 1993).

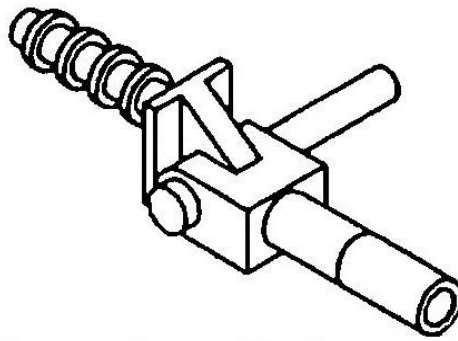


**Fig 3-12.** Weightman design

### **3.2.13 Mathys prosthesis**

The Mathys prosthesis (Fig 3-13) is an all-plastic implant. The prosthesis consists of a polyacetal-resin proximal component, a polyester metacarpal component, a metal core, and a screw. The two pieces are implanted separately and are fixed in the medullary canals by an expanding mechanism. A cone shaped metal piece is pressed into the stem by a screw to secure the stems into the medullary canals. The two parts are snapped together afterwards. The main problem was the migration of the prosthesis so, within a few months postoperatively, the range of motion was very poor (Eiken and Hagert 1981; Hagert 1978; Vermeiren *et al.* 1994).

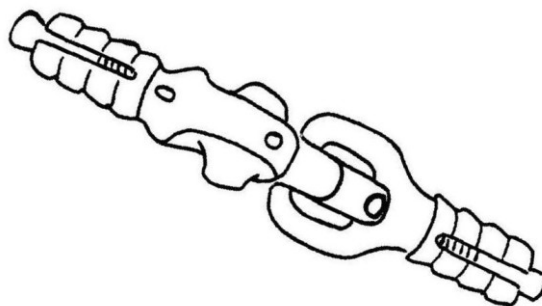


**Fig 3-13.** Mathys design

The later design of the Mathys RM (Robert Mathys, Bettlach, Switzerland) implant consists of two Polyetheretherketone (PEEK) components. There is an internal titanium screw for initial fixation and the stems are coated with titanium for bone ingrowth (Joyce 2004). PEEK has been proven as a biocompatible biomaterial and with sufficient strength for a joint replacement (Morrison *et al.* 1995).

### 3.2.14 Link arthroplasty prosthesis

The Link implant (Fig 3-14) is a cobalt chrome alloy self-locking cemented hinge prosthesis. It consists of two parts: the metacarpal is a hollow flat cylinder with a chord and the phalanx component is a flat disc with the same outside diameter and width as the metacarpal chord. At a certain position, shown in Fig 3-14, the two parts lock together with little disruption to the periarticular structures. The Link arthroplasty stabilises the excess lateral movements while it provides a functional flexion – extension arc of motion. A follow-up study of 51 joints has shown 64 % good results with an arc of motion more than 40° (Devas and Shah 1975; Eiken and Hagert 1981).

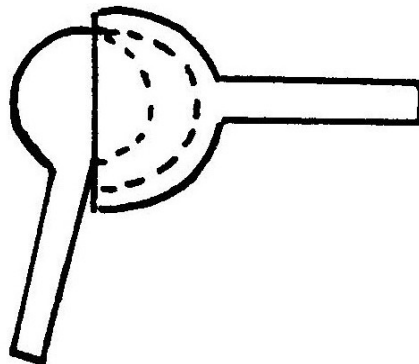


Fig 3-14. Link design

### 3.2.15 WEKO Prosthesis

The WEKO prosthesis (Fig 3-15) consists of five parts. It has two titanium porous coated medullary sockets, a prong, a prosthesis head and the axis for coupling the head and the prong. The prosthesis itself is available in one size, while the medullary sockets are available in six sizes. The bearing surfaces are made from CoCrMo coated with titanium-niobium. The range of motion is 5° of extension and 90° of flexion, while the lateral movement is restricted to 4°- 6°. A two-year follow-up study of the prosthesis has shown all the prostheses have to be removed due to rapid migration and rotation inside the medullary cavities (Radmer *et al.* 2003). The stem of the implant was changed to a cylindrical one with a star shaped cross-section to reduce the stress on the sleeves. In a ten-year follow up study 16% of the prostheses had to be removed, with rotational stability and osseointegration problems and the fact that the range of motion deteriorates with time (Wessels 2005).

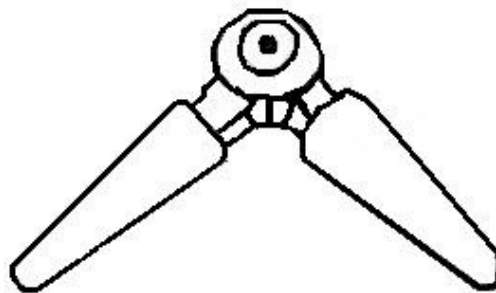
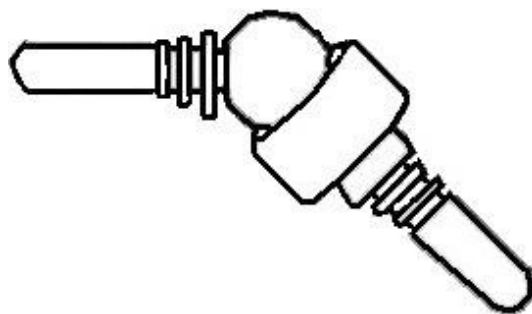


Fig 3-15. WEKO design

### 3.2.16 Digital Operative Arthroplasty DJOA prosthesis

The digital joint operative arthroplasty (DJOA) (Fig 3-16) is a non-constrained implant that acts as hinge joint. It consists of two stainless steel components with a polyethylene coating. The articular surface has a slot to accommodate the rim of the proximal surface and

the design allows 90° maximum flexion. The prosthesis is implanted without cement using grooved, tapered polyethylene inserts for fixation. The DJOA design 3 implant uses a press-fit fixation of ellipsis-shaped polyethylene stems wedged into the intramedullary canals. The stainless steel surface of the metacarpal component is spherical and the articular surface of the proximal phalangeal component is cylindrical. The clinical results were not encouraging for the former designs of the DJOA. It has been reported that 5.5 years after implantation none of the prostheses qualified as ‘good’ (Rittmeister *et al.* 1999). The proximal component does not match the anatomical shape of the metacarpal, the design is unable to provide adequate coaptation and the use of polyethylene was questioned due to its osteolytic behaviour (Linscheid 2000).



**Fig 3-16.** DJOA design

### **3.2.17 Daphne Prosthesis**

The Daphne prosthesis (Fig 3-17) manufactured by Tecres (Verona, Italy) consists of two pyramidal segments linked at the base by a cylindrical articulated joint. The flexible segments are made from polymethylmethacrylate (PMMA) and the flexible joints are made from AISI 316L stainless steel. The segments are not fixed inside the phalangeal and metacarpal medullary canals so have a ‘‘piston-like’’ longitudinal motion. The mechanical and biocompatibility tests of the prosthesis and its materials have given a positive answer in

terms of biocompatibility and high resistance to wear. Further follow-up studies in clinical use are necessary for implant evaluation (Petrolati *et al.* 1999).

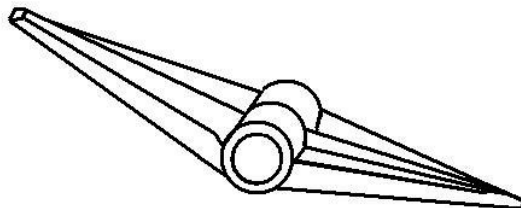


**Fig 3-17.** Daphne design

### **3.3 Flexible one-piece prostheses**

#### **3.3.1 Swanson prosthesis**

The Swanson implant design (Fig. 3-18) is the most widely used MCP joint replacement implant (Beevers and Seedhom 1995b; Blazar and Bozentka 1997; Shapiro 1999). The function of the implant is based on the concept that the implant acts as a dynamic spacer by keeping the bones ends apart and in good alignment (Eiken and Hagert 1981; Hagert 1978). The implant is fixed in the joint by the principle of encapsulation (Gillespie *et al.* 1979; Swanson 1969). Swanson summarises his concept as follows: Joint resection + implant + encapsulation = new joint (Swanson 1972). The Swanson implant is now manufactured from a silicone material called 'Flexspan' while the first implant in 1962 was manufactured from conventional silicone elastomer (CSE). Later designs were made from high performance (HP) elastomer and in 1986 it was replaced by HP-100 (Goldfarb and Stern 2003; Joyce 2004; Joyce and Unsworth 2002a).

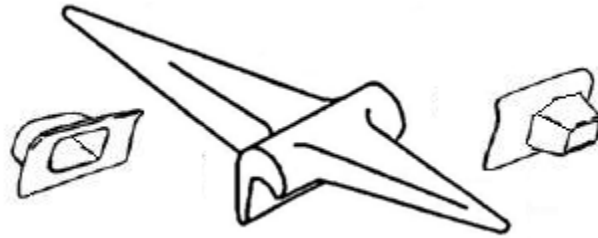


**Fig 3-18.** Swanson design with grommets

The centre of rotation was erratic and did not confine itself to any pattern (Gillespie *et al.* 1979). In an *in vitro* study of the instantaneous centre of rotation (ICR) the Swanson implant presents a large range of instantaneous centres of rotation ICRs indicating significant pistoning of the stems in and out of the bone and toggling during flexion. Abnormal pistoning or implant toggle may result in wear debris and implant fracture (Weiss *et al.* 2004). The pistoning motion may cause bone erosion (Levack *et al.* 1987). The metacarpophalangeal arthroplasty with the Swanson implant improves the cosmetic appearance of the hand, reduces pain, corrects deformity and provides a more functional arc of motion for the patient (Goldfarb and Stern 2003; Ishikawa *et al.* 2002; Kirschenbaum *et al.* 1993; McArthur and Milner 1998; Pereira and Belcher 2001).

The reported rates of fractures for the Swanson MCP implant present a great variation from no fractures at an average of 5.25 years follow-up study (Bieber *et al.* 1986) to 82.4 % fracture rate at a 5 year follow-up period (Kay *et al.* 1978). The differences in the fracture rate are due to the different implant materials, prosthesis failure determination, condition of the adjacent joints, patient individuality, different follow-up periods and different postoperative care (Joyce and Unsworth 2002a; Nalebuff 1984). The Swanson implant mainly fractures at the junction of the distal stem and hinge, and secondly across the hinge

## Chapter 3

due to subluxing forces that often dominate in the rheumatoid hand (Joyce and Unsworth 2002a). At an average of 14-year follow-up study, a fracture rate of 67 % was reported for the Swanson MCP implant (Goldfarb and Stern 2003). It has been concluded that fracture of HP-100 Swanson implants is not related to rheologic properties of the implanted elastomer as it remains intact after implantation while oxidation of the silicone rubber *in vivo* may be implicated in fracture of the implant (Naidu 2007; Naidu *et al.* 1997).

Due to the problems of fracture, press-fit titanium circumferential grommets were introduced in 1987 to attempt to reduce the incidence of prosthesis fracture from sharp bony edges and shearing forces. The grommets were introduced to protect the flexible hinge implant midsection, so to prevent abrasion and tear of the implant material (Swanson *et al.* 1997). Two studies with follow-up periods of 5.8 years and 3.9 years, respectively, have shown a reduction in the implant fractures due to the use of grommets (Schmidt *et al.* 1999b; Swanson *et al.* 1997). On the other hand, it has been stated that the use of grommets just delayed the fracture of the implant (Minamikawa *et al.* 1994a). While others found that the use of grommets did not prevent implant fracture (Trail *et al.* 2004). Report of two cases with evidence of symptomatic titanium particulate tissue inflammation due to titanium debris of the grommets has been also reported (Khoo *et al.* 2004). It has been also noted that with grommets more bone stock has to be removed (Khoo 1993).

The range of motion and ulnar drift after Swanson MCP implant arthroplasty has been monitored by many follow-up clinical studies (Beckenbaugh *et al.* 1976; Bieber *et al.* 1986; Ferlic *et al.* 1975; Fleming and Hay 1984; Goldfarb and Stern 2003; Hagert *et al.* 1975;

## Chapter 3

Kay *et al.* 1978; Kirschenbaum *et al.* 1993; Mannerfelt and Andersson 1975; McArthur and Milner 1998; Opitz and Linscheid 1978; Schmidt *et al.* 1999a; Schmidt *et al.* 1999b; Swanson 1972; Synnott *et al.* 2000; Wilson *et al.* 1993). The mean immediate postoperative range of motion was 46° and the final postoperative was 36° compared with the 30° preoperative (Goldfarb and Stern 2003). A post-operative arc of motion for Swanson MCP implants less than 45° of flexion has been also reported (Beevers and Seedhom 1995b). Ulnar drift has a high recurrence postoperatively and was averaged 20° for fractured implants and 10° for intact implants (Goldfarb and Stern 2003).

Fracture of the silicone implant remains a problem, but fortunately it does not usually ruin the result of the arthroplasty as the encapsulation process is mainly responsible for the joint stability (Schmidt *et al.* 1999b; Vasenius *et al.* 2000). Also, the status of the implant does not affect the range of motion in flexion-extension movement, but the ulnar drift which is important in both the function and the cosmetic appearance was affected by the implant fracture as the implant afterwards is unable to support the repetitive loading patterns experienced during daily activities (Fowler and Nicol 2002; Goldfarb and Stern 2003).

Literature reviews identified no reports of immunologic reaction, connective tissue disease, or other systemic effects associated with the use of the Swanson finger implant (Foliart 1995; Foliart 1997). After all, silicone induced particulate synovitis and lymphadenopathy have been reported due to long-term use of silicone elastomeric joint implants (DeHeer *et al.* 1995; Hirakawa *et al.* 1996; Khoo 1993; Minamikawa *et al.* 1994b).

The patient satisfaction with the Swanson implant arthroplasty is very high (Goldfarb and Stern 2003). The study by Fleming and Hay (1984) showed 91% patient satisfaction which was most influenced by postoperative hand appearance and pain relief rather than by objective measures (Mandl *et al.* 2002; Massy-Westropp *et al.* 2003; Schmidt *et al.* 1999b; Synnott *et al.* 2000). The outcome is also influenced by the postoperative therapy regime (Massy-Westropp and Krishnan 2003).

### 3.3.2 Niebauer prosthesis (Cutter)

The Niebauer prosthesis (Fig. 3-19) was developed at the same time as the Swanson implant. The implant is made of silicone rubber reinforced by a Dacron fibre mesh for added strength internally and externally (Beevers and Seedhom 1993; Hagert 1978). The fixation of the implant into the medullary canals was due to in-growth of fibrous and bony tissue into the implant stems. The hinge was reinforced with a Dacron weave and the stems are covered with a Dacron mesh sleeve for immediate fixation (Goldner *et al.* 1977). Bending was intended to take place only at the hinge (Hagert 1975c; Niebauer and Landry 1971; Niebauer *et al.* 1969). The motion of the stems of the Niebauer implant and the bone erosions indicates an insufficient intramedullary fixation (Hagert 1975a; Hagert 1975b).

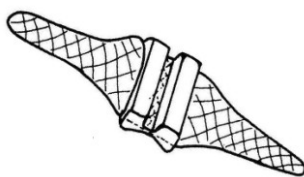


**Fig 3-19.** Neibauer design

The Niebauer implant is too weak to withstand the forces in the MCP joints (Hagert 1975a). The two different materials that the implant is made of appeared as a contributing factor to

the implant fracture as the stress of the interface between the two materials causes the softer material to yield (Hagert 1975c). A follow-up study after 2.5 years showed average flexion motion of 35°, fracture rate of 38.2 % and 44.1 % recurrence of clinical deformity (Beckenbaugh 1976). In a 3-year follow-up study reported a fracture rate of 53.7% (Hagert 1975a). A 6.5 years follow-up study has shown 54° active motion and 62% deformity recurrence (Goldner *et al.* 1977). According to this study the overall fracture rate was 6.8% but for the 37 implants followed for 6.5 year follow-up was 29.7%. A follow-up study for an average of 11.5 years showed good pain relief, short-term correction of ulnar drift, but some recurrence afterwards, no significant gain in motion, but a more extended and functional arc of motion (Derkash *et al.* 1986).

### **3.3.3 Soft Skeletal Implant Avanta (previously known as the Sutter)**

The Avanta Soft Skeletal Implant previously called the Sutter prosthesis (Fig. 3-20) is manufactured by Avanta (SanDiego, California, US). The implant was introduced in 1987 and was also based on the concept of flexible implant encapsulated by connective tissue, similar to the Swanson implant (Moller *et al.* 2005). The Sutter prosthesis has a centre of flexion palmar to its longitudinal axis, which makes extension easier to be achieved (Joyce *et al.* 2003; McArthur and Milner 1998). The Sutter prosthesis is manufactured from ‘Silflex’ a silicone rubber material (Bass *et al.* 1996; Joyce *et al.* 2003). Different fracture rates of the implant have been reported. A fracture rate of 45 % at a follow-up of more than 3 years has been reported (Bass *et al.* 1996). A fracture rate of 27 % has been also reported (Joyce *et al.* 2003). While in a long-term follow-up study reported a fracture rate of 52 % compared with 67 % for the Swanson implant (Goldfarb and Stern 2003).

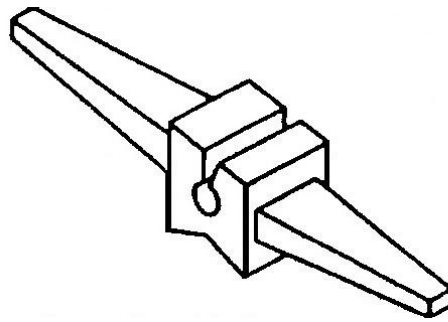


**Fig 3-20.** Sutter – Avanta design

Fracture rates of 20 % have been reported at a two-year follow-up study and 7° higher range of motion than the Swanson implant (Moller *et al.* 2005). The Sutter prosthesis fractures at the junction of the distal stem and hinge due to the relatively small radii at these junctions (Joyce 2004). *In vitro* testing of the Sutter was able to reproduce the mode of fractures seen *in vivo* (Joyce *et al.* 2003). Finite element analysis of the implant has noted that the implant would fracture only at the hinge (Penrose *et al.* 1997; Williams *et al.* 2000). It has been reported that “the Avanta (Sutter) prosthesis achieved wide acceptance without any studies confirming better performance to the Swanson” (Moller *et al.* 2005; Parkkila *et al.* 2005). Apart from the straight implant design there is also the Avanta preflexed silastic implants available (Joyce 2004).

### **3.3.4 Neuflex prosthesis**

The Neuflex implant (Fig. 3-21) manufactured by DePuy Orthopaedics Inc. (Warsaw, Indiana, US) was introduced in 1998 and is preflexed by 30° so to mimic the natural resting position of the fingers. *In vitro* tests have shown greater longevity than the Sutter design (Joyce 2004; Joyce and Unsworth 2005). A better arc of motion than that of the Swanson in the Preflex design reduced the strain across the hinge by 35 % (Erdogan and Weiss 2003). In a comparative study of the instantaneous centre of rotation (ICR), the Neuflex implant

matched more closely the intact MCP joint in comparison with the Swanson and Avanta silastic implants (Weiss *et al.* 2004). It allows a more functional degree of motion that probably leads to a decreased implant failure rate. In a comparative follow-up study of two-years between the Swanson and Neuflex implants, the Neuflex implant presents a better mean flexion arc of  $72^{\circ}$  in comparison with  $59^{\circ}$  for the Swanson (Delaney *et al.* 2005). The Neuflex implant *in-vitro* fracture occurs only across the pivot of the central hinge section in contrast with previous *in-vitro* and *in-vivo* experience with Swanson and Sutter designs that both fracture at the junction of the distal stem and the hinge (Joyce and Unsworth 2005). Neuflex implant has a collar to reduce pistoning and also reduce wear of the material and that more clinical trials are necessary to support that hypothesis that the implants last for longer in comparison with the Swanson implants (Trail 2005). The Neuflex compared with the Sutter implant presents higher patient satisfaction regarding the occupational performance of the prosthesis (Pettersson *et al.* 2006a).

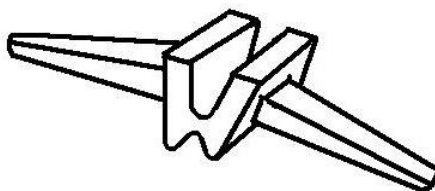


**Fig 3-21.** Neuflex design

### **3.3.5 Helap Flap prosthesis**

The Helap prosthesis (Fig 3-22) is a one piece silicone rubber implant reinforced by Dacron to give increased strength. Its features involve a dorsal ulnar based flap to maintain the central position of the extensor tendon, wide stem shoulders to prevent sliding down in the medullary canals and flat rectangular stems to prevent rotation of the implant. A short

follow-up study of 1.5 year has shown over-correction of the ulnar deviation resulting to some patients finger position being in radial deviation (Levack *et al.* 1987). An average arc of motion from 10° to 48° has been described, while in 21% of the joints flexion was less than 30°. The follow-up period was inadequate for definite evaluation of the prosthesis and further studies are necessary (Beevers and Seedhom 1995b; Levack *et al.* 1987).

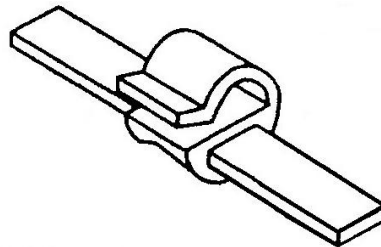


**Fig 3-22.** Helap Flap design

### **3.3.6 Calnan – Reis prosthesis**

The Calnan-Reis prosthesis (Fig. 3-23), introduced in 1968, was a one-piece implant manufactured from polypropylene and fixed by cement (Calnan and Reis 1968a; Calnan and Reis 1968b). The results were very poor and an unspecified clinical trial has been held for this design (Reis and Calnan 1969). It has been stated that this design provided inadequate space for bone separation, weak lateral stability, uncontrolled range of motion and mechanical irritation due to soft tissue pinching at the hinge (Nicolle and Calnan 1972).

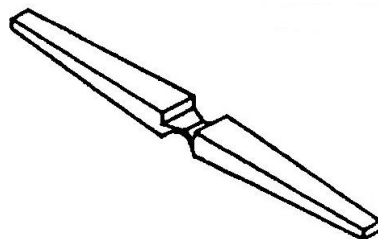


**Fig 3-23.** Calnan- Reis design

### 3.3.7 Calnan-Nicolle prosthesis

In 1972 Nicolle & Calnan introduced a modification of the above Calnan-Reis prosthesis. A silicone rubber capsule (Fig. 3-24) prevents the fibrous tissue ingrowth and also protects the hinge from the bone edges. A clinical trial presented 59° arc of motion and 18 % ulnar drift recurrence (Nicolle and Calnan 1972).

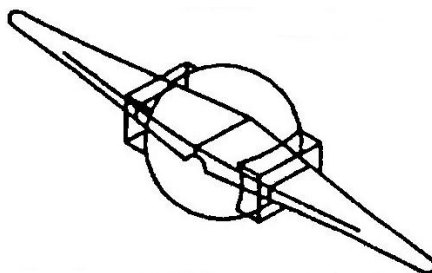


**Fig 3-24.** Calcan – Nicolle design

### 3.3.8 Lundborg prosthesis

The Lundborg prosthesis (Fig 3-25) consists of two titanium fixtures and a silicone flexible spacer as the joint mechanism. Each end of the silicone spacer is mounted on a titanium plate with a short, slightly conical stem to provide a press-fit mechanism into the fixtures for maximum stability (Lundborg *et al.* 1993; Moller *et al.* 1999a). The prosthesis fixation is based on osseointegration and the titanium fixtures were screw-shaped for stable anchorage in the bone marrow canal. The replacement of the silicone spacer if it failed is easy without the removal of the titanium fixtures (Moller *et al.* 1999b). A follow-up study after 2.5 years showed an average active range of motion of 57° in rheumatoid cases and 50° in all the cases. The fracture rate was 6 % and patient satisfaction was high (Lundborg *et al.* 1993). A later follow-up study showed 98 % radiographic osseointegration,

postoperative median range 40° and 25 % fracture of the silicone spacer (Moller *et al.* 1999a).

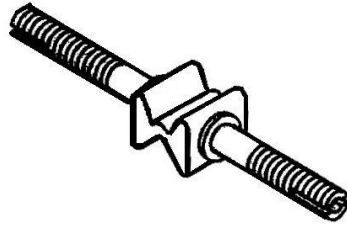


**Fig 3-25.** Lundborg design

Thirty one MCP joint implants that were evaluated for more than 5 years showed 97 % osseointegration, and 24.5 % fracture rate of the silicone spacer (Moller *et al.* 2004). Similar results have been observed for septic arthritis, compared with rheumatoid arthritis and osteoarthritis, with 34° range of motion and no loosening of the titanium fixtures (Lundborg and Branemark 2001). Cancellous bone grafting from the iliac crest was used for rheumatoid arthritis patients as the quality of cancellous bone is not good. There is a concern for the high fracture rate of the silicone spacer and an improved spacer has to be developed (Moller *et al.* 2004).

### **3.3.9 Ascension Silicone implant**

One can add to the Silicone flexible MCP implants with the 30° Silicone MCP Ascension (Fig 3-26), but no studies are available up to date (Joyce 2004).

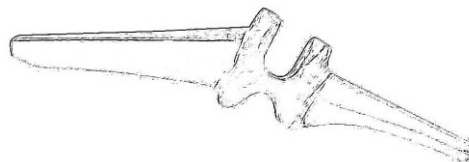


**Fig 3-26.** Ascension silicone implant design

### 3.4 Surface replacement prostheses

#### 3.4.1 Pyrolytic Carbon MCP implant

The Pyrolytic Carbon MCP implant (Fig 3-27) is a two-piece prosthesis that has an articulating, unconstrained design with a hemispherical head and grooved, offset stems. A long-term follow-up study of 11 years has been reported that showed an average of 13° improvement in the arc of motion and 94 % of the implants give evidence of osseointegration (Cook *et al.* 1999). Pyrolytic carbon has an elastic modulus similar to that of cortical bone (Cook *et al.* 1989).

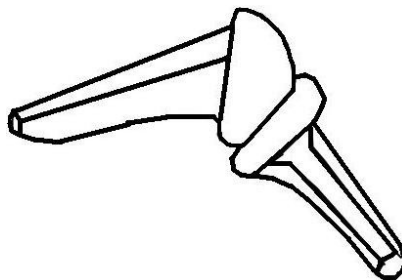


**Fig 3-27.** Pyrolytic Carbon design

After being implanted into human MCP joints it has been biologically and biomechanically compatible, wear resistant and durable material for arthroplasty (Cook *et al.* 1983; Cook *et al.* 1999; Joyce 2004; Murray 2003). The Pyrolytic Carbon implant is indicated for primary rheumatoid arthritis or post-traumatic arthritis and general MCP joints that had little deformity, subluxation, or dislocation and not for severe rheumatoid arthritic joints (Beckenbaugh 2003; Cook *et al.* 1999). Fixation problems have raised the question of whether Pyrolytic carbon is suitable for uncemented fixation (Daecke *et al.* 2006; Herren *et al.* 2006). Pyrolytic carbon has been suggested as a noteworthy alternative in MCP treatment after a follow-up study of ten months for seven prostheses in two patients. There was improvement in grip and pinch strength as well as in passive range of motion, but no

change or deterioration in the active range of motion. There was recurrence of ulnar drift in one of the patients with no evidence of implant failure which supports the need of minor deformities and early implantation of unconstrained designs in rheumatoid patients (Kujala *et al.* 2006). The pyrocarbon surface replacement prosthesis has proved inadequate for rheumatoid arthritic patients and generally for patients with major deformities (Cook *et al.* 1999). Comparison of Proximal Interphalangeal arthroplasty between Pyrolytic Carbon implants and Silicone implants from osteoarthritic patients show similar results without any superiority of the Pyrolytic carbon compared with the silicone implant (Branam *et al.* 2007). An intraoperative fracture of Pyrocarbon proximal interphalangeal (PIP) joint has been reported (Skie *et al.* 2007).

### 3.4.2 Avanta SR implant

The Avanta SR (Surface Replacement) prosthesis (Fig. 3-28) consists of a cobalt-chrome alloy metacarpal hemispherical head that articulates against an UHMWPE phalangeal component. The intrinsic stability of the prosthesis and it was found to be more than the normal joint (Kung *et al.* 2003).

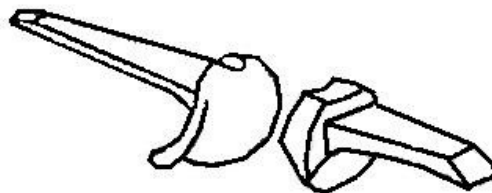


**Fig 3-28.** Avanta SR design

The prosthesis is fixed with bone cement. A few *in vitro* tests have been undertaken with a wear volume of 3.12 mm<sup>3</sup> per million cycles (Joyce 2004). Cement removal is difficult in

the necessity of revision and also there is concern about the effect of heat polymerization (Linscheid 2000).

### 3.4.3 Moje implant

The Moje ceramic-on-ceramic implant (Fig. 3-29) consists of an inclined metacarpal head and a phalangeal component with matching concave surface (Joyce 2004). A press-fit method for fixation is used. There are no clinical results available for MCP prosthesis, but the metatarsophalangeal and proximal interphalangeal implants presents good short-term outcomes (Ibrahim and Taylor 2004; Pettersson *et al.* 2006b). Fracture problems have been reported on the metatarsophalangeal joint implant (Pavier 2005).

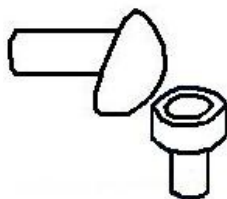


**Fig 3-29.** Moje design

### 3.4.4 Elogenics implant

A new two-piece unconstrained prosthesis is the Elogenics (Fig.3-30) implant with conforming spherical surfaces by Zimmer Europe (Winterthur, Switzerland) has shown low wear rates during *in vitro* testing to five million cycles of flexion and extension (Joyce *et al.* 2006; Rieker *et al.* 2003). Both components are manufactured from titanium alloy and the metacarpal component has an UHMWPE hemispherical ball/socket. Short to mid – term studies have shown good results with no necessity of implant removal (Hagena and Mayer 2005; Mayer and Hagena 2005).

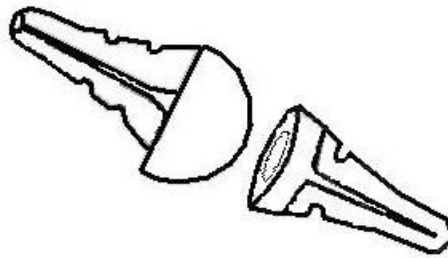


**Fig 3-30.** Elogenics design

### **3.4.5 Total Metacarpophalangeal Replacement (TMR) implant**

The Total Metacarpophalangeal Replacement (Fig 3-31) is an unconstrained surface MCP joint implant that consists of three components: a spherical metacarpal component with an offset cylindrical stem that fits within an UHMWPE plug and an UHMWPE phalangeal cup. Both the metacarpal and phalangeal stems have fins that provide fixation within the medullary canals. Sliding and rotation between the metacarpal head and the UHMWPE plug reduces stress transmission to the area of fixation due to a pistoning effect. A five-year follow-up study of 13 implants has shown joint movement improvement from 27° to 60°. It should be noted that in all the patients the condition of the ligaments was good (Harris and Dias 2003; Joyce 2004).



**Fig 3-31.** Total metacarpophalangeal replacement design

### 3.4.6. Andigo implant

The Andigo design (Fig. 3-32) metal-on-metal uncemented prosthesis is manufactured from cobalt-chrome alloy, is a two piece implant and the medullary stems are coated with hydroxyapatite for bone ingrowth (Joyce 2004).



Fig 3-32. Andigo design

### 3.4.7 Digitale implants

The Digitale implant (Fig. 3-33) is a two-piece titanium-coated, stainless steel stems into which fits a hinge unit manufactured by Procerati (Paris, France) (Joyce 2004).

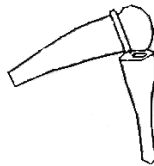
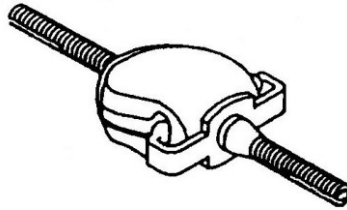


Fig 3-33. Digitale design

### 3.4.8 Hagert prosthesis

The Hagert prosthesis (Fig 3-34) consists of a joint mechanism attached between two bone fixtures. The joint mechanism allows three dimensional movements. It consists of an ultra-high-density polyethylene articular head on the metacarpal side and a socket of titanium on the phalangeal side. Two small ball-and-socket joints provide the assembly mechanism for

stability of the joint mechanism. A follow-up study of 3.4 years has been held with only 5 patients. The range of motion comes up to 65° flexion and the fracture rate was 20 % (Hagert *et al.* 1986).



**Fig 3-34.** Hagert design

### **3.4.9 Sibly & Unsworth (Durham) prosthesis**

Durham prosthesis is a surface replacement prosthesis (Fig. 3-35) that is non cemented (Sibly and Unsworth 1991a). Laboratory tests of this design named the Durham design has been presented but no *in vivo* results have been published (Joyce *et al.* 1996).

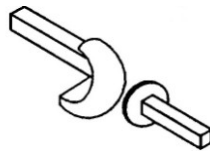


**Fig 3-35.** Sibly-Unsworth design

### **3.4.10 Kessler prosthesis**

The Kessler prosthesis (Fig. 3-36) was designed for the replacement of the destroyed metacarpal head. In a preliminary clinical trial, with eight patients, the results showed pain relief and preservation of length and shape of the MCP joint. The average range of motion was 60°, but a further follow-up study and larger number of implants are necessary for adequate evaluation (Beevers and Seedhom 1995b; Kessler 1974).

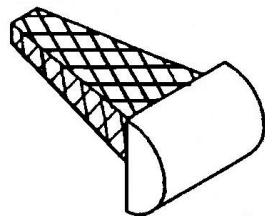


**Fig 3-36.** Kesler design

### **3.5 Discussion**

A frustration among hand surgeons in not being able to match the success of the large total joint arthroplasties has been reported (Linscheid 2000). There are fundamental differences of the large human joints, like hip, in comparison with the metacarpophalangeal joint, which is a skin-deep articulation supported in all the range of motion by small ligaments and a variety of tendons in all the sides and although the magnitudes of the forces are relatively small in comparison with other joints, the proportion of force per unit size is probably much greater in the hand (Flatt 1980). The necessity for more durable implants as today patients are healthier and live longer has been also mentioned (Goldfarb and Stern 2003). The lack of standardized procedure for abrasion wear of silicone and lack of standard procedures for testing finger implants prior to use *in vivo* elastomers has been reported (Joyce 2003; Peimer 1989).

In this review of the literature many discontinued implants have been presented with few follow up studies and a lot of failures. The hinge implants, due to the allowance of unidirectional motion during flexion and extension motion only, were susceptible to the lateral abnormal forces due to the rheumatoid disease process. Hinge implants have been found to be inappropriate as an implant concept for the metacarpophalangeal joint. One

## Chapter 3

piece silicone implants are the most used implants and they have the longest presence in the history of small joint replacement arthroplasty. The most used of the flexible implants is the Swanson design and this has been characterized as the gold standard that any new implant is compared to.

In one piece silicone implants there is a difference in the site of failure between the finite element analysis studies and the *in vivo*/ *in vitro* results. In finite element analysis the failure is predicted in the central hinge of the implant while from *in vitro* results and retrieved implants the main site of failure is initiated in the dorsal aspect of the distal stem due to abrasion (Joyce 2009). Although the one piece silicone implants are spacers that provide alignment and flexibility to the joint, due to the high scoring in pain relief, ease of implantation and revision procedure, patient satisfaction and more flexible range of motion, they are the implants of choice among hand surgeons. The cost of silicone implants due to the material used and the quantity of implants used is lower than that of the surface implants and maybe this is a reason for implant selection.

Newer silicone implant designs such as the Neuflex, Avanta or Ascension silicone rubber designs differ from the Swanson implant; they provide a preflexion that stress relief the implant during normal function. It has been reported that the Neuflex design with the increased range of motion does not result in any difference in the revision rate or implant fracture compared with the Swanson design (Kimani *et al.* 2009). For the surface replacement implants it can be seen that there are a few new designs that use material combinations that have been proven reliable in the larger joints of the human body, like the

## Chapter 3

hip and knee. However there is a lack of long term follow-up multi-centre studies to provide us with reliable data for comparison with the results of the older one piece silicone implants.

There are also cases where failure rates published for the same implant differ like in Weko design where 16% and 100 % failure rate has been reported (Radmer *et al.* 2003; Wessels 2005). Most of the time the results are influenced by the patient selection, surgical technique as well as the number of the implants that are involved in the study.

This chapter has detailed some of the current and past designs of MCP joint replacement implants and some of the failures and design problems. In the next chapter the design considerations for a new novel metacarpophalangeal joint prosthesis will be considered.

## Chapter 4

### Design considerations for a new metacarpophalangeal prosthesis

#### 4.1 Introduction

Metacarpophalangeal joint prostheses are designed to relieve pain, improve the cosmetic appearance of the deformed finger, restore the functional range of motion, correct and prevent further deterioration of the deformities, provide stability of the joint and adequate strength to carry out daily activities (Beevers and Seedhom 1995a; Linscheid 2000). A successful design of a small joint replacement arthroplasty has been suggested that it should (Flatt and Fischer 1969):

- Restore a functional range of motion
- Provide adequate stability
- Provide a mechanical advantage equivalent to the normal joint
- Resist the rotational stresses and seat firmly
- Be easily implantable
- Accommodated to a range of sizes for different individuals

Further requirements have been set by (Linscheid 2000):

- Be manufactured from biocompatible materials
- Provide adequate wear strength material characteristics
- Allow soft tissue reconstruction

In this section the full design requirements for a metacarpophalangeal joint replacement will be considered. During this process the design criteria involve the consideration of the

engineering challenges, the patient expectations, the surgical aspects, as well as the manufacturing limitations; none of them should be considered separately as shown in Fig 4-1.

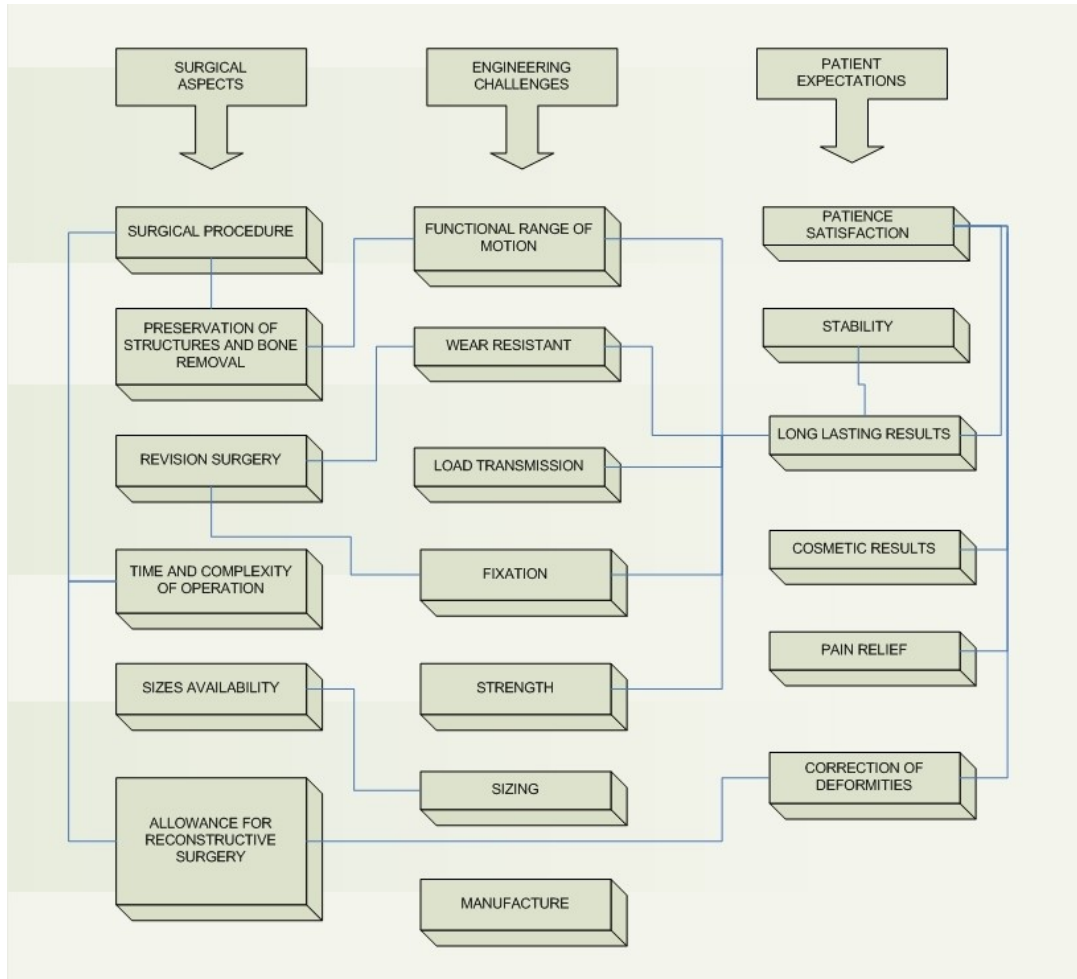


**Fig 4-1.** Interrelations of the surgical aspects, patient expectations and engineering challenges in the design of a new prosthesis

## 4.2 Anatomy and conformity of the bearing surfaces

The eccentric attachment of the collateral ligaments at the metacarpophalangeal joint results in a complex sliding and rolling action of the articulating surfaces (Pagowski and Piekarski 1977). The radius of the articulating concave surface of the proximal phalange is much

larger than the convex portion of the metacarpal head (Pagowski and Piekarski 1977). Dimensions of the bearing surfaces can be selected according to published data on human metacarpophalangeal joint dimensions and dimensions of current metacarpophalangeal joint implants (Unsworth and Alexander 1979; Unsworth *et al.* 1971). Non conforming bearing surfaces can also allow lubricant to become entrained between the surfaces and allow wear debris to escape (Beavers and Seedhom 1995a).

If the soft tissues surrounding the joint are in a poor condition, then there may be a problem with joint stability, and any contribution to stability from the bearing surfaces must be welcomed. Conforming surfaces may alter the moment arms, movement and lubrication of the joint but would also result in lower joint contact stress (Ash and Unsworth 2000). The lubrication of the design concept as well as the functionality of the joint will both contribute to the amount of conformity that the new implant will have and it will be presented in Chapter 7. In the normal metacarpophalangeal joint the area of the metacarpal head is larger than the area of the proximal phalange socket. The normal anatomy of the metacarpophalangeal joint has shown that the radius of the metacarpal head and proximal phalange are not reciprocal. Also, there is a difference among the fingers of the hand and the radius is different in the sagittal and coronal plane (Unsworth and Alexander 1979). The right and left hand fingers are not symmetrical but the necessity of fewer available sizes and the compromise of standard size implants make the moment arms of the joint after arthroplasty different from the normal ones (Ash and Unsworth 2000; Beavers and Seedhom 1999).

### **4.3 Range of motion**

Taking into consideration the biomechanical analysis of the normal and diseased metacarpophalangeal joint (Pylios and Shepherd 2007), as well as, the information presented in Chapter 2, a functional range of motion rather than a full range of motion should be considered for the new implant design. A design that will provide a range of motion of up to 70° of flexion and 5° of extension as well as 40° arc of motion for abduction and adduction with rotational freedom will be able to help patients to fulfil most of the daily activities (An *et al.* 1985; Hume *et al.* 1990; Rand and Nicol 1993). A functional, rather than a full range of motion will also likely reduce the stresses and strains within the implant at the extreme positions of flexion and extension.

### **4.4 Centre of rotation**

The centre of rotation of the natural metacarpophalangeal joint is located within the metacarpal head, but its exact location is open to debate (Ash *et al.* 1996). The moment arm of the joint is a factor that plays an important role in the movement of the joint. The right placement of the centre of rotation will guide the moment arms and the balance of the flexor and extensor tendons and muscles (Linscheid 2000).

### **4.5 Strength of the implant**

The implant itself should be designed to withstand the normal forces experienced in the human hand. The implant design should also withstand the shear stresses that are experienced in the diseased joint and try to balance the high eccentric forces eliminating

any overload of the implant that will lead to recurrence of deformity and excess wear or breakage of the implant or even distortion of the implant. The hand strength is highly deteriorated preoperative and the rheumatoid arthritic patients experience very low hand strength, but the osteoarthritis patients have more strength during pinch and grasp action. The review of the literature has shown that after joint arthroplasty the strength of the patients is better but the increase is very small in comparison with the strength of the normal hand (Pylios and Shepherd 2007). A load of 200-250 N can be expected for the implant *in vivo* and a lateral force of 100 N, but during motion of the finger a lower load at the range of 14-100 N is expected. A lower load of 50 N has been selected as maximum load in lubrication analysis of metacarpophalangeal joint replacement (Joyce 2007b).

#### **4.6 Stability of the implant**

Due to the effects of rheumatoid arthritis and osteoarthritis the normal joint biomechanics are deteriorated and the internal forces due to tendons, ligaments and muscles are not in balance. The end result is the known deformities of ulnar drift and volar subluxation with disabling consequences for the patient (Wise 1975). The ulnar drift alters the opposability of the thumb towards the other fingers that is the hallmark of human dexterity (Linscheid and Dobyns 1979). The insertion of the implant together with the necessary soft tissue reconstruction procedures should balance the forces among the different structures that are supporting the joint. That is especially important in rheumatoid arthritis where the deformities are major in comparison with osteoarthritis. In early rheumatoid arthritis in which the condition of the muscles, tendons and ligaments are in better condition, the implant design should provide an internal stability as in the case of rheumatoid arthritis the

disease process does not stop with the insertion of the implant and may continue after implantation (Madhav and Stern 2007).

### **4.7 Wear performance**

The wear of materials used in joint replacement is a concern as the amount of wear debris is responsible for many problems concerning the outcome of the joint replacement (Savio *et al.* 1994). Osteolysis is a main adverse effect and also silicone synovitis, due to the silicone rubber wear which is one of the main materials used for flexible MCP implants (DeHeer *et al.* 1995; Khoo 1993; Lanzetta *et al.* 1994; Peimer *et al.* 1986).

### **4.8 Fatigue**

The implant itself should be capable to sustain the normal function of the human metacarpophalangeal joint. The annual rates of movements available in the literature should be used for an estimation of the expected lifetime of the implant design. The lifestyle of the user and the nature of the user's work should be taken into account. The age and gender of the patient is vital for the long term results and successful outcome of the implant design. A sliding distance of 368 km is equivalent of 12.5 years of use *in vivo*, which extrapolates to 29.44 km sliding distance per year (Joyce *et al.* 1996). In finger joint simulators a cycle is the motion from 0° flexion up to 90° of flexion and back to 0°. This corresponds to  $1.34 \times 10^6$  cycles that the implant will experience for this annual distance for a radius of the metacarpal head of 7 mm (Joyce *et al.* 1996). Other calculations have shown similar sliding distances per year but the number of movements were calculated to be  $15 \times 10^6$  and  $12 \times 10^6$  for the normal and diseased fingers, respectively (Fowler and Nicol 2001b). A yearly number of finger movements of 1 million has been calculated, although the

movement was up to 90° (Stokoe *et al.* 1990). The movements described in another study were less in magnitude with 64% and 77% of the overall movements less than 10° of flexion (Fowler and Nicol 2001b). The finger implants, therefore, tend to experience a higher number of movements with a smaller arc of motion than the full range of motion movements that are conventionally used for testing them *in vitro*.

## **4.9 Fixation method**

### **4.9.1 Introduction**

The type of fixation is based on the available bone and the dimensions of the joint. The cortical thickness is greater in men (20-70 years) 5.2 to 4.6 mm than in women (20-70 years) 4.8 to 3.15 mm. It decreases slowly with age in men but rapidly after 50 years in women (Morgan *et al.* 1967). A cortical thickness of 2.67 mm and 1.48 mm in the metacarpal midshaft and metaphysis, respectively for joint replacement patients aged 25 to 68 years has been reported (Swanson *et al.* 1986). Intramedullary cavities (Fig 4-2) vary in size (Table 4-1) among the human population and among fingers of the same person that makes a general type of fixation difficult. The ring finger cross section of the medullary cavity is half that of the index and middle fingers (Linscheid 2000). Fixation of the prosthesis is vital for replacement success. Failure of fixation can be caused by a reaction to wear debris, micro motion of the implant towards the bone and stress shielding (Haupt 2000).

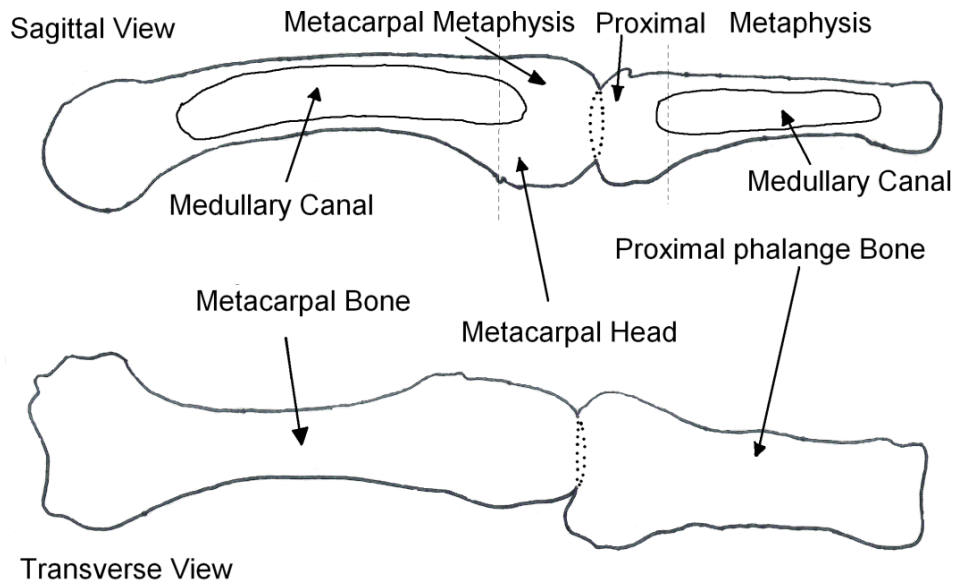


**Fig 4-2.** Sagittal and transverse view of metacarpophalangeal joint and medullary cavities position

### **4.9.2 No fixation**

No fixation of the implant has been proposed for flexible implants like the Swanson design. The implant is free to piston inside the medullary cavities and the fixation is provided by the encapsulation process (Swanson 1969). This type of fixation is illustrated in Figure 4-3(a).

### **4.9.3 Cement**

Polymethylmethacrylate cement (Fig.4-3(c)) has been used as an implant fixation technique since the 1960s and was introduced by Professor Sir John Charnley (Charnley 1970). It is a self-curing cement that acts as a filler which sets hard inside the body and provides mechanical interlocking between the bone and implant interface (Beavers and Seedhom 1995a). There is concern for cell necrosis due to the polymerization of the cement which results in an exothermic reaction. No recognisable adverse reactions to the thermal effect of

methylmethacrylate polymerization on small tubular bones or on the overlying tissue with a temperature rise of up to 60 degrees (Schultz *et al.* 1987b). Although the amount of cement that could be used in the finger joints is limited by the small size of the bones, there is concern about the heat dissipation and rise in the temperature could cause bone necrosis. There is also concern for revision arthroplasty and the difficulty of removing the cement and the damage it may cause to the remaining bone (Beevers and Seedhom 1995a). Cement particles may also contribute to third-body wear (Caravia *et al.* 1990). There are two interfaces: the bone-cement and cement-implant. The cement-implant interface loosening can be minimised by coating with bone cement or a polymethylmethacrylate polymer. The problems at the bone-cement interface are based on bone cement and cementing technique factors (pores, inherent weakness, toxicity) (Park 1992).

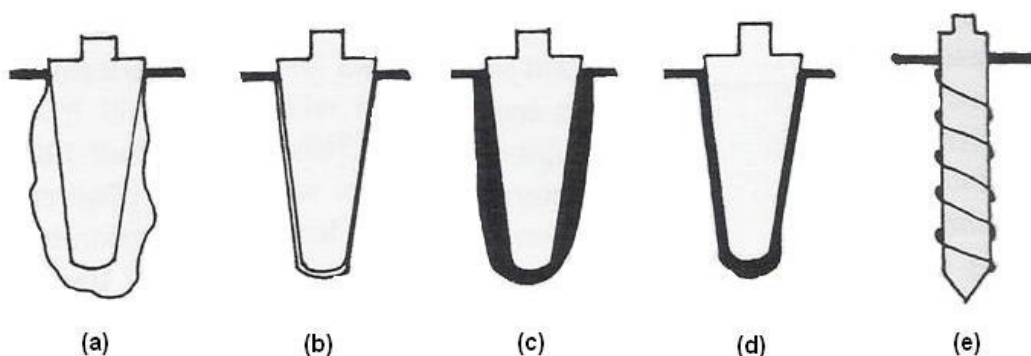


**Fig 4-3.** Different types of fixation (a) No fixation (b) Press fit fixation (c) Cement fixation (d) Coated prosthesis (e) Osseointegration fixation (Adapted from (Haupt 2000))

#### ***4.9.4 Interference or press fit***

Interference or press-fit techniques (Fig 4-3(b)) is when the implant is inserted uncemented inside the reamed hole of the bone and it becomes surrounded by dense fibrous tissue which provides good fixation at the bone/implant interface (Beevers and Seedhom 1995a). When a

joint prosthesis is implanted into the bone, the normal stress pattern in the bone is changed, which can result in bone resorption and may eventually cause loosening of the prosthesis. Loosening can produce wear debris from the bone-joint interface which can become trapped between the bearing surfaces, causing third-body wear. It can also be deposited in the surrounding soft tissues, causing inflammation and pain (Ash and Unsworth 2000). Polyethylene fin fixation has been used for the Total Metacarpophalangeal Replacement (TMPR) by Finsbury Orthopaedics (Leatherhead, Surrey,UK) (Harris and Dias 2003).

### ***4.9.5 Bone in-growth or osseointegration fixation***

Bone in-growth is a method of fixation (Fig 4-3 (e)) where a porous coating is applied on the surface of the implant stem and the surrounding bone grows inside the porous coating, forming an interlock mechanism for implant fixation (Beevers and Seedhom 1995a). There are several designs that use the concept of bone in-growth or osseointegration. The Lundborg and Hagert designs uses this concept with very good fixation of titanium screws, but very poor functional outcome of the use of the design *in vivo* (Hagert *et al.* 1986; Lundborg *et al.* 1993). The osseointegration of the titanium screws in small bones was very good in metacarpophalangeal implants and wrist implants (Lundborg *et al.* 2007; Lundborg *et al.* 1993). The Pyrocarbon implant uses osseointegration on a coated prosthesis (Fig 4-3 (d)) as the type of fixation, although there is some debate if actual osseointegration takes place with pyrocarbon finger implants *in vivo* (Cook *et al.* 1999; Daecke *et al.* 2006; Herren *et al.* 2006).

## 4.10 Minimal bone resection

Minimal bone resection is necessary as the metacarpophalangeal joint has limited bone stock. Further, with rheumatoid arthritis patients there is deterioration in the bone stock available due to osteoporosis (Ash and Unsworth 2000). In Figure 4-4 the level of resection of the metacarpal head is presented (Weiss 2000). The insertion of the implant actually changes the transmission of the load from externally to internally as the stem will distribute the forces into the cancellous bone. The bone-implant interface is vital for the success of the implant in the long term (Ash and Unsworth 2000).

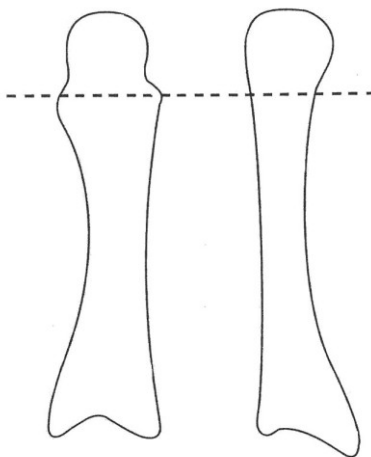


**Fig 4-4.** Level of resection of the metacarpophalangeal head (Weiss 2000)

## 4.11 Sizing of the prosthesis

There is a commercial need to limit the number of sizes that the final design should be available in. In the human population there are a variety of different sizes for the dimensions of the metacarpophalangeal joints (Unsworth and Alexander 1979) but the number of sizes of any implant should be limited. So compromise should be done according

to the frequency that the dimensions are observed. The Swanson silicone implant is available in 10 sizes, while the Elogenics is available in 4 sizes for the metacarpal head and 3 sizes for the proximal part. In Table 4-1 dimensions of metacarpophalangeal joint anatomical characteristics are presented from the literature (Lazar and Schulter-Ellis 1980; McArthur et al. 1998; Schulter-Ellis and Lazar 1984; Unsworth and Alexander 1979). The index finger has been selected as the initial model joint for this study since the index finger has a history of use as a standard for human metacarpal studies (Barker *et al.* 2005b; Berme *et al.* 1977; Brook *et al.* 1995; Chao and An 1978; Chao *et al.* 1976; Li *et al.* 2003). Moreover the index finger is involved in both the grasp and pinch actions and it is one of the fingers that it is more active during a power grip (Wise 1975). The deformities from rheumatoid arthritis are more frequent and more severe in the fingers that participate more in the grasp action (Wise 1975). Further, osteoarthritis mainly affects the index finger (Nunez and Citron 2005).

### **4.12 Allowance of soft tissue reconstruction**

The correction of the deformity is vital for restoration of normal kinematics and cosmetic improvement of the metacarpophalangeal joint. The correction of deformity involves various reconstruction processes but in long term follow-up studies there is recurrence of them. Correction of deformities of the other joints of the hand and wrist , should be done prior to arthroplasty of the metacarpophalangeal joint (Bogoch and Judd 2002). Soft tissue management of the metacarpophalangeal joint is vital and sometimes more important than the actual insertion of the silastic implant (Nalebuff 1984; Trail 2006).

## Chapter 4

**Table 4-1.** Anatomical dimensions of metacarpal head and proximal phalange All dimensions are in mm. MC: Metacarpal Bone, PP: Proximal phalange bone, IM: internal measurements, EM: External measurements, SD: Standard deviation

Anatomical dimension	Bone	Index	SD	Middle	SD	Ring	SD	Little	SD	Note	Reference
Proximal Cartilage	MC	0.78	0.2	0.8	0.19	0.64	0.15	0.69	0.20	IM	(Lazar and Schuller-Ellis 1980)
Proximal Metaphysis	MC	11.42	2.89	10.38	2.83	9.69	1.75	9.56	1.97	IM	(Lazar and Schuller-Ellis 1980)
Medullary Canal	MC	44.10	5.76	42.92	5.42	36.46	5.14	32.83	4.46	IM	(Lazar and Schuller-Ellis 1980)
Metacarpal length	MC	68.84		66.64		58.53		53.86		IM	(Lazar and Schuller-Ellis 1980)
Radius head sagittal	MC	7.63	1.48	7.63	1.01	6.69	0.88	6.22	0.89		(Lazar and Schuller-Ellis 1980)
Radius head sagittal	MC	7.95	0.85	7.48	0.62	7.35	0.65	6.60	0.82		(Unsworth and Alexander 1979)
Radius head transverse	MC	7.00	0.54	8.25	1.06	7.47	0.67	6.71	1.26		(Unsworth and Alexander 1979)
Radius head sagittal	MC	7.90	1.22	7.69	1.20	6.69	1.60	6.46	1.08		(Lazar and Schuller-Ellis 1980)
Ulnar Cortex	MC	2.08	0.48	2.11	0.52	1.11	0.50	1.65	0.55	IM	(Lazar and Schuller-Ellis 1980)
Radial Cortex	MC	2.12	0.54	2.13	0.51	1.73	0.34	1.76	0.37	IM	(Lazar and Schuller-Ellis 1980)
Medullary Canal	MC	4.16	1.27	3.85	1.13	3.37	1.01	4.32	0.99	IM	(Lazar and Schuller-Ellis 1980)
Thickness frontal	MC	8.36		8.09		6.21		7.73		IM	(Lazar and Schuller-Ellis 1980)
Volar Cortex	MC	2.49	0.62	2.53	0.53	1.90	0.49	1.60	0.39	IM	(Lazar and Schuller-Ellis 1980)
Dorsal Cortex	MC	2.09	0.49	1.92	0.49	1.77	0.52	1.47	0.43	IM	(Lazar and Schuller-Ellis 1980)
Medullary Canal	MC	4.79	1.04	5.04	1.10	4.26	0.94	4.15	1.09	IM	(Lazar and Schuller-Ellis 1980)
Thickness sagittal	MC	9.37		9.49		7.93		7.22		IM	(Lazar and Schuller-Ellis 1980)
Metacarpal Length	MC	69.22	4.25	67.27	3.42	57.70	3.03	53.86	2.93	EM	(Lazar and Schuller-Ellis 1980)
Thickness frontal midshaft	MC	8.34	0.34	8.42	1.04	6.70	0.53	7.60	0.64		(Lazar and Schuller-Ellis 1980)
Thickness sagittal midshaft	MC	9.28	0.83	9.48	1.21	7.80	0.59	7.13	0.81		(Lazar and Schuller-Ellis 1980)
Metacarpal length	MC	69.06	3.6	68.8	4.8	57.6	4.3	54.9	3.4		(Unsworth and Alexander 1979)
Width of head	MC	17.27	1.71	16.80	1.63	14.50	1.35	14.38	2.55		(Unsworth and Alexander 1979)
Phalange length	PP	43.2	2.0	47.0	3.0	43.7	2.3	35.0	1.8		(Unsworth and Alexander 1979)
Phalange length	PP	41.65	2.24	45.98	2.45	43.40	2.22	34.35	2.17	EM	(Schuller-Ellis and Lazar 1984)
Proximal metaphysic	PP	9.01	1.75	8.76	2.49	8.40	2.03	7.49	1.29	IM	(Schuller-Ellis and Lazar 1984)
Medullary canal	PP	24.10	3.25	27.83	3.34	26.96	4.24	20.55	3.03	IM	(Schuller-Ellis and Lazar 1984)
Distal Metaphysis	PP	7.31	1.68	8.09	1.17	7.14	1.04	5.69	1.00	IM	(Schuller-Ellis and Lazar 1984)
Phalange length	PP	40.42		44.68		42.50		33.73		IM	(Schuller-Ellis and Lazar 1984)
Radius socket sagittal	PP	6.18	1.06	6.65	0.95	6.01	0.65	5.49	0.81		(Schuller-Ellis and Lazar 1984)
R socket sagittal	PP	8.59	0.96	8.70	1.13	7.93	0.93	7.60	1.01		(Schuller-Ellis and Lazar 1984)
Phalange thickness at midshaft frontal	PP	10.12	1.06	10.40	0.83	9.77	0.73	8.93	0.88	EM	(Schuller-Ellis and Lazar 1984)
Phalange thickness at midshaft sagittal	PP	6.91	0.59	7.58	0.60	6.91	0.36	6.17	0.68	EM	(Schuller-Ellis and Lazar 1984)
Ulnar cortex	PP	1.82	0.58	2.16	0.44	2.04	0.45	2.04	0.74	IM	(Schuller-Ellis and Lazar 1984)
Radial Cortex	PP	2.08	0.55	1.96	0.67	1.88	0.57	1.98	0.57	IM	(Schuller-Ellis and Lazar 1984)
Medullary canal width	PP	6.86	1.42	6.62	1.27	5.96	0.92	5.20	1.24	IM	(Schuller-Ellis and Lazar 1984)
Thickness at midshaft frontal	PP	10.76		10.74		9.88		9.22		IM	(Schuller-Ellis and Lazar 1984)
Volar cortex	PP	1.40	0.26	1.53	0.30	1.34	0.33	1.13	0.27	IM	(Schuller-Ellis and Lazar 1984)
Dorsal cortex	PP	1.85	0.39	1.84	0.39	1.78	0.46	1.54	0.49	IM	(Schuller-Ellis and Lazar 1984)
Medullary canal width	PP	3.74	0.84	4.23	0.91	3.80	0.74	3.43	0.64	IM	(Schuller-Ellis and Lazar 1984)
Thickness phalange at midshaft sagittal	PP	6.99		7.60		6.92		6.10		IM	(Schuller-Ellis and Lazar 1984)
Length of phalange	PP	40.0	1.5	43.3	1.8	40.8	0.9	32.3	1.1	EM	(McArthur <i>et al.</i> 1998)
Width of medullary canal at midpoint (sagittal)	PP	6.3	1.0	7.3	1.0	6.9	1.0	6.9	1.0	IM	(McArthur <i>et al.</i> 1998)
Width of medullary canal at midpoint (Transverse)	PP	4.2	0.8	4.3	0.5	4.4	0.5	3.6	0.5	IM	(McArthur <i>et al.</i> 1998)

## **4.13 Patient considerations**

### ***4.13.1 Pain relief, improved cosmetic appearance and function***

Pain relief is achieved by replacing the two bone ends and, therefore, preventing bone-on-bone contact. The available metacarpophalangeal joint designs relieve the pain adequately (Linscheid 2000). The high patient satisfaction observed with Swanson implants is based mainly on the relief of pain after arthroplasty (Fleming and Hay 1984; Goldfarb and Stern 2003). The cosmetic appearance is vital as the hand is used for communication and any deformity has a psychological impact on the individual apart from the physical disability that any malformation contributes in the normal hand function. The release of the tendons and muscles that form the deformation is a necessary procedure during the operation. Any deformities in adjacent joints, such as the wrist or proximal joints of the finger have to be addressed prior to any intervention in the metacarpophalangeal joint. The end result of the implant arthroplasty is a more extended arc of motion that may help the individual to act more functional than before. Also the correction of the deformities is vital for the cosmetic appearance of the hand and also pain relief is vital for the normal function of the hand.

### ***4.13.2 Simplicity of surgical procedure and surgical tooling***

The simplicity of the surgical procedure is very important as the number of instruments necessary to perform the insertion procedure, especially when several prostheses are implanted simultaneously, determine the time of the surgery in total. The number of available sizes of implant will also govern the number of required instruments. The complexity of the design will also affect the number of instruments that will be needed for implantation of the prosthesis. The number of instruments should be small to eliminate the cost and the complexity of the surgical procedure. Trial implants should also be available to

demonstrate the best size for a specific patient. The trial implants are placed according to the recommended procedure as the normal ones and are used to check the range of motion and stability (Murray 2007).

### **4.14 Revision arthroplasty**

The revision surgery should be taken into account as the previous experience of metacarpophalangeal joint design have a high ratio of revision arthroplasty due to implant breakage or an additional operation to correct recurrence of deformities. So the time and simplicity of the revision operation is important and also the simplicity of replacement of the implant is also important. After the removal of the previous implant, available bone stock should be enough to support the new implant.

### **4.15 Manufacturing considerations**

The manufacturing procedure is vital for the success of the implant. A difficult and costly manufacturing process will probably deteriorate the success of the prosthesis design. In the complexity of the design and the impact that it has on the manufacturing process, the effect that a complex design will have on the operating time and the complexity during any revision arthroplasty has to be added.

### **4.16 Summary**

In summary the new metacarpophalangeal joint replacement should be able to provide flexion up to 70 degrees, extension up to 5 degrees, radial and ulnar deviation arc of motion up to 40 degrees, free rotation or at least 10-15 degrees and to be able to sustain a force up to 256 N. To be accommodated to the dimensions of the space remaining with minimal bone removal and maximal reservation of tendons, ligaments and surrounding structures.

## Chapter 4

According to Table 4-1 the metacarpal part of the prostheses for minimal resection of the medullary cavities should be from 24 to 44 mm in length for the proximal part 16 to 28 mm in length (Lazar and Schulter-Ellis 1980; Schulter-Ellis and Lazar 1984). It should also provide alignment of the joint and pain relief to the patient. Bone cement should not be used for fixation as has been described earlier. The design should be able to reduce the stress of the bearing surfaces and enhance the lubrication of the contact surface.

## Chapter 5

### Concept design of the new metacarpophalangeal joint replacement

#### 5.1 Introduction

The concept design stage involved brainstorming to consider all the possible designs that meet the product design specification presented in the previous chapter. The initial sketches and a brief description of the various concept designs are presented. The process of selecting one of the concepts to develop will then be described.

#### 5.2 The concept designs

##### 5.2.1 Design 1 – (Three piece elastomer and surface replacement design)

Concept design 1 (Fig 5-1) is a three-part assembly that involves a one-piece elastomer part and two other hard surface (metal or polyethylene) parts.

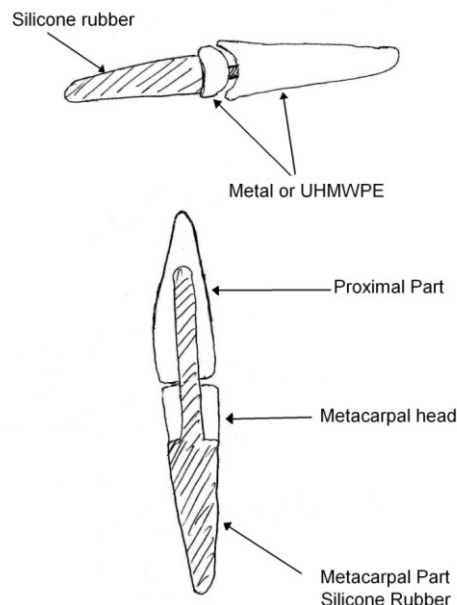


**Fig 5-1.** Concept design 1

The metacarpal part is a ball shaped part through which the elastomer part passes. The proximal phalange is a socket shaped part with a stem attached for intramedullary insertion. The one-piece elastomer part also passes through the socket hole and stem. The metacarpal part of the elastomer acts as the cushion material for the metacarpal ball component and also transmits the forces inside the medullary cavity. The proximal part of the elastomer actually pistons freely inside the hollow of the proximal metal or polyethylene part that encapsulates it. This design is believed to support the implant during grasp actions where high forces are experienced.

### **5.2.2 Design 2 – (Four piece elastomer and surface replacement design)**

Design 2 (Fig 5-2) is very close to the design 1 philosophy but it consists of four parts. The extra middle part provides 30 degrees flexion to the design to match the natural resting position of the metacarpophalangeal joint. It also consists of a one-piece elastomer that pistons freely through the middle part and the hollow of the proximal component. The metacarpal part sits firmly on the elastomer part that acts as the backing material.

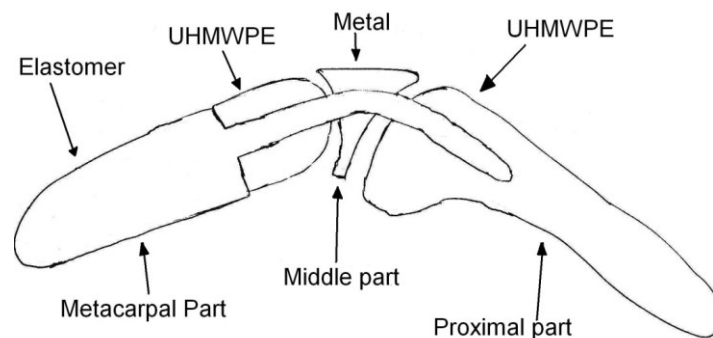


**Fig 5-2.** Concept design 2

### **5.2.3 Design 3 – (Two balls and double socket middle part design)**

This concept design (Fig 5-3) is a four-part model assembly that has two balls, one middle part with two sockets and an elastomer part. The elastomer part pistons freely inside the

stems and passes through the middle part and acts as an internal ligament. The two balls and the middle parts are aligned. The elastomer part will provide the internal stability that is necessary to the deteriorated metacarpophalangeal joint.

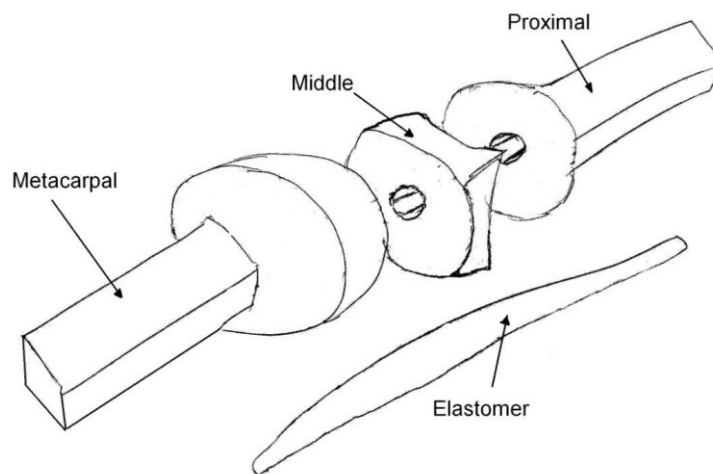


**Fig 5-3.** Concept design 3

***5.2.4 Design 4 – (Two balls and double socket middle part preflex design with internal elastomer part)***

Design 4 (Fig 5-4) is a four-part model that follows the design concept of design 3 but it has the middle part with 30 degrees angle of flexion so that the proximal and metacarpal balls have 30 degrees between them to match the resting position of the natural finger. The final range of motion of the design is the sum of the angle between the metacarpal and middle part and the proximal phalange component and the middle part, plus the initial 30 degrees flexion. With this concept design to achieve 60 degrees of flexion requires only 30 degrees of flexion. So 30 degrees of flexion of elastomer + 30 degrees preflexion = 60 degrees of flexion of the final assembly. It is supposed to provide constrain at pinch and grasp actions with the double ball and socket configuration and also the elastomer part to provide internal stability that will act as an internal ligament and will provide a highly constrained design.

During flexion/extension and ulnar/radial deviation the silicone will provide the internal stability that is needed for rheumatoid patients. It is believed that this design can be used for patients with both rheumatoid arthritis and osteoarthritis. The elastomer part will be protected as it is enclosed within stems, rather than interacting with the bone, as in the case with the Swanson design.

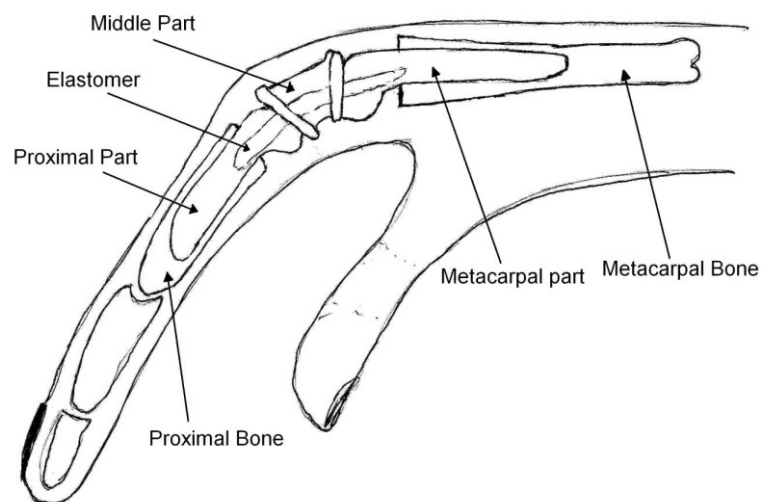


**Fig 5-4.** Concept design 4

### ***5.2.5 Design 5 – (Two socket stems and elastomer ball design)***

Concept design 5 (Fig 5-5) is a three-part assembly that consists of an elastomer sphere with two stems inserted into the other two cup-shaped stems. The concept is the encapsulation of the elastomer spacer inside a harder material such as a metal or polyethylene, which will protect it from wear and crack initiation. The two elastomer stems are at 30 degrees to each other to provide the natural resting position of the normal metacarpophalangeal joint. The elastomer sphere will act as the backing material during the high axial forces that the implant experiences in the metacarpophalangeal joint during many daily activities. Also the low elastic modulus of the elastomer and its property to deform when compressed will reduce the contact stresses that will be applied axially during daily activities.

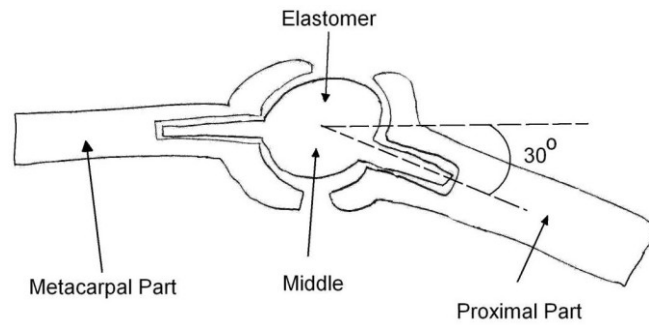


**Fig 5-5.** Concept design 5

### **5.2.6 Design 6 – (Volar plate approach design)**

Design 6 (Fig 5-6) is a three-part assembly and follows the concept of intrinsic stability that is provided by the volar plate. The elastomer part acts as an internal volar plate. There is a concern about the placement of the centre of rotation and the ability of the pistoning effect due to its complex pathway inside the polyethylene stems. Also, rotation of the ball and socket configuration may be a problem due to the fact that the elastomer part does not pass centrally inside the polyethylene parts but passes more volarly.

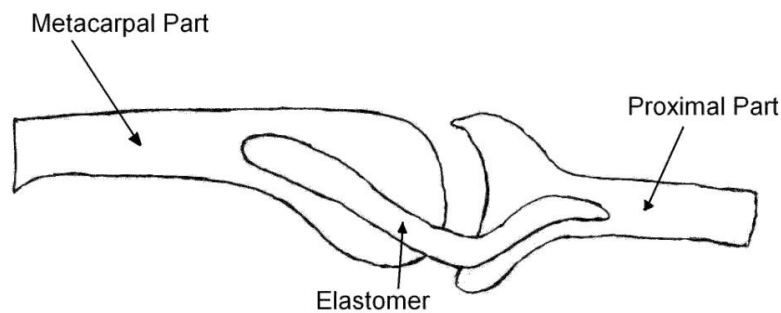


**Fig 5-6.** Concept design 6

### **5.2.7 Design 7 – (Four stem elastomer design)**

This design is a three-part assembly. The spherical elastomer part has four stems instead of two in design 5. Figure 5-7 shows the transverse section of the design and the offset placement of the stems according to the central axis of the design. It is believed that it will provide a more constrained movement in ulnar and radial deviation and a more secure

flexion-extension movement. There is a concern for the high shear stresses that will be experienced in the four elastomer stems.

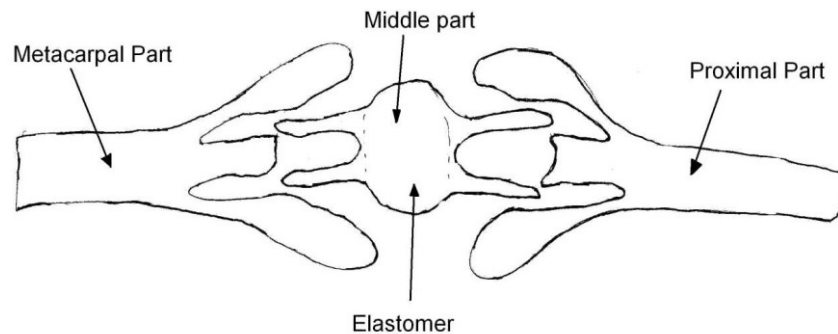


**Fig 5-7.** Concept design 7

**5.2.8 Design 8 – (Five part – two elastomer part design)**

This design (Fig 5-8) is a five- part assembly that incorporates features from designs 3 and 7 to give more intrinsic stability. It is more complex than the other designs and that makes it very complicated for manufacturing and assembly during the surgical operation. Also, there is a problem with the rotation of the two balls in relation with the middle part.

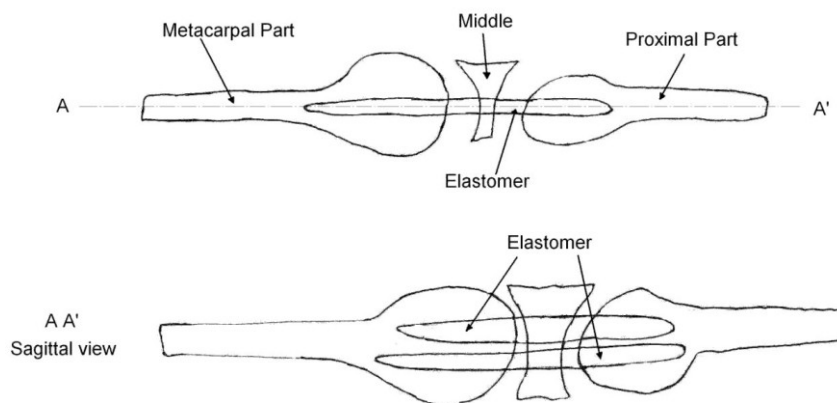


**Fig 5-8.** Concept design 8

**5.2.9 Design 9 – (Two sockets and middle ball design)**

Design 9 (Fig 5-9) is a four-part assembly that involves a spherical middle part and two cups attached to the stems. The three previous parts should be made by hard materials like

metal or polyethylene and there is also an elastomer part that passes through the middle ball and the two cups to provide the intrinsic stability to the whole design.

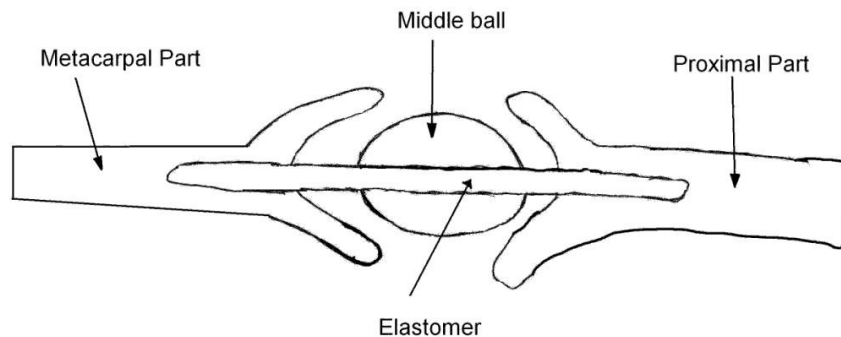


**Fig 5-9.** Concept design 9

### ***5.2.10 Design 10 – (One piece elastomer design)***

Design 10 (Fig 5-10) is a one piece design that follows the past concept of a one piece silicone design like the Swanson, Sutter and Neuflex (Linscheid 2000). This actually acts as a spacer instead of an artificial joint and the placement of the centre of rotation as well as a more preflex design to match the resting position of the natural joint will help to protect the elastomer material from overstretching and will probably make it last for longer. There is concern about the wear of the elastomer against the bone and the pistoning effect inside the medullary cavities. Also there is a concern if the elastomer by itself has the ability to withstand the ulnar deviated shear stresses of the rheumatoid metacarpophalangeal joint that are present after implantation and also if the material can transmit the higher forces experienced with osteoarthritic patients that are younger, stronger and more demanding than the rheumatoid patients.

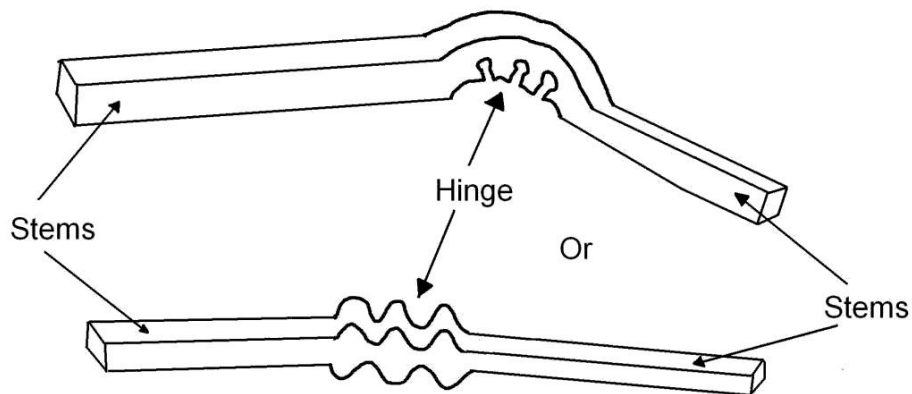


**Fig 5-10.** Concept design 10

**5.2.11 Design 11 – (Surface replacement ball and socket design)**

This two- part assembly (Fig 5-11) follows the concept of surface replacement of the joint that has been used successfully in the hip and knee joint replacements. This is the most accurate representation of the natural anatomy of the metacarpophalangeal joint. It is a ball and socket articulation with the metacarpal as the ball and the proximal phalange as the socket.

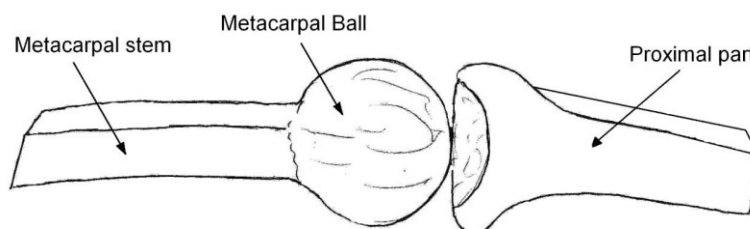


**Fig 5-11.** Concept design 11

**5.2.12 Design 12 – (Surface replacement socket and ball design – reversed design)**

This design (Fig 5-12) follows on from design concept 11 of the surface replacement but the ball and socket configuration is here reversed and the socket is in the metacarpal part and the ball in the proximal phalange part. Studying other ball and sockets joints of the body like the hip and wrist we see that the moving parts of the joint have the ball while the stable parts

have the socket. The moving part of the metacarpophalangeal joint is the proximal phalange as the proximal phalange slides on the metacarpal head, so the ball is placed in this part according to this concept idea. There are concerns, as with design 11, about the wear debris and the use of this design in rheumatoid patients.

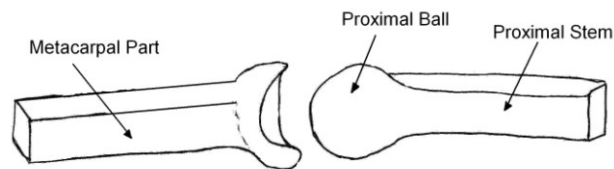


**Fig 5-12.** Concept design 12

### **5.2.13 Design 13 – (Three piece elastomer hinge design)**

Design 13 (Fig 5-13) is a three part assembly that involves an elastomer middle part with two stems that are inserted in two hollow-shaped metal or polyethylene parts that are inserted in the medullary cavities of the metacarpal and proximal phalange. The elastomer will actually piston inside the metal or polyethylene parts instead of the impingement and pistoning on the sharp bone ends.

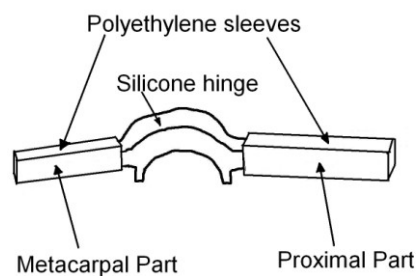


**Fig 5-13.** Concept design 13

## **5.13 Evaluation of the concept designs**

A total of 13 different concept designs have been presented above but only one can proceed to the detailed design process. The evaluation of these designs has been undertaken using the ‘six thinking hats’ method developed by Edward de Bono (Bono 1999). The six thinking

## Chapter 5

hats method is a way of brainstorming, but a structured approach for problem solving and has been proposed as a method for the medical device design process (Aichinson *et al.* 2009; Cowan *et al.* 2006; King and Fries 2003). The six hats are namely white, red, black, green, blue and yellow and each hat represents a different thought process. The white hat focuses on the facts and data available. The red hat looks into the problem with intuition and gut feelings. The black hat concentrates on the bad points of the decision, that may not work properly or what will be the potential problems of this decision. The yellow hat concentrates on the positive aspects of your decision and what are the consequences if everything goes well. The green hat is the way to provide creative solutions to the problems; what needs to be done, what needs to be modified. Finally the blue hat is the directional hat that has to be used by the leader of the meeting for decision making or directions of the conversation. The hat is not listed in Table 5.1 as this hat is used to decide the order that the other hats should be used (Bono 1999; King and Fries 2003).

In Table 5-1 the six thinking hats method results are shown and in Table 5-2 a scoring system is used to score every design concept according to 15 criteria of evaluation that have been derived from the design criteria described in Chapter 4. The scoring system was from a scale of 1 to 10. The higher the score on its criteria corresponds to the higher satisfaction of this criteria to the design. The fifteen criteria for scoring involved manufacturing, biomechanical and surgical points of interest. As the aim of this procedure was to compare the different designs, the design criteria (Chapter 4) were used, so there was no weighting on its criteria. Figure 4-1 describes the interrelation between the criteria for the new implant and the different point of view that this design involves in the design process. The scoring method presented here is another tool in the evaluation process.

**Table 5-1.** Table according to six thinking hats method

<b>Alternatives/data available</b>	<b>Likes/good points</b>	<b>Concerns/bad points</b>	<b>Modifications to overcome concerns</b>	<b>Gut feeling/reactions</b>
<i>White hat</i>	<i>Yellow Hat</i>	<i>Black Hat</i>	<i>Green Hat</i>	<i>Red hat</i>
<b><u>Design 1</u></b> <b>(3 piece elastomer and surface replacement design)</b>	Low elastic modulus of metacarpal part, free pistoning of the elastomer inside the proximal part	Concerns about wear of elastomer on bone-polyethylene interface	High endurance elastomer	High stress in the elastomer
<b><u>Design 2</u></b> <b>(4 piece elastomer and surface replacement design)</b>	Advantage of the preflexion, elastomer as backing material to distribute the axial forces	Same as above	Close elastic modulus of elastomer and polyethylene to reduce the stresses at their interface	Same as above
<b><u>Design 3</u></b> <b>(2 balls and double socket middle part design)</b>	Encapsulation of elastomer with protection from the initiation of cracks on its surface	High concerns for stress concentration in the elastomer during flexion, wear of the elastomer from the stems	Free pistoning of the elastomer inside the two stems	Advantage of the elastomer as an internal ligament
<b><u>Design 4</u></b> <b>(2 balls and double socket middle part preflexed design with internal elastomer part)</b>	Encapsulation possible, protection from crack initiation, preflexion advantage of the stress distribution in elastomer during flexion	Wear of elastomer by the stems, high shear stress applied to elastomer	Wear resistant elastomer material	Elastomer acts as an internal ligament, ball and socket configuration provide high constrained design and support during high loads
<b><u>Design 5</u></b> <b>(2 socket stems and elastomer ball design)</b>	The elastomer ball with the two stems will act as a backing material so it will deform during high forces	Possible wear of the elastomer – polyethylene interface	Wear resistant elastomer material	There is a preflexion that will reduce the stress in the elastomer at flexion-extension movement
<b><u>Design 6</u></b> <b>(volar plate approach design)</b>	The elastomer will act as an internal volar plate to prevent the hyperextension of the proximal part towards the metacarpal part similar to the volar plate in the normal joint	Problematic placement of the centre of rotation and non conformed surface interface of the polyethylene bearing surfaces	Alteration of hole diameters to give a more flexible design to overcome the inconformity of the surfaces	Simple design with anatomical restrictions
<b><u>Design 7</u></b> <b>(four stem elastomer design)</b>	This design provides a higher internal stability in movement with a more constrained movement at	Too bulky design with complex interrelation of the surfaces and the parts involved, difficult to	Simpler design to make it easier in manufacture	Distribution of the stresses internally but very complex in manufacture and assembly during surgery

Chapter 5

	ulnar and radial deviation in comparison with the flexion-extension movement	manufacture		
<b><i>Design 8</i></b> <b>(5 part – 2 elastomer part design)</b>	Very constrained design for high deformities	Very complex design with many parts and difficult to manufacture, long operation time length	Less restrictions by the design	Very restricted movement in flexion- extension with good surrounding tissue condition requirement
<b><i>Design 9</i></b> <b>(2 sockets and middle ball design)</b>	Constrained design with internal elastomer ligament	High stress in the elastomer part and concern about the wear in the ball and socket interface	Change of design to reduce the high forces in the elastomer part	Concerns for dimensioning due to the ball and socket configuration
<b><i>Design 10</i></b> <b>(one piece elastomer design)</b>	Simple and cheap to manufacture	Possibly unable to sustain the shear forces that are experienced in rheumatoid patients, concern of wear of elastomer by the bone and in case of silicone rubber possible silicone synovitis	Wear resistant elastomer material, possible design alterations to reduce the stress of the shear forces on elastomer	Very simple design and in previous implant designs have been proven inadequate to sustain the shear forces but has given high patient satisfaction and cosmetic improvement (eg. Swanson, Neuflex)
<b><i>Design 11</i></b> <b>(surface replacement ball and socket design)</b>	The closest design to the normal metacarpophalangeal joint anatomy	Relies on good condition of the joint with minor deformities, concern about wear due to surface contact	More constrained design	Adequate for osteoarthritic patients but inadequate for rheumatoid arthritic patients with major deformities and in balance in tendons and surrounding tissues
<b><i>Design 12</i></b> <b>(surface replacement socket and ball design reversed design)</b>	Possibly more constrained than design 11 to provide stability due to shear stresses	Same as above	Soft tissue reconstruction to provide adequate stability	Adequate only for osteoarthritic patients and patients with minor deformities and good condition of the surrounding tissues and tendons
<b><i>Design 13</i></b> <b>(3 piece elastomer hinge design)</b>	Protection of the crack initiation of the elastomer surfaces due to encapsulation of the elastomer stems	Possible wear of elastomer due to pistoning effect and impingement of the elastomer on the polyethylene stems	Wear resistant elastomer	Possible protection of the elastomer stems but again unable to support the high axial and shear forces that are carried out by the elastomer itself

**Table 5-2.** Concept design criteria scoring table

<b>Concept design</b>	<b>1</b>	<b>2</b>	<b>3</b>	<b>4</b>	<b>5</b>	<b>6</b>	<b>7</b>	<b>8</b>	<b>9</b>	<b>10</b>	<b>11</b>	<b>12</b>	<b>13</b>
<b>Criteria</b>													
Ease of implantation	7	6	6	7	6	5	6	5	6	8	7	7	6
Protection of silicone synovitis	5	5	6	6	6	5	5	5	6	3	0	0	4
Protection against osteolysis	6	6	7	7	6	6	6	6	6	6	6	6	6
Ease of manufacturing	6	5	6	6	5	4	4	4	5	7	7	7	6
Size accommodation	5	5	5	5	5	5	5	5	5	6	6	6	6
Range of motion	6	7	6	8	6	5	5	5	6	7	7	7	6
Revision operation simplicity	5	5	5	5	5	5	5	5	5	6	6	6	5
Amount of bone removal	7	7	7	7	7	7	7	7	7	8	7	7	7
Sustain applied forces	6	7	7	8	5	5	5	6	6	5	6	6	6
Suitable for RA patients	7	8	7	8	7	6	6	6	7	6	4	4	6
Suitable for OA patients	6	7	7	7	6	5	5	5	5	4	8	8	5
Centre of rotation placement	6	5	5	6	6	5	5	5	5	6	8	8	6
Operation time length	5	5	5	5	5	5	5	4	5	6	6	6	5
Allow soft tissue reconstruction	7	7	7	7	6	6	6	6	6	8	7	7	7
Constrained design	6	6	7	7	6	6	5	6	6	6	5	5	6
<b>Total (Max :150)</b>	<b>84</b>	<b>86</b>	<b>88</b>	<b>93</b>	<b>81</b>	<b>75</b>	<b>75</b>	<b>75</b>	<b>81</b>	<b>86</b>	<b>82</b>	<b>82</b>	<b>88</b>

The criteria presented in Table 5-2 include biomechanical, manufacture and surgical points of interest. The ease of implantation, allowance of soft tissue reconstruction, operation time, amount of bone removal and revision operation simplicity refer to surgical points of interest especially for the implantation procedure and consideration regarding the revision surgery something quite common for MCP joint arthroplasties. The criteria ease of manufacturing and size accommodation refer to manufacturing challenges of the concept designs. The biomechanically related criteria refer to wear resistance issues such as protection against silicone synovitis and osteolysis. Strength of the design is another biomechanical issue such as sustaining the applied forces, suitability for Rheumatoid arthritic (RA) patients, suitability for osteoarthritic (OA) patients and finally functionality of the design such as the range of motion, centre of rotation placement and how constrained the design should be.

According to Table 5-2 concept design 4 appears the highest score among the different concept designs. The selection of the concept that will be used in the detailed design process

is a complicated process. Generally a group of people, including engineers, surgeons, sales and marketing people, from different backgrounds get involved in this procedure and the selection apart from the objective criteria involves subjective criteria and feelings in their decision. In the process of this new metacarpophalangeal joint replacement the scoring and all the decisions have been made by the author with the help of Dr Duncan Shepherd.

It can be seen that design 10 that represents the one piece silicone implants concept scored third highest score, although it has been characterized as the gold standard. That happens as the one piece silicone criteria, such as high patient satisfaction, pain relief and ease of implantation, surgeon acceptability and probable cost of manufacture scored high. However, if it is looked at biomechanically, for longevity and wear of the materials the score is not so high.

In Fig 5-4 we have seen the drawing of the concept design and in the following Fig 5-14 the 3D design drawing of the design is presented before going to the detailed design of the concept regarding sizing, material selection and evaluation of it.

Design 4 is based on the proposed design for a novel wrist arthroplasty (Pylios and Shepherd 2007; Shepherd and Johnstone 2005).

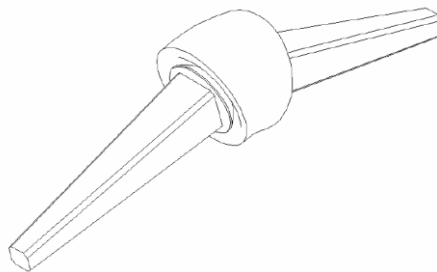


**Fig 5-14.** 3D design of concept selection 4.

## **Chapter 6**

### **Risk analysis**

#### **6.1 Introduction**

Every medical device prior to approval with CE marking needs to have completed the risk analysis procedure. It is a legal procedure that it is also a very useful process to evaluate your design during the development stages. The Medical Device Directive (MDD) and EN ISO 14971 are now well established and are used by medical device manufacturers as a yardstick for the minimum standard of quality required (EN14971; MDD). During manufacture faults can occur. It is understood that some manufacturing faults are inevitable, but they must be detected and eliminated in products which affect the health and welfare of patients. Some faults are considered critical and life threatening. These faults are described by the MDD as risks. A risk is the probability of a hazard causing harm to a patient or healthcare worker.

In the MDD and ISO EN 14971 there are no indications regarding the acceptance of any risk and the acceptance of a level of risk is a decision made by the manufacturer after consultation with the regulatory bodies and the medical profession. All assessments (and recommendations to proceed) should be made after weighing the benefits gained by the patient against the overall effect of the risk occurring. These assessments should be recorded and retained in case of any possible legal action resulting. Risk analysis is a rolling requirement for any product at any stage in its evolution, and should be updated regularly depending on the information gained during development.

## 6.2 Undertaking risk analysis

Once the characteristics of the medical device have been defined, it is necessary to identify all the possible hazards associated with the device such as energy hazards (mechanical force, moving parts), biological hazards (bio-incompatibility, toxicity), hazards related to the use of the device (inadequate labelling, packaging or instructions for use). Risks are taken in order to achieve something; a risk is not taken without some benefit. It is important to balance risk against benefit. If the risk is above an acceptable level, ways must be identified to reduce the risk to acceptable levels. This may include redesigning part of the device, improving the packaging, making labelling or instructions for use clearer.

Brain storming with all the people involved in the development of a medical device should enable all the potential hazards to be identified. A report on the risk analysis is produced so that a decision can be made as to whether the remaining risks associated with the device are acceptable and outweighed by the benefits to the patient. The risk analysis results will be placed into the technical file of the device. A risk analysis is not just a one-off process and it is important to review the risk analysis at regular interval during development process.

For each potential hazard associated with a medical device, there is a frequency of occurrence,  $O$ , a severity of failure,  $S$ , and an ability to detect the failure,  $D$ . Each of these elements was scored on a scale of 1 to 10, as shown in table 6-1, for the hazards identified for the novel metacarpophalangeal joint replacement. The identification of probability and risk of each hazard can be done by either using a bottom-up Failure Mode and Effect Analysis (FMEA) or a top-down Fault Tree Analysis (FTA) (Hill 1998; Viceconti *et al.* 2009).

**Table 6-1.** Rating of occurrence, severity and detection for potential hazards

<b>Rating</b>	<b>Occurrence, O</b>	<b>Severity, S</b>	<b>Detection, D</b>
1	<1 in 10 <sup>6</sup>	No harm	Always seen
2			
3		Unnoticed by customer	
4			
5	1%	Customer notices	Easily spotted
6			
7		Customer complains	
8			
9			
10	>50%	Product will not function at all	No detection

### **6.3 Risk analysis of the novel metacarpophalangeal joint replacement**

The risk analysis should be considered for its individual part of the assembly as well as the implant as a whole. Packaging and labelling are important, but are not being considered during this study, as we are only concerned with the design. The risk analysis presented for a radio-carpal joint replacement will be used as the guide for our analysis (Shepherd 2002). As has been already mentioned, risk analysis is not a one-off procedure, but here only the final risk analysis will be presented. The results are presented in Table 6-2 below.

#### **6.3.1. Design description and characteristics**

The characteristics of the new metacarpophalangeal implant design are:

- I. It is intended for long term implantation for replacement of the diseased metacarpophalangeal joint. It is intended to relieve pain, realign and improve functionality of the joint.
- II. It is intended to be used by surgeons familiar with finger joint replacements.
- III. The selected concept design, is a modular design which consists of two polyethylene stems inserted into the metacarpal and proximal phalange bones respectively, two

metal balls attached to the stems, an elastomer middle part and an elastomer that acts as an internal ligament and which fits inside the corresponding cavities of the two stems and the holes of the balls and middle part to provide alignment of the whole design.

### **6.3.2 Identification of hazards and estimation of risks**

The identification of the potential hazards has been carried out by the writer of this thesis and the Failure Mode and Effect Analysis (FMEA) has been used for the estimations of the risk of any potential hazard. The results of this procedure are presented in Table 6-2 below. The estimation of the risks was made based on the risk priority number *RPN*. The scoring of the potential risk is based on the decision and identification of the writer; different writers and/or larger decision bodies could score differently the potential hazards. As can be seen in Table 6-2 the critical part of the design is the elastomer part and the wear performance of the implant that have been scored an *RPN* 300 and 240 respectively. For that reason in Chapters 8, 9 and 10 that follow the lubrication analysis and contact stress analysis of the implant is presented. Wear test performance of possible material combinations is also investigated so to find out ways to reduce the risks of the possible hazards presented in this risk analysis. The final design is presented in Chapter 11.

**Table 6-2.** Results of risk analysis.

Item	Function	Possible hazard or failure mode	Effect of hazard or failure	Causes of hazard or failure	O	S	D	RPN	Action to reduce or eliminate risk	
<b>Elastomer part</b>	Provides alignment of the implant and acts as internal ligament for the joint replacement	<i>Breaks</i>	Lost of alignment	High shear stresses	10	6	5	300	Suitable material & design	
			>>	Fatigue failure	10	6	5	300	>>	
<b>Middle part</b>	Acts as backing material and provides the cups for the metacarpal and proximal phalange balls	<i>Wear</i>	Silicone synovitis	Piston effect	6	6	3	108	>>	
			Wear debris reaction	Mixed or boundary lubrication between the metacarpal and proximal phalange balls and the middle part interface	6	8	5	240	Material properties & design	
			>>	Piston effect of the elastomer part	3	5	4	60	>>	
<b>Metacarpal head</b>	Provides the articulating surface for the metacarpal bone	<i>Breaks</i>	Device non functional	High forces	1	8	8	64	Design requirements	
			<i>Wear</i>	Osteolysis	Inadequate lubrication	1	8	8	64	>>
<b>Metacarpal stem</b>	Interface of implant bone and attached to me metacarpal ball	<i>Breaks</i>	Device non functional	High forces	2	8	8	128	Design requirements & material	
			>>	Bending moments	2	8	8	128	>>	
			>>	Stem and ball interface failure	1	5	4	20	>>	
			<i>Wear</i>	Osteolysis	Sliding motion in the metacarpal bone	3	7	7	147	>>
			>>	Sliding of the Metacarpal ball towards the stem	1	5	4	20	>>	
<b>Proximal head</b>	Acts as the articulating surface for the proximal phalange	<i>Breaks</i>	Device non functional	High forces	1	8	8	64	>>	
			<i>Wear</i>	Osteolysis	High asperities contact	1	8	8	64	>>
			<b>Proximal stem</b>	<i>Breaks</i>	Device non functional	High forces	2	8	8	128
>>	Bending moments	2			8	8	128	>>		
<b>Implant</b>	Provide adequate stability and functionality in the metacarpophalangeal joint diseased by RA and OA	<i>Breaks</i>	Device non functional	Design problem	5	10	6	300	Reevaluate the design requirements	
			>>	Stem and ball interface failure	1	5	4	20	>>	
			<i>Wear</i>	Osteolysis	Sliding motion in the proximal phalange bone	3	7	7	147	>>
			>>	Sliding of the proximal phalange ball towards the stem	1	5	4	20	>>	
			>>	Piston effect of the elastomer part inside the shaft of the stem	2	8	8	128	>>	
		<i>Inadequate performance</i>	Device non functional	Design problem	3	10	5	150	Reevaluate the design process	

## Chapter 7

### Lubrication analysis of metacarpophalangeal joint replacement

#### 7.1. Introduction

In this chapter a lubrication analysis of the new metacarpophalangeal joint replacement concept will be presented that will help with the decision on some of the design aspects of the design concept, namely radius of the ball, thickness of the elastomer layer and the radial clearance.

#### 7.2. Lubrication theory

The purpose of lubrication is to separate two surfaces sliding past each other with a film of lubricant, which can be sheared causing as little frictional resistance as possible. The ideal form of lubrication regime is the separation of the two opposing surfaces by a film of fluid. Fluid film lubrication (Fig 7-1a) occurs when the lubricant film is sufficiently thick to prevent the surfaces from coming into contact. This lubrication regime provides low friction and high resistance to wear. The lubricant films are normally many times thicker than the surface roughness of the bearing surfaces. Surface roughness is expressed by the arithmetic mean height of the roughness peaks and valleys,  $R_a$ , (Hamrock 1994).

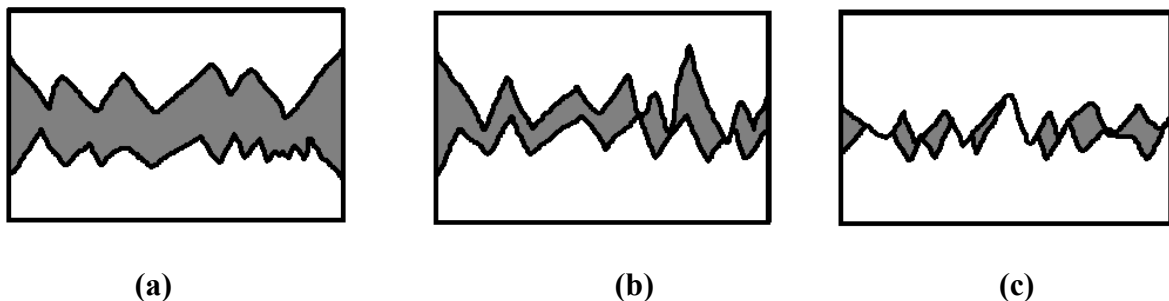


**Fig 7-1.** Lubrication regimes (a) Fluid film lubrication, (b) Mixed Lubrication, (c) Boundary lubrication

In boundary lubrication (Fig 7-1c) there is no separation between the two bearing surfaces by a fluid film, so the surfaces are in contact and there is surface interaction between mono

or multi molecular layers. That happens as the conditions are severe and the loads are high, so that the fluid film cannot be preserved (Hills 2000). The contact lubrication mechanism is governed by the physical and chemical properties of very thin surface films of molecular proportions (Hamrock 1994).

Mixed lubrication (Fig 7-1b) is the transition zone between the fluid film and boundary lubrication. The total load experienced between the two surfaces is shared between the asperity contact and the micro-fluid film lubrication associated with a number of miniature bearings formed by surface irregularities (Jin 2002). Interaction takes place between one or more molecular layers of boundary lubricating films.

In joint replacement implants it is conventional to have hard-on-hard bearing surfaces such as metal-on-polyethylene, metal-on-metal or ceramic-on-ceramic (Linscheid 2000). However, soft layered joints have been proposed for the replacement of diseased joints (Unsworth *et al.* 1987; Unsworth *et al.* 1981). A layer of low elastic modulus material has been used to replicate the function of the normal articular cartilage and enhance the lubrication regime. The reduction of the contact stresses, by increasing the contact area between the opposing surfaces, will enhance the lubrication film and separate the two surfaces from direct contact; it is believed that this will increase the life of the implant (Dowson *et al.* 1991).

Theoretical studies predict that soft layered joints benefit from micro-elastohydrodynamic lubrication which means that the surface asperities will be flattened and the reduced compound surface roughness will allow thinner lubrication films to preserve the separation of the two surfaces (Auger *et al.* 1993; Dowson *et al.* 1991). Squeeze film lubrication phenomena will further enhance the lubrication film (Auger *et al.* 1993; Dowson *et al.*

1991). Several materials have been proposed as the soft layer such as polyurethanes, hydrogels and silicone rubbers (Zheng-Qiu *et al.* 1998). There are some concerns about the soft layered joints in situations where the fluid film breaks down, such as during heavy loading or at the start up of motion, as there will be direct contact between the two surfaces. Under these conditions the friction and probably the wear will increase to unacceptable levels (Caravia *et al.* 1993). Application to joint replacements has shown that the abrupt change in stiffness between the soft layer and the rigid substrate and the relative low strength of the interface resulted in high shear stresses and de-bonding of the soft layer from the substrate (Stewart *et al.* 1998). Composite polyurethane layers with graded elastic modulus have been constructed to overcome this abrupt change in the soft layered joints (Stewart *et al.* 1997). The aim of this part of the study was to investigate the lubrication in the application of the soft layered joint concept in a novel MCP joint implant design and compare with the ‘conventional’ hard-on-hard material combinations.

## 7.3. Materials and Methods

### 7.3.1. Model

The idea of the new novel metacarpophalangeal implant design is shown in Fig 7-2. Although the initial design is quite complex to apply the lubrication analysis to, the model has been simplified so that known analytical methods can be applied to predict the minimum film thickness.

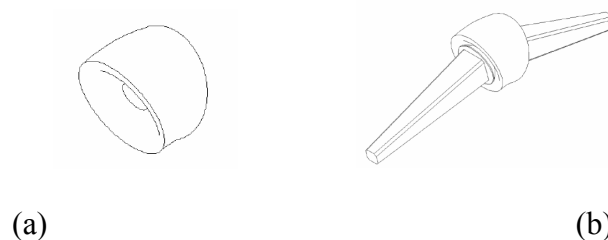


**Fig 7-2.** The design concept of the new metacarpophalangeal implant (a) middle part, (b) implant assembly

The simplified model is to use the model of two balls and the two-sided socket in the middle as illustrated in Figure 7-3. In Figure 7-3 we can see that there is symmetry in the model so a simplified configuration of the ball and socket model and then the equivalent ball-on-plane model can be used, as shown in Figure 7-4.

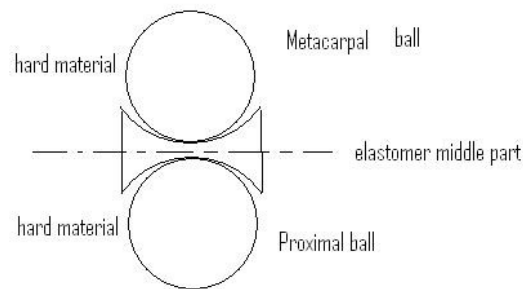


**Fig 7-3.** Model of the design in Figure 7-2

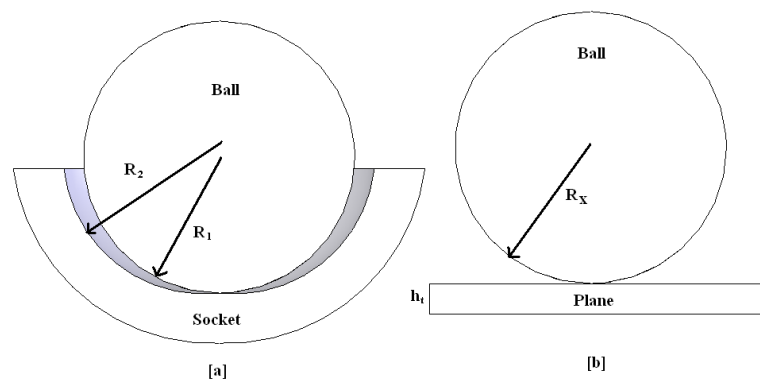


**Fig 7-4.** Simplified model (a) Ball-and-socket model for lubrication analysis, (b) equivalent ball-on-plane model for lubrication analysis

### 7.3.2 Lubrication analysis equations for soft layered joints

Analytical methods were used to calculate the minimum film thickness for different design parameters and operating conditions for the soft layered joints (Pylios and Shepherd 2008a). The metacarpophalangeal joint was modelled as a ball-and-socket joint and the equivalent ball-on-plane model shown in Figure 7-4 was used. The minimum film thickness ( $h_{min}$ ) was calculated using the Dowson & Yao formula (Dowson and Yao 1994):

## Chapter 7

$$h_{\min} = 1.59R_x \left( \frac{\eta u}{E' R_x} \right)^{0.56} \left( \frac{h_t E'}{E'' R_x} \right)^{0.36} \left( \frac{L}{E' R_x^2} \right)^{-0.20} \quad (7-1)$$

where  $\eta$  is the lubricant viscosity,  $u$  is the entraining velocity,  $h_t$  is the thickness of the soft layer,  $L$  is the applied load,  $R_x$  is the equivalent radius (calculated from Equation 7-2), and  $E'$  and  $E''$  are elastic moduli that can be calculated from Equations 7-3 and 7-4, respectively.

The equivalent radius was calculated from

$$\frac{1}{R_x} = \frac{1}{R_1} - \frac{1}{R_2} \quad (7-2)$$

where  $R_1$  and  $R_2$  are the radii of the ball and socket of the lubrication model, respectively.

Note that the radial clearance is given by:  $c = R_2 - R_1$ .

The equivalent modulus  $E'$  was calculated from:

$$E' = \left( \frac{1 - \nu_2^2}{E_{adj}} \right)^{-1} \quad (7-3)$$

where  $\nu_2$  is the Poisson's ratio of the soft layer material and  $E_{adj}$  is calculated from equation 7-5.

$E''$  was calculated from:

$$E'' = \left( \frac{(1 + \nu_2)(1 - 2\nu_2)}{(1 - \nu_2)E_{adj}} \right)^{-1} \quad (7-4)$$

where

$$E_{adj} = \frac{4LR_x h_t}{\pi \alpha^4} \left[ \frac{(1 + \nu_2)(1 - 2\nu_2)}{1 - \nu_2} \right] \quad (7-5)$$

and  $\alpha$  is the contact radius calculated from (Yao *et al.* 1994):

$$\alpha = 0.94h_t^{0.38} \left( \frac{LR_x}{E_2} \right)^{0.21} \quad (7-6)$$

It should be noted that Equation 7-1 is based on the constrained column's model that is restricted to elastomer materials with Poisson's ratio of 0.4 or less. The Poisson's ratio of the available elastomer materials on the other hand approaches 0.5. The adjusted modulus  $E_{adj}$  in Equation 7-5 was used to overcome this problem, so  $\nu_2 = 0.4$  was used throughout this study for the hard-on-elastomer material combinations (Auger *et al.* 1993).

### **7.3.3 Lubrication analysis equations for 'conventional' material combinations**

For the 'conventional' material combination, such as a metal against a polymer, the minimum film thickness was calculated according to the theory of Hamrock and Dowson (Hamrock and Dowson 1978) :

$$h_{\min} = 2.798R_x \left( \frac{\eta u}{E' R_x} \right)^{0.65} \left( \frac{L}{E' R_x^2} \right)^{-0.21} \quad (7-7)$$

where  $R_x$  is the equivalent radius,  $\eta$  is the viscosity,  $u$  is the entraining velocity,  $E'$  is the equivalent elastic modulus and  $L$  is the applied load.

The equivalent radius  $R_x$  was calculated from equation 7-2.

The equivalent elastic modulus  $E'$  was calculated from:

$$\frac{1}{E'} = 0.5 \left( \frac{1-\nu_1^2}{E_1} + \frac{1-\nu_2^2}{E_2} \right) \quad (7-8)$$

where  $E_1$ ,  $\nu_1$  and  $E_2$ ,  $\nu_2$  are the elastic modulus and Poisson's ratio of the ball and the socket, respectively. The bearing surfaces were assumed to be semi-infinite and the elastohydrodynamic theory was used for the lubrication analysis.

### 7.3.4 Parameters

The parameters that have been used in the lubrication analysis are shown in Table 7-1. The radius of the metacarpal head has been investigated in the range 4 to 10 mm, according to published data on the MCP joint and implant dimensions (Beevers and Seedhom 1999; Joyce 2007b; Unsworth and Alexander 1979).

**Table 7-1.** Values of the parameters used in the lubrication analysis

Parameter	Average value	Range
Radius of ball (mm)	7.5	4-10
Radial clearance (mm)		0.08-3.5
Viscosity (Pa s)	0.005	0.003-0.01
Entraining velocity (m/s)	0.017	0.0009-0.033
Load (N)	14	2-100
Thickness of elastomer (mm)	2	0.5-3
Elastic modulus of elastomer (MPa)		5-25

The angular velocity is translated to entraining velocity by equation 7-9 (Jagatia and Jin 2002).

$$u = \frac{\omega R_1}{2} \quad (7-9)$$

where  $\omega$  is the angular velocity and  $R_1$  is the radius of the metacarpal.

The values given in the literature for angular velocity are 12.5 ( $\pm 26.25$ ) degrees/s for normal and 10.5 ( $\pm 20.38$ ) degrees/sec for diseased and 14 ( $\pm 29.41$ ) degrees/s for normal and 9.9 ( $\pm 17.98$ ) degrees/s for diseased of the middle and index MCP joint, respectively (Fowler and Nicol 2001b). The result was that the rheumatoid arthritic patients appear to have

slower and smaller movements. The angular velocity for the metacarpophalangeal joint for a rapid pinch action has been measured to be  $509 \pm 84$  degrees/s (Cole and Abbs 1986). The angular velocity has been calculated from 14 degrees/s to 509 degrees/s and for 7.5 mm radius of metacarpal head the entraining velocity is 0.0009 m/s to 0.033 m/s. The average entraining velocity that has been used is 0.017 m/s, while a range from 0.0009 m/s to 0.033 m/s have also been considered as the range of angular velocity of a finger joint varies.

An applied load in the range 2 N to 100 N was investigated, which represents values used in previous analysis of MCP joints and has been used in a finger joint simulator (Joyce 2007b; Joyce and Unsworth 2000). Although loads of up to 256 N (Weightman and Amis 1982) in pinch and 980 N (Beevers and Seedhom 1995a) in grasp actions have been reported, for the lubrication analysis these values are abnormal as during high load there is no sliding motion of the finger so any lubrication analysis is not appropriate. The sliding motion in the finger is associated with low loads. In previous lubrication analysis of metacarpophalangeal joint prostheses the maximum load has been considered as 50 N (Joyce 2007b).

The viscosity of the synovial fluid was assumed to be 0.005 Pa s and has been considered Newtonian and isoviscous for the purpose of the lubrication analysis (Jalali-Vahid *et al.* 2001). A range of 0.003 to 0.01 Pa s has been used to study the effect of the viscosity of the lubricant on lubrication regimes of the implant (Joyce 2007b).

The radial clearance was varied from 0.08 mm to 3.5 mm going from very constrained to less constrained surfaces (Scholes *et al.* 2005; Swieszkowski *et al.* 2006).

## Chapter 7

The elastic modulus of the elastomer has been considered in the range of 5 to 25 MPa with a Poisson's ratio of 0.5 (Dowson *et al.* 1991; Quigley *et al.* 2002).

The thickness of the elastomer was varied between 0.5 and 3 mm (Unsworth and Strozzi 1994).

In this part of the study the following bearing material combinations were investigated:

- Cobalt Chrome molybdenum alloy (CoCr) –on- Ultra High Molecular Weight Polyethylene (UHMWPE) (Metal-on-Polyethylene material combination (MoP)).
- Cobalt Chrome alloy (CoCr) –on- Cobalt Chrome alloy (CoCr) (Metal - on – Metal material combination (MoM)).
- Zirconia - on – Zirconia (Ceramic – on – Ceramic material combination (CoC))
- Cobalt Chrome alloy (CoCr) –on- Polyurethane (Metal – on – Elastomer material combination (MoE))

The properties of the materials that have been used for the lubrication analysis are presented in Table 7-2 below.

**Table 7-2.** Materials properties

Material	Elastic modulus (GPa)	References	Poisson's ratio	References	Roughness ( $\mu\text{m}$ ) Ball,socket	References
CoCrMo Alloy	210	(Pylios and Shepherd 2004)	0.3	(Pylios and Shepherd 2004)	0.003,0.01	(Joyce 2007b)
UHMWPE	1	(Pylios and Shepherd 2004)	0.4	(Pylios and Shepherd 2004)	1.29	(Pylios and Shepherd 2004)
Zirconia	198	(Joyce 2007b)	0.29	(Pylios and Shepherd 2004)	0.003,0.006	(Joyce 2007b; Pylios and Shepherd 2004)
Polyurethane	5-25	(Quigley <i>et al.</i> 2002)	0.5	(Dowson <i>et al.</i> 1991)	0.163	(Scholes <i>et al.</i> 2002)

### 7.3.5 Lubrication regimes

Although the calculation of the minimum film thickness is important for the lubrication analysis, the indication of the lubrication regime that the two opposing surfaces operate under is vital for the evaluation of the wear of the two surfaces. The calculation of the lambda ratio (Equation 7-10) indicates the lubrication regime under which the two bearing surfaces operate and can be calculated from:

$$\lambda = \frac{h_{\min}}{\sqrt{(R_{a1})^2 + (R_{a2})^2}} \quad (7-10)$$

where  $h_{\min}$  is the predicted minimum film thickness and  $\sqrt{(R_{a1})^2 + (R_{a2})^2}$  is the compound surface roughness for the two bearing surfaces. If the calculated lambda ratio,  $\lambda$ , is more than 3 then there is fluid film lubrication with effective separation of the two surfaces. At intermediate values of lambda ratios from 1 to 3 mixed lubrication is indicated and less than unity, boundary lubrication (Johnson *et al.* 1972). The values of the compound surface roughness for the materials used in the analysis are shown in Table 7-3 below.

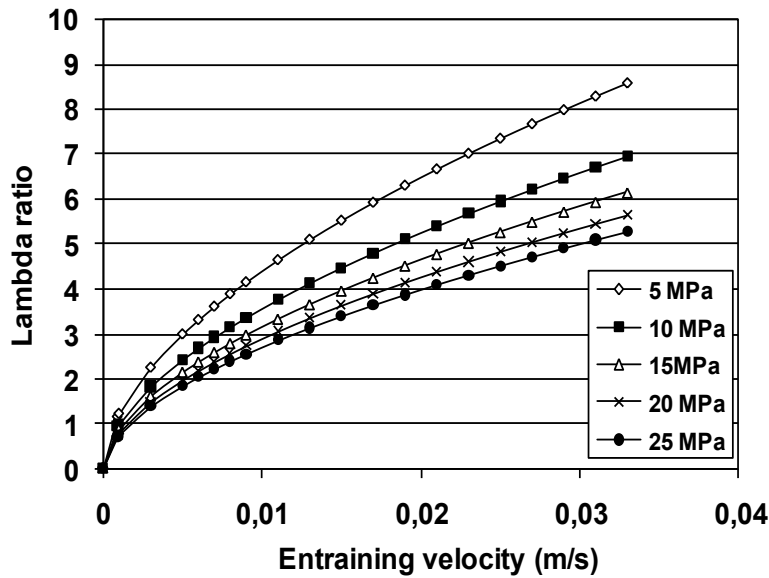
**Table 7-3.** Compound surface roughness of materials combinations

Material combination	Surface roughness ( $\mu\text{m}$ )
CoCr-CoCr	0.0104
CoCr -UHMWPE	1.29
Zirconia – Zirconia	0.0067
CoCr - Polyurethane	0.163

## 7.4 Results

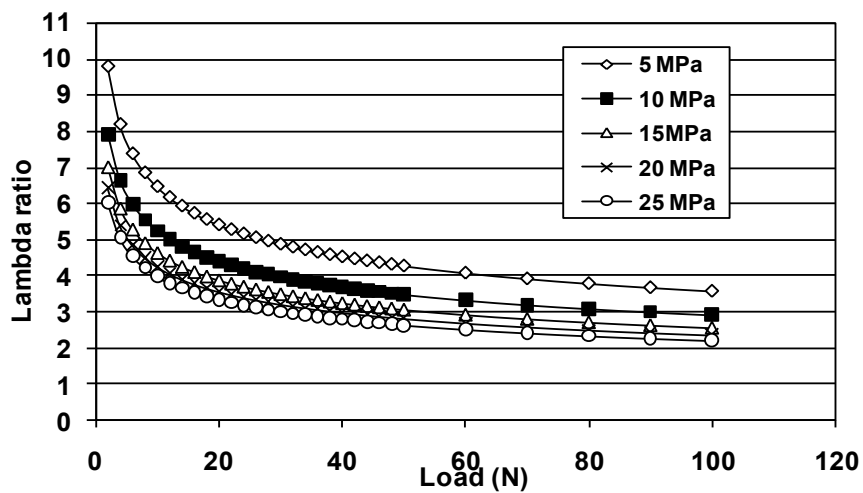
The effect of the various parameters on the predicted lambda ratio on soft layered compared with the conventional material combinations is presented in Figures 7-5 to 7-16.

Figure 7-5 shows that the lambda ratio is enhanced when the entraining velocity increases. In human fingers, as has been reported earlier, conditions of high velocity are connected with low load.



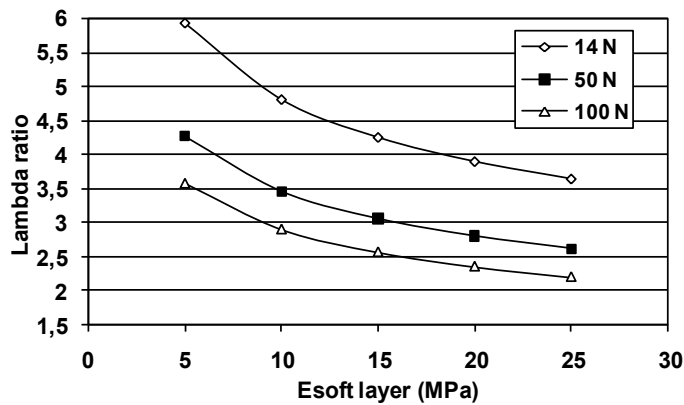
**Fig 7-5.** Effect of velocity on predicted lambda ratio for soft layered joints ( $L=14$  N,  $h_t=2$  mm,  $R_1=7.5$  mm,  $c=0.08$  mm)

The effect of the load on lambda ratio for hard-on-elastomer material combinations is shown in Figure 7-6. The lambda ratio decreases when the load increases.



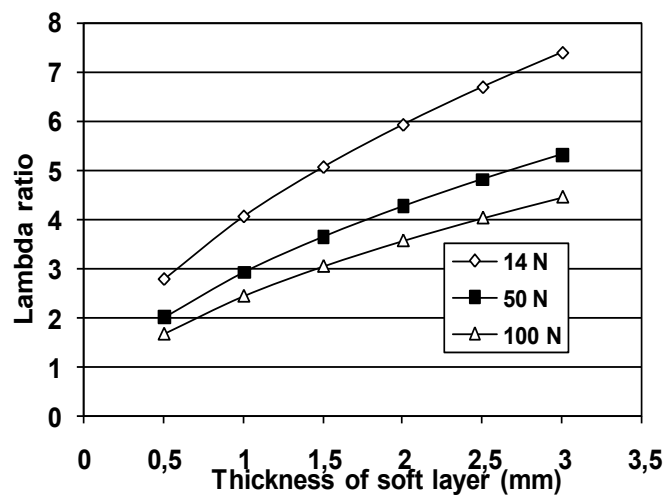
**Fig 7-6.** Effect of load on predicted lambda ratio for soft layered joints ( $u=0.017$  m/s,  $h_t=2$  mm,  $R_1=7.5$  mm,  $c=0.08$  mm)

The effect of the elastic modulus of the elastomer is shown in Figure 7-7. The increase in the elastic modulus of the soft layer material decreases the lambda ratio. The harder the material, the smaller the contact radius, and as a result there is a smaller film thickness and lambda ratio as well.



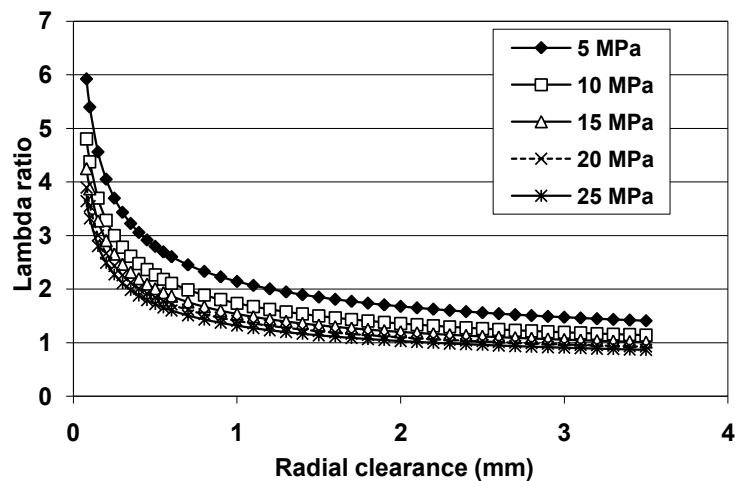
**Fig 7-7.** Effect of elastic modulus of soft layered on predicted lambda ratio ( $u=0.017$  m/s,  $h_t=2$  mm,  $R_1=7.5$  mm,  $c=0.08$  mm)

The effect of the increase of the thickness of the elastomer layer is shown in Figure 7-8. Any increase in the thickness of the elastomer layer, increases the lambda ratio.

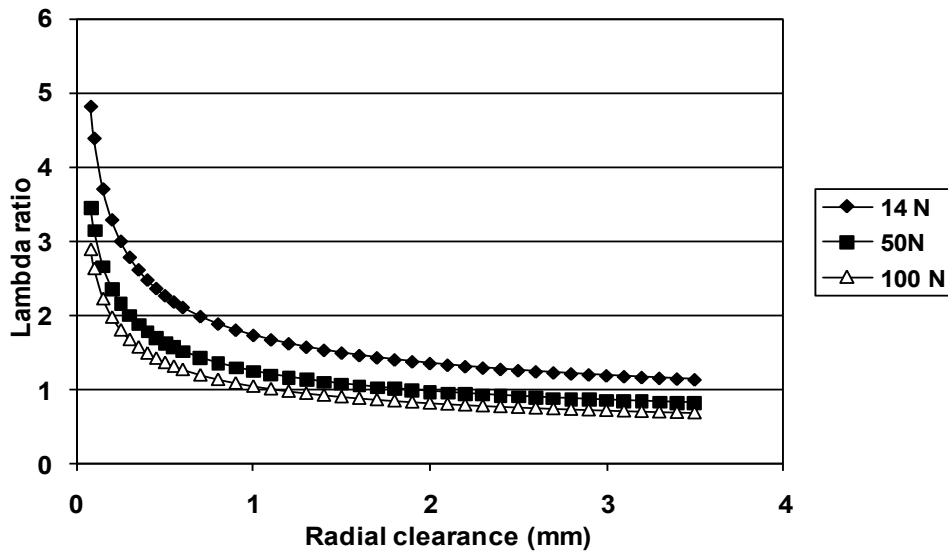


**Fig 7-8.** Effect of thickness of soft layered on predicted lambda ratio ( $u=0.017$  m/s,  $E_{\text{soft layer}}=5$  MPa,  $R_1=7.5$  mm,  $c=0.08$  mm)

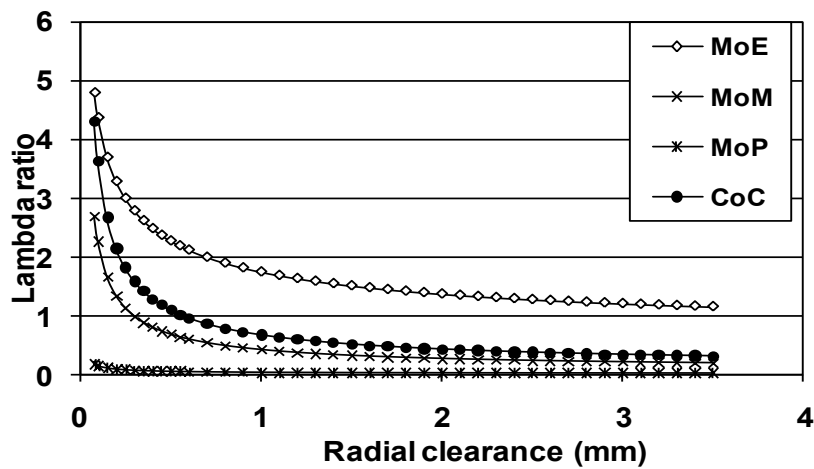
The smaller the radial clearance the higher the lambda ratio as shown in figures 7-9 and 7-10. The smaller the clearance the higher the conformity of the articulating surfaces that leads to higher stability of the implant design. Figure 7-9 shows the effect of the radial clearance on Lambda ratio for different elastomer elastic moduli. Figure 7-10 shows the effect of clearance on the lambda ratio with varying load. In Figure 7-11 the effect of radial clearance on lambda ratio is presented, with varying material combinations.



**Fig 7-9.** Effect of clearance on lambda ratio for different Elastic modulus of soft layered ( $u=0.017$  m/s,  $ht=2$  mm,  $R1=7.5$  mm, load =14 N)



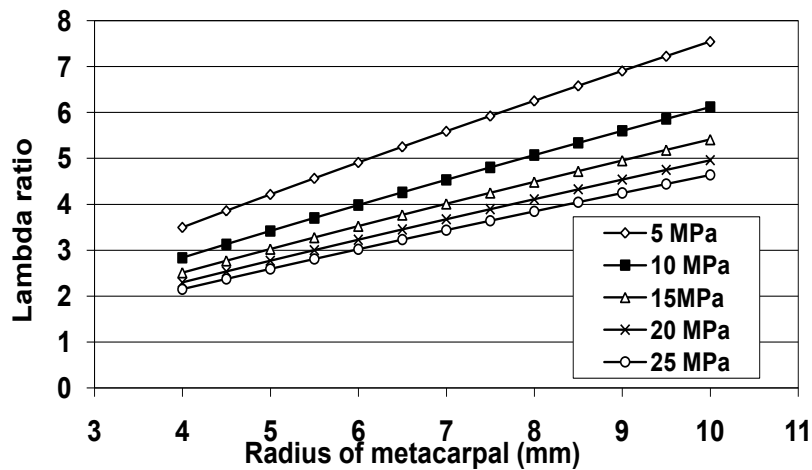
**Fig 7-10.** Effect of clearance on lambda ratio according to load ( $u=0.017$  m/s,  $ht=2$  mm,  $E=10$  MPa,  $R_1=7.5$  mm)



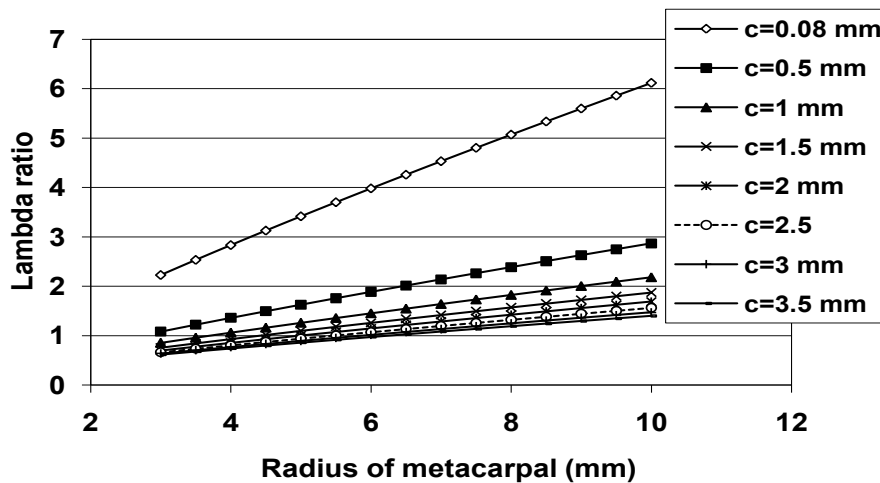
**Fig 7-11.** Effect of clearance on Lambda ratio according to material combination ( $u=0.017$  m/s,  $ht=2$  mm,  $L=14$  N,  $c=0.08$  mm)

Figure 7-12 shows the effect of the radius of the metacarpal on the lambda ratio with varying radial clearance for metal on elastomer material combinations. Increasing the radius of the metacarpal head increases the lambda ratio, as shown in Figure 7-12 and 7-13. Figure

7-13 shows the effect of the increase of the radius of the metacarpal head on the lambda ratio with varying radial clearance for metal – on- elastomer material combinations.



**Fig 7-12.** Effect of metacarpal head radius on predicted lambda ratio for soft layered joints ( $u=0.017$  m/s,  $L=14$  N,  $h_t=2$  mm,  $c=0.08$  mm)



**Fig 7-13.** Effect of radius of metacarpal on Lambda ratio according to clearance ( $u=0.017$  m/s,  $L=14$ N,  $h_t=2$  mm,  $E=10$  MPa)

The effect of viscosity on lambda ratio is presented in Figures 7-14 and 7-15. The average viscosity that has been used in this study is  $0.005$  Pa s (Jalali-Vahid *et al.* 2001), as this is the viscosity of the diseased joint due to arthritis that the implant will experience. The effect

of viscosity on lambda ratio with varying material combination and load is presented in Figures 7-14 and 7-15 respectively.

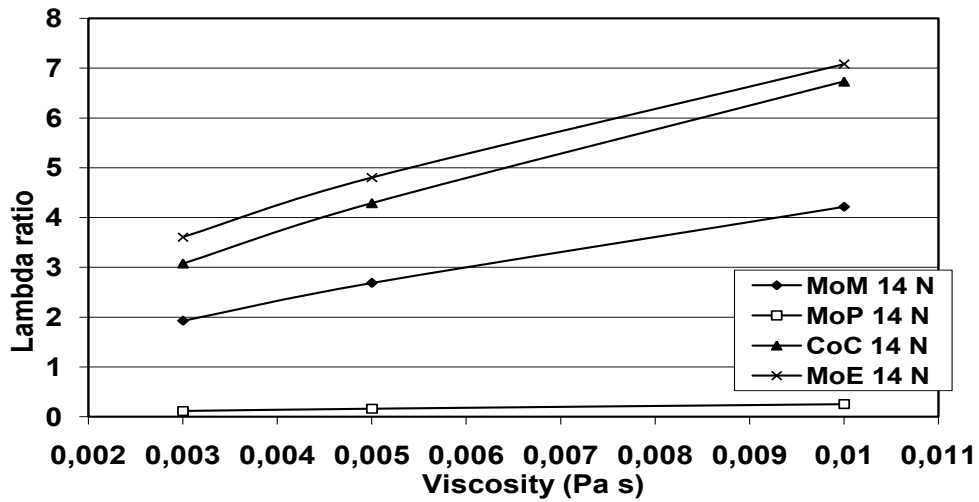


**Fig 7-14.** Effect of viscosity on Lambda ratio according to material combination ( $u=0.017$  m/s,  $h_t=2$  mm,  $L=14$  N,  $c=0.08$  mm)

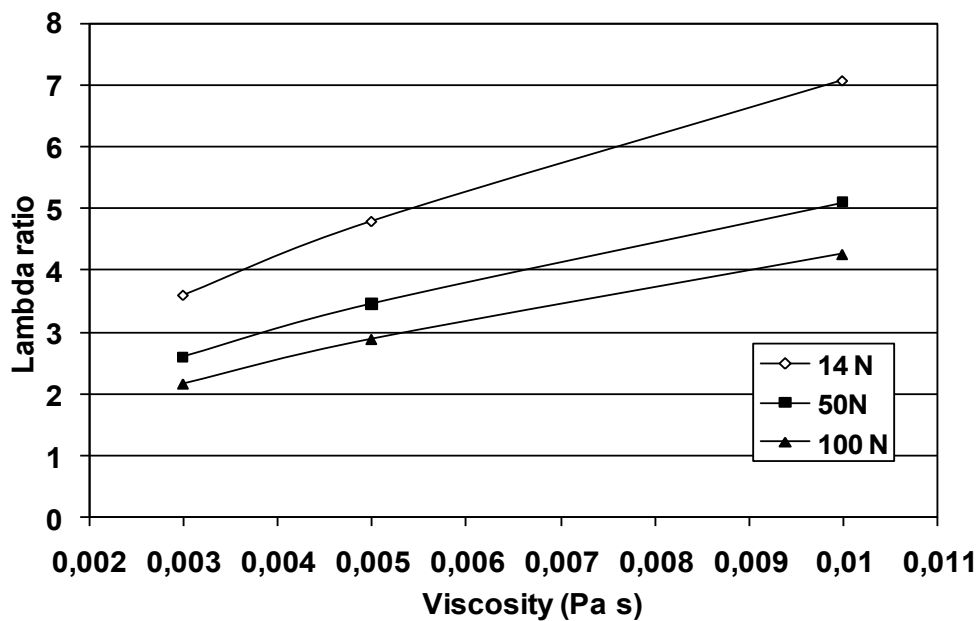


**Fig 7-15.** Effect of viscosity on Lambda ratio for metal on elastomer material combination according to load ( $u=0.017$  m/s,  $h_t=2$  mm,  $E=10$  MPa,  $c=0.08$  mm)

## 7.5. Discussion

The predicted lambda ratio for the hard-on-elastomer material combinations in MCP joint replacement implants can be enhanced by decreasing the clearance, decreasing the elastic modulus of the soft layer, increasing the radius of the metacarpal head, decreasing the applied load, increasing the thickness of the soft layer and increasing the entraining velocity. The load and entraining velocity are operating parameters, while the radial clearance, the radius of the metacarpal head, the thickness and the elastic modulus of the elastomer are design parameters. The operating parameters cannot be controlled, but the design parameters can be chosen during design to enhance the film thickness.

In the human finger during grasp actions conditions of severe wear may occur when the load is high and the velocity is low. Under these conditions other modes of lubrication come into action, like squeeze film lubrication that is enhanced by the soft layer performance. For normal hand function it is better to concentrate in the lower range of values of load which the prosthesis is most likely to operate under.

The lambda ratios of the soft layer, for the same operating and design parameters, present higher lambda ratios values than the conventional material combinations. Ceramic-on-Ceramic has the highest Lambda ratio of the conventional materials, followed by the Metal-on-Metal and finally by the Metal-on-Polyethylene.

Although the increase in thickness of the soft layer increases the lambda ratio, according to elastohydrodynamic theory, it also increases the shear stress between the soft layer and the substrate (Unsworth and Strozzi 1994). Shear stress is connected with the debonding phenomena between the layer and the substrate (Matthewson 1981). A compromise between

film thickness enhancement and shear stress reduction has to be done and for hip joints, incorporating the soft layer concept, an intermediate layer thickness of 2 mm has been considered the best option (Unsworth and Strozzi 1994).

A metal-on-elastomer material combination showed evidence of fluid film lubrication according to this lubrication analysis. If we take into account the asperity perturbation of the elastomer, the metal-on-elastomer material combination provides evidence that its lubrication regime is enhanced in comparison with the hard-on-hard material combinations, like metal-on-metal and metal-on-polyethylene. Under some circumstances (small clearance, low load, high entraining velocity, low elastic modulus of the elastomer and large thickness of the elastomer) fluid film lubrication is possible. Only the elastohydrodynamic lubrication has been considered in the calculation of the minimum film thickness in this analysis, while the microelastohydrodynamic lubrication and the squeeze film lubrication also enhance the lubrication film of the metal-on-elastomer and possible thinner lubrication films will be adequate to separate the surfaces from coming into contact (Auger *et al.* 1993; Dowson *et al.* 1991).

With hard-on-hard material combinations like metal-on-metal or ceramic-on-ceramic, under some specific design and operating parameters, full fluid film lubrication is possible, while the metal-on-polyethylene and pyrocarbon-on-pyrocarbon implants operate under a boundary or mixed lubrication regime, as has been shown in a previous study (Joyce 2007b). The only available wear test data of a MCP two-piece implant is the *in vitro* study of the Elogenics<sup>TM</sup> that incorporate a metal-on-polyethylene bearing couple (Joyce *et al.* 2006). There was evidence that scratches appear on the surface that indicates asperity contact and a mixed or boundary lubrication regime.

## Chapter 7

The application of the theory for the calculation of lubrication film thickness on the soft layer material combinations provides a rigid backing for the soft layer. In the metacarpophalangeal joint design concept presented here, the soft layer is not attached to a rigid backing. However, as the design consist of two metal balls in contact with the soft middle part, it is assumed to have the same effect as a soft layer with a rigid backing. The final design has a hole in the middle that probably deteriorates the lambda ratio that has been calculated here. However, the purpose of this analysis was mainly to compare the different materials combinations and not to undertake a full analysis.

The findings of this part of the study propose the application of the elastomer, a well known material used in metacarpophalangeal joint arthroplasty, from a different point of view and its application in a new metacarpophalangeal joint implant design.

The predicted lambda ratio for the hard-on-elastomer material combinations in MCP joint replacement implants are enhanced by decreasing the clearance, decreasing the elastic modulus of the soft layer, increasing the radius of the metacarpal head, decreasing the applied load, increasing the thickness of the soft layer and increasing the entraining velocity. Specific values of these parameters will be presented in Chapter 11 with the final design considerations as the final design dimensions will be a compromise among wear results, lubrication analysis, stress analysis and accommodation to the size of metacarpophalangeal joint of the specific design.

## **Chapter 8**

### **Wear of medical grade silicone rubber against titanium and ultra high molecular weight polyethylene**

#### **8.1 Introduction**

The selected concept design, as described in chapter 5, involved an elastomer part to move freely inside the cavities of the metacarpal and proximal phalange parts. The aim of this part of the study was to investigate the wear of silicone rubber against Titanium and Ultra High Molecular Weight Polyethylene to ascertain if this material may be suitable for the final design.

#### **8.2 Materials and Methods**

##### ***8.2.1 Apparatus***

A pin-on-disc apparatus was designed to fit to a BOSE ElectroForce 3300 materials testing machine (Bose Corporation, ElectroForce Systems Group, Minnesota, USA), as shown in Figures 8-1 and 8-2 (Pylios and Shepherd 2008b). The detail engineering drawings of the pin-on-disc design apparatus are shown in Appendix A. The pin and disc apparatus was manufactured by Tru-turn Rapid Engineering Ltd (Kings Norton, Birmingham, UK). The testing machine has a rotary motor fitted to its base (to rotate the disc) and a linear motor fitted to the crosshead to apply an axial force from the pin to the disc. The pin and disc were contained within an environmental chamber into which a lubricant was added. The temperature of the lubricant was maintained by a heater and circulation pump (Cole-Parmer, Vernon Hills, Illinois, US). The Bose 3300 machine provides a loading system for the pin against the disk material that is precisely monitored. Also the disk is moved on a reciprocative motion relative to the pin that provides the wear path and the sliding distance

for evaluation of the wear rate of the material combinations. As the testing machine is fully calibrated each year, it is an appropriate machine to use for wear testing.

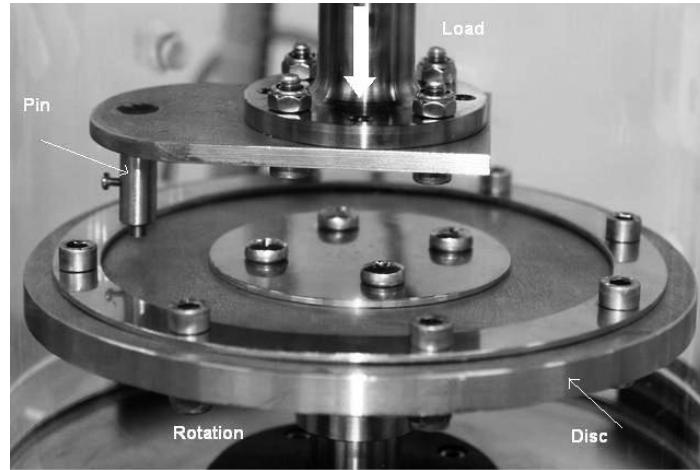


**Fig 8-1.** The pin-on-disc set up

Two lubricants were used in the study: full strength Ringer's solution (Fisher Scientific, Loughborough, UK) and bovine serum solution that consists of 25% Bovine serum (Harlan Sera-Lab Ltd, Harlan Sera-Lab, Loughborough, UK) and 75% distilled water (volume/volume) (Joyce and Unsworth 2001). During the experiments the lubricant was maintained at a temperature of 37°C for simulation of body temperature that any prosthesis will experience (Joyce *et al.* 1996). The lubricant was replaced after the completion of each test.

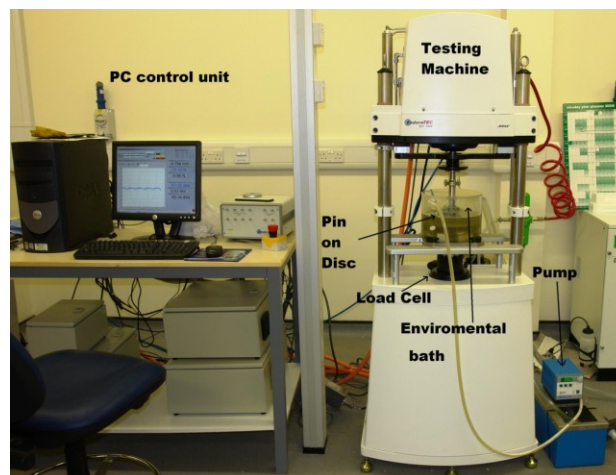


**Fig 8-2.** The experimental set-up of the wear test

### 8.2.2 Materials

Two materials were used to manufacture the pins: Ultra High Molecular Weight Polyethylene (UHMWPE) (CHIRULEN<sup>®</sup> 1020, Meditech Vreden, Germany) and Titanium (Grade 2, ATI Titanium International, Birmingham, UK). The pins were flat ended, 25 mm in length and 5 mm in diameter. The disc material was Medical Grade Solid Silicone Rubber 71-MED (CS Hyde Company, Lake Villa, Illinois, USA), which has similar material properties to the type used in Swanson flexible implants see Appendix B (Hutchinson *et al.* 1997; Savory *et al.* 1994). The material was provided from the company in sheets of 3 mm thickness and they were cut to a diameter of 170 mm to fit to the test apparatus, using a scalpel and template. According to the manufacturers the silicone rubber had a tensile strength of 8.3 MPa and hardness (Shore A) of  $50 \pm 5$ .

The surface roughness ( $R_a$ ) of each of the four titanium and four UHMWPE pins was measured using a Taylor Hobson Form Talysurf Series 120L stylus instrument (Taylor Hobson Ltd, Leicester, UK), shown in Figure 8-3. The mean surface roughness of the titanium pins was  $0.1948 \pm 0.0159 \mu\text{m}$ , with the UHMWPE having a mean of  $1.1876 \pm 0.039 \mu\text{m}$ .



**Fig 8-3.** Taylor Hobson Form Talysurf Series 120L

### ***8.2.3 Experimental procedure***

The ASTM standards G132-96 and F732-00 were used as a guide for the wear test procedure (ASTM 1996; ASTM 2000). Before testing the samples were carefully cleaned using the following procedure:

- Rinse in water to remove any bulk material
- Immerse in a solution of Neutracon 1% for disinfection
- Place in an ultrasonic bath for 10-15 min at 37°C
- Rinse in distilled water
- Dry with lint free wipe
- Allow to dry in a laminar air flow cabinet for 2 hours

The mass of the samples (titanium or UHMWPE pins and the silicone rubber disc) were measured before and after testing using an Ohaus GA200D balance (Ohaus, New Jersey, US) to the nearest 0.1 mg. Fluctuations in the mass of a specimen were not observed. Three measurements of mass were made per sample and the mean value was used for the subsequent calculations of wear factors. Laboratory sheets shown in Appendix C have been used for every material.

A control pin and disc material were kept unloaded inside the bath to take account of any lubricant absorption. The sliding speed of the reciprocation motion was 0.079 m/s and the stroke length was 15.7 cm per cycle. Each test was run for 31,850 cycles. Each cycle was regard as starting from 0° rotation up to 150° and back again to 0°. It was not possible to rotate the disc through 360 ° due to technical problems to avoid damage of the load cell, leakage problems and restriction due to the cables attached to the load cell. Tests were run

for a total distance of 10 km. This distance was chosen as the pistoning of the Swanson or Sutter design of implant inside the medullary cavities of a bone has been calculated to be about 0.5 mm per flexion (Penrose *et al.* 1997). Assuming 1 million finger flexions per year 10 km would be 20 years of use (Joyce and Unsworth 2000).

The load used for the wear test was 10 N ( $9.96\text{N} \pm 1.2\text{ N}$ ) as has been previously used for material evaluation for finger implants (Joyce *et al.* 1996; Joyce and Unsworth 1996). It gives a nominal contact stress of 0.51 MPa.

Eight tests were run in total, four in bovine serum and four in Ringer's solution. For each lubricant two UHMWPE and two Titanium pins were tested. After testing the mass of all the samples were measured.

### **8.2.4 Wear evaluation**

Wear of the materials was defined as the mass loss with respect to the initial mass, to which any mass gain of the control material due to lubricant absorption was added. Therefore the mass uptake of the controls and test material was assumed to be equal.

The wear factors  $k$  ( $\text{mm}^3/\text{N m}$ ) were calculated from Equation 8-1 (Joyce and Unsworth 1996):

$$k = \frac{V}{Fx} \quad (8-1)$$

where  $V$  is volume of wear ( $\text{mm}^3$ ),  $F$  is the applied load (N) and  $x$  is the sliding distance (m).

$$\text{Given that } V = \frac{m}{\rho} \quad (8-2)$$

where  $\rho$  is the density of the material ( $\text{kg}/\text{m}^3$ ) and  $m$  is the mass of the wear debris (kg), equation 8-1 can be rewritten as

$$k = \frac{m}{\rho Fx} \quad (8-3)$$

The density of the silicone rubber was 1.15 g/cm<sup>3</sup>.

### 8.3. Results

There was no mass loss for the titanium and UHMWPE pins and also no lubricant absorption for the pins or disc material control samples. The surface roughness of polyethylene and titanium pin materials was unchanged, while the silicone rubber surface roughness deteriorated and the wear path was visual with the naked eye. Scanning Electron Microscopy (SEM) with JEOL 6060 Microscope (Jeol Ltd., Herts., UK) shown in Figure 8-4 located in the Centre of Electron Microscopy of Metallurgy and Materials department of University of Birmingham UK) was used to observe the wear pattern on the silicone (Fig 8-5 & 8-6). The SEM was undertaken with the help of Dr Laura Leslie, colleague in the Biomedical Engineering Research Group. The samples were cut to size using a scalpel blade and mounted onto SEM stubs (AGAR Scientific, Stansted, UK). These are metal discs measuring approximately 30 mm diameter and 10 mm height. The sample length and width cannot be larger than the disc and the height of the sample must be as small as possible to ensure it does not make contact with the camera in the microscope chamber. The sample must be of a conductive material and is secured to the stub using a circular piece of conductive sticky tape (AGAR Scientific, Stansted, UK). The samples were gold sputtered using an EMSCOPE SC500 (EM systems, Cheshire, UK). A spot size of 60 was used along with High Voltage (HV) of 15 kV and Working Distance (WD) of 10 mm.



**Fig 8-4.** Scanning Electron Microscopy JEOL 6060

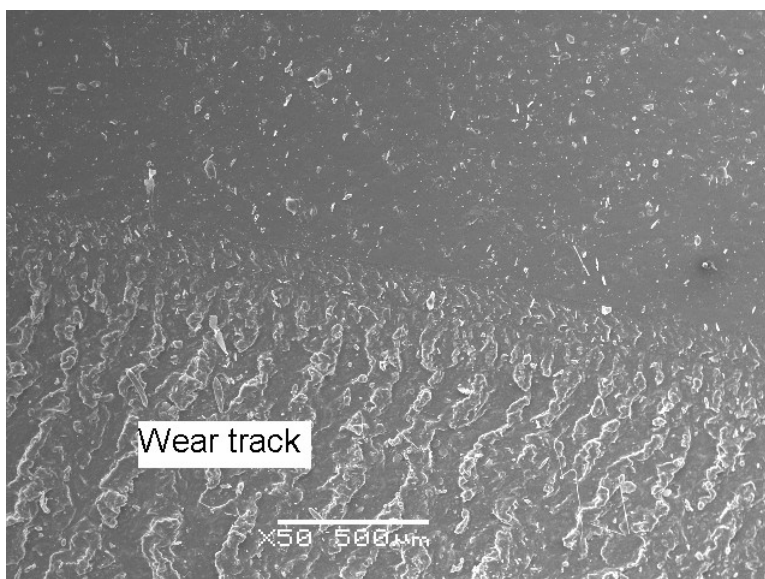


**Fig 8-5.** SEM image of the wear track on the silicone (Titanium pin).

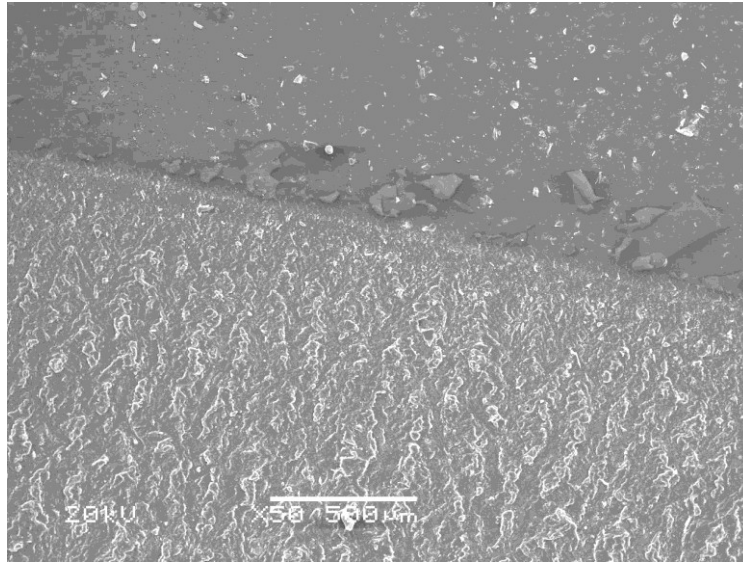


**Fig 8-6.** SEM image of the wear track on the silicone (UHMWPE pin)

It can be seen that there was no cutting of the pin into the silicone. The wear test results are shown in Table 8-1, where the  $k$  factors for the silicone rubber have been calculated for each lubricant and pin material. It can be seen that for titanium against silicone the wear factors were  $40.0 \times 10^{-6} \text{ mm}^3/\text{N m}$  and  $66.5 \times 10^{-6} \text{ mm}^3/\text{N m}$  for bovine serum and Ringer's solution, respectively. The wear factors for UHMWPE against silicone were higher with values of  $84.4 \times 10^{-6} \text{ mm}^3/\text{N m}$  and  $88.3 \times 10^{-6} \text{ mm}^3/\text{N m}$  for bovine serum and Ringer's solution, respectively.

**Table 8-1.** Calculated  $k$  factors for silicone rubber against Ti and UHMWPE.  $K$  factors are a mean of two samples. (RS: Ringer's solution, BS: Bovine serum)

	Lubricant	Pin material	Wear mass (mg)( $\pm$ SD)	$k$ $10^{-6}(\text{mm}^3/\text{Nm})(\pm$ SD)
1	RS	Ti	7.7 ( $\pm$ 0.5)	66.5 ( $\pm$ 4.3)
2	RS	UHMWPE	10.2 ( $\pm$ 0.4)	88.3 ( $\pm$ 3.1)
3	BS	Ti	4.6 ( $\pm$ 0.6)	40.0 ( $\pm$ 4.9)
4	BS	UHMWPE	9.7 ( $\pm$ 0.3)	84.4 ( $\pm$ 2.5)

## 8.4. Discussion

It was found that the wear factors of silicone against titanium are smaller than silicone against UHMWPE. The wear factors with bovine serum as the lubricant were smaller than

using Ringer's solution as the lubricant. A similar result has been found in other studies as the bovine serum is believed to act as a boundary lubricant (Joyce and Unsworth 2001). The wear factors in this study for medical grade silicone against titanium and ultra high molecular weight polyethylene ( $40-80 \times 10^{-6} \text{ mm}^3/\text{N m}$ ) are higher than those quoted for metal on polymer total hip replacement implants typically  $2 \times 10^{-6} \text{ mm}^3/\text{N m}$  (Hall *et al.* 1996). However, it is the volume of wear generated, as well as wear particle size, that is important and this depends on the force and sliding distance. In hips the forces and sliding distances are high. With the Swanson implant, the novel wrist implant and the current concept for metacarpophalangeal joint replacement, the silicone is not used as a bearing surface, rather it slides against either titanium (Swanson silicone implants designs) and ultra high molecular weight polyethylene (novel wrist implant (Shepherd and Johnstone 2005)). The force and sliding distance are much smaller and therefore the volume of wear will be small. Wear factors for other elastomers, such as polyurethane or hydrogels, are typically in the range  $10^{-6} - 10^{-9} \text{ mm}^3/\text{N m}$  (Jin *et al.* 1993). Silicone rubber appears to have a higher coefficient of friction sliding against metal than hydrogels against metal and, therefore, a higher wear rate for silicone rubber is expected (Sawae *et al.* 1996). Due to the higher wear of silicone rubber sliding against UHMWPE it can be concluded that the adhesive forces experienced in this material combination are higher; this is analogous to the findings of two elastomer materials sliding against each other that appear to have higher friction than metal on elastomer friction (Caravia *et al.* 1995). Also, the surface roughness of the UHMWPE pins was much higher than that of the titanium pins and a more severe lubrication regime is expected to be experienced in the UHMWPE on silicone rubber material combination.

Wear tests of other elastomers have been undertaken by using the elastomer material as the pin material (Jin *et al.* 1993; Schwartz and Bahadur 2006). Pin-on-plate tests have shown

that the plates wear more than the pins (Joyce *et al.* 1996) so a higher wear factor is expected to have been calculated in comparison with the wear factor for the silicone rubber if it has been used as the pin material. However, a silicone pin would not be suitable as it would deflect during sliding.

The Archard wear equation is a way for wear evaluation where the wear is proportional to the hardness of the counterface but as it is generally difficult to define the hardness of visco-elastic polymeric materials. The dimensional wear factor method has been used in this study for the evaluation as it has been used in most of the wear tests for materials used in finger joint replacements (Jin *et al.* 2006; Joyce *et al.* 1996).

The material combination of titanium on silicone rubber has been proven to produce less wear than UHMWPE on silicone rubber. The effect of the lubricant was higher for the titanium on silicone rubber rather than the UHMWPE on silicone rubber material combinations. According to the results presented here a Titanium-on-Silicone rubber or more generally a metal-on-elastomer material combination interface will produce less wear than a Polyethylene-on-Silicone rubber interface. The choice of the titanium material as pin material was first due to the use of this material in grommets of Swanson implant and secondly as possible material for finger joint replacement. Final decisions on the material selection of the metacarpophalangeal joint design will be presented in Chapter 11.

## **Chapter 9**

### **Finite element analysis of elastomer part**

#### **9.1 Introduction**

The elastomer part will help to constrain and align the metacarpal and proximal phalanx parts of the novel prosthesis design. According to the risk analysis presented in Chapter 6 it is the most vital part and most likely site of failure of the whole prosthesis. Finite element analysis of this part will be conducted and several alterations will be used to validate the most appropriate design for this vital part.

#### **9.2 Finite element analysis of elastomer**

Elastomers have been used predominantly for the small joint replacements and especially for the metacarpophalangeal joints. Several studies have been found in the literature that have attempted to model elastomer finger implants (Biddiss *et al.* 2004; Lewis *et al.* 1998; Penrose *et al.* 1997; Podnos *et al.* 2006; Williams *et al.* 2000). There are some primary problems of modelling elastomers using finite element analysis. Some researchers have considered the elastomer as a material that behaves in a linear manner (Abdul Kadir *et al.* 2008; Penrose *et al.* 1997; Williams *et al.* 2000). That is a very simplified approach as elastomers are hyperelastic incompressible materials and a different approach should be considered to gain more realistic results. The most common approach is the use of a constitutive equation for the material behaviour within its operational conditions. The strain energy function has been extensively used in the definition of the mathematical model for the hyperelastic model. These constitutive equations known as hyperelastic material models are expressed in terms of the strain energy potential. One type of strain energy potential or

## Chapter 9

(strain energy density) commonly used for modelling elastomers is the polynomial form (Boast and Coveney 1999):

$$U = \sum_{i+j=1}^N C_{ij} (\bar{I}_1 - 3)^i (\bar{I}_2 - 3)^j + \sum_{i=1}^N \frac{1}{D_i} (J_{el} - 1)^{2i} \quad (9-1)$$

where  $U$  is the strain energy per unit of reference volume,  $N$  is a material parameter,  $C_{ij}$  and  $D_i$  are temperature depended material parameters,  $\bar{I}_1$  and  $\bar{I}_2$  are first and second deviatoric strain variants and  $J_{el}$  is the elastic volume ratio.

Unlike the elastic models, the deformation modes (principal nominal strain,  $\varepsilon_i$ ) for hyperelastic models are described in terms of the principal stretches  $\lambda_i$  as:

$$\lambda_i = 1 + \varepsilon_i \quad (9-2)$$

The deviatoric strains are expressed in terms of the deviatoric stretches:

$$I_1 = (\bar{\lambda}_1)^2 + (\bar{\lambda}_2)^2 + (\bar{\lambda}_3)^2 \quad (9-3)$$

$$I_2 = (\bar{\lambda}_1)^{-2} + (\bar{\lambda}_2)^{-2} + (\bar{\lambda}_3)^{-2} \quad (9-4)$$

The deviatoric stretch is given by:

$$\bar{\lambda}_i = J^{-1/3} \lambda_i \quad (9-5)$$

with the assumption of incompressibility and isothermal response,  $J=1$ . So:

$$\lambda_1 \lambda_2 \lambda_3 = 1 \quad (9-6)$$

The total volume ratio  $J$  in equation (9-5) is related to the elastic volume ratio as:

$$J_{el} = \frac{J}{J^{th}} \quad (9-7)$$

where the expansion volume is given by:

$$J^{th} = (1 + \varepsilon^{th})^3 \quad (9-8)$$

## Chapter 9

The initial shear modulus and bulk modulus in terms of the material constants are given respectively by:

$$\mu_0 = 2(C_{10} + C_{01}) \quad (9-9)$$

$$K_0 = \frac{2}{D_1} \quad (9-10)$$

For a material that is incompressible, the compressibility parameter  $D$  is assumed to be equal to zero. Particular forms of the polynomial model can be obtained by setting specific coefficients in Equation 9-1 to zero. If all  $C_{ij}$  with  $J \neq 0$  are set to zero, the reduced polynomial form is obtained:

$$U = \sum_{i=1}^N C_{i0} (I_1 - 3)^i + \sum_{i=1}^N \frac{1}{D_i} (J_{el} - 1)^{2i} \quad (9-11)$$

If in the reduced polynomial form  $N=1$  then we have the Neo-Hookean model.

$$U = C_{10} (I_1 - 3) \quad (9-12)$$

If in the general polynomial form  $N=1$  we come up with the Mooney-Rivlin model.

$$U = C_{10} (I_1 - 3) + C_{01} (I_2 - 3) \quad (9-13)$$

Deformation of the real material involves mechanisms that are imperfectly understood, and we are reduced to constructing phenomenological models.

Since increasing hand mobility is a goal of the surgery, displacement loading rather than force loading was applied to the model of the implant (Biddiss *et al.* 2004). It is also possible to define the displacement of the proximal phalanx with respect to the metacarpal bone. The displacement of the bones on either side of an implant is more readily quantifiable and it is considered that the main reason for reconstructing a finger joint with an implant is to provide mobility rather than strength (Williams *et al.* 2000).

## Chapter 9

Podnos *et al.* (2006) described that there was good correlation between the reaction moment from two dimensional plane strain models and those from three-dimensional solid models of the hinge area. Therefore two-dimensional plane strain models were used, since for the same computational effort they allow higher mesh density than three dimensional models and therefore more accurate results (Podnos *et al.* 2006). There is no information available which would allow the definition of exact boundary and load conditions that correspond to the implant's behaviour *in vivo* (Podnos *et al.* 2006).

Some assumptions have been used to make the analysis simpler and save on computational time. The following assumptions have been considered for the analysis:

- The material is elastic in behaviour
- The material is isotropic permitting only isotropic thermal expansion
- The stress-strain relationship is highly non-linear
- The material is approximately incompressible
- All deformation occurs instantaneously; hence viscous effects are modelled by including a separate viscoelastic or hysteresis model.

For the analysis in this study the Mooney-Rivlin constitutional model has been used to evaluate the critical elastomer part of the concept design. It is a more general form of the strain energy potential. It provides a better fit than the neo-Hookean form and is most widely used for modelling elastomer materials (Boast and Coveney 1999).

### 9.3 Software for Finite Element Analysis

The Comsol Multiphysics Ver 3.3 (Stockholm, Sweden) has been used for the finite element analysis. This software provides the Mooney-Rivlin hyperelastic model that has been selected for the analysis of the model.

### 9.4 Model for analysis

Stress-strain data from uniaxial tension tests from the Swanson finger implant material (silicone rubber known as Flexspan) was taken from literature (Kult and Jira 2001; Kult and Vavrik 2001) and fitted with the Mooney-Rivlin constitutive model described in section 9.1 and equation 9-13. The elastomer part is a one piece elastomer that has two stems inserted in the metacarpal and phalangeal sleeves of the assembly. As the stems will just slide inside the cavities, the elastomer part is expected to act in a similar way to the one-piece silicone implants. In Figure 9-1a and 9-1b straight and preflexed elastomer part designs are presented. In previous finite element analysis of finger implants the whole implant has been modelled but the stress on the stems was minimal in comparison with the central hinge area (Penrose *et al.* 1996; Penrose *et al.* 1997; Williams *et al.* 2000). From the modelled Swanson and Neuflex metacarpophalangeal implants the stems have been excluded as they do not experience high stress concentrations (Biddiss *et al.* 2004). The elastomer part in this study behaves similarly to the one piece silicone implants so respectively the central part of the elastomer part has been modelled shown in Figures 9-1 (c) & (d). The central part of the elastomer part is the part that will sustain the repetitive bending because of the flexion and extension motion of the metacarpophalangeal joint (Biddiss *et al.* 2004; Penrose *et al.* 1996; Penrose *et al.* 1997; Williams *et al.* 2000). The dimensions of the model shown in Figure 9-1 are 3.5 mm by 7 mm in length.

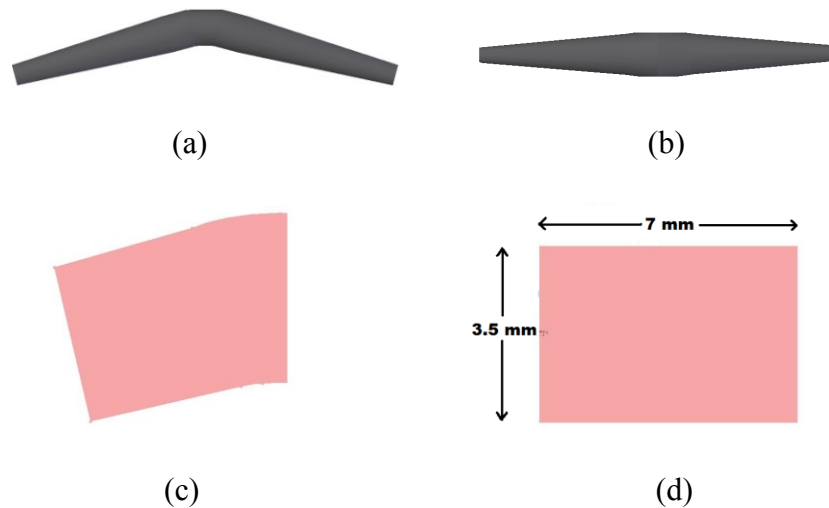


**Fig 9-1.** (a) Preflexed design elastomer part, (b) Straight design elastomer part, (c) Preflexed model for finite element analysis, (d) Straight model for finite element analysis.

## 9.5 Method of loading

The model of the elastomer part was loaded and fixed according to Fig 9-2. Nodes on the right edge were constrained in all degrees of freedom and a tangential displacement was applied to the distal side. The distal end deflected downwards to represent the normal function of the implant *in vivo* e.g. during grasping. The displacement was a function of angle and was applied until 85° of flexion was reached, which is more than the functional range of motion described in Chapter 4. The same type of fixation and displacement was applied to both designs (straight and preflexed). As the cross-section of the elastomer part is circular, lateral deflection that represents radial and ulnar deviation of the implant are of lower amplitude than the flexion-extension directed loading during function of finger implants *in vivo*, and, therefore, can be evaluated with the results from the flexion-extension range of motion.

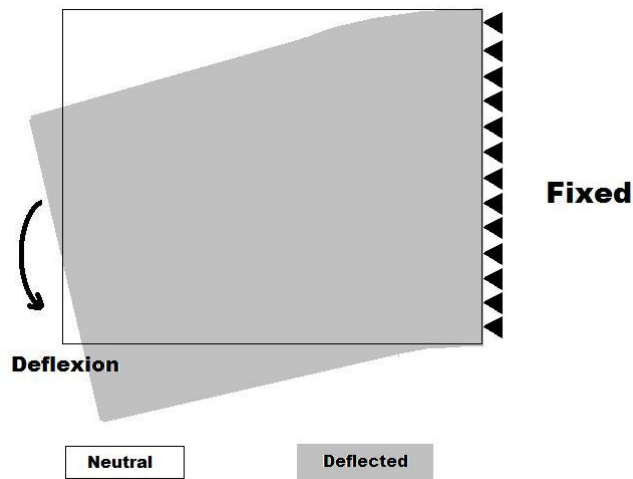


**Fig 9-2.** Loading of FEA model by deflection: tangential applied displacement loading.

## 9.6 Determination of coefficients of Mooney-Rivlin model

A script in Matlab 7 (Natick, USA) was used to determine the coefficients for the Mooney-Rivlin model, shown in Appendix D, and fits the stress-strain data available from the literature (Kult and Vavrik 2001) similar to the approach of using the Mooney-rivlin model to analyse MCP Swanson implant (Lewis *et al.* 1998; Nikas and Sayles 2004). The applicable coefficients of the Mooney-Rivlin model calculated in this analysis are  $C_{10} = 0.21$  MPa and  $C_{01} = 0.056$  MPa. The error between the literature data of stress-strain of silicone rubber and the fit of the Mooney-Rivlin constitutional model has been calculated according to equation 9-14.

$$x_{error}(\%) = \frac{|x_{calc} - x_{literature}|}{x_{literature}} \times 100 \quad (9-14)$$

The maximum error has been calculated up to 16 % that match the error of similar approach for finite element analysis of silicone finger implants (Biddiss *et al.* 2004). The stress-strain data of the literature and the fitted curve of the Mooney-Rivlin model are calculated by the script described in Appendix D, presented in Fig 9-3.

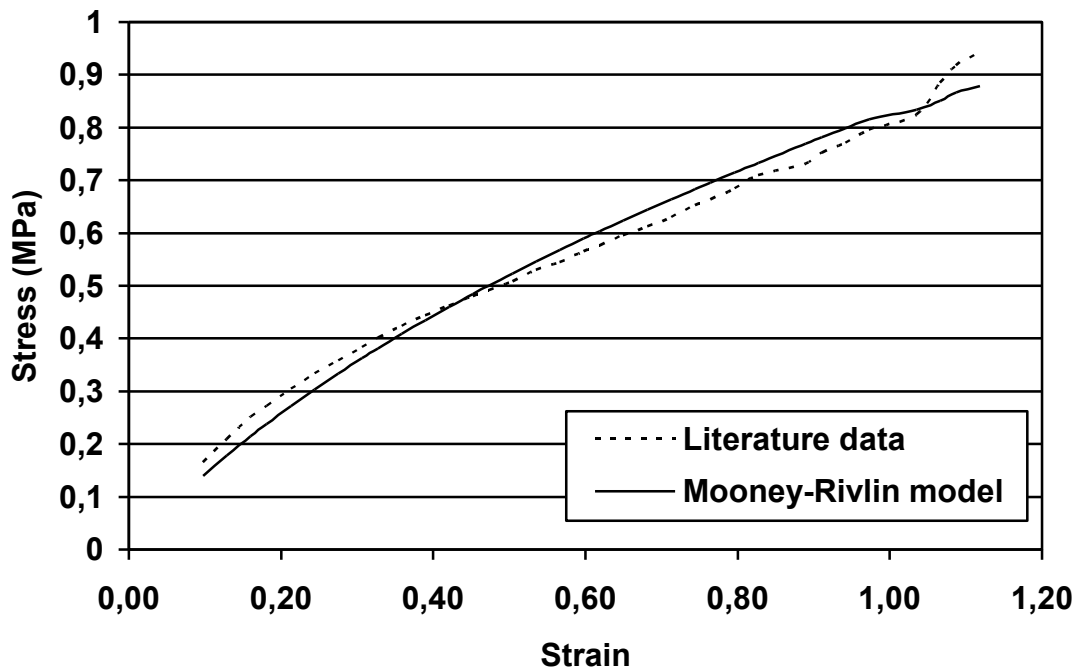


**Fig 9-3.** Fit of Mooney-Rivlin model to literature data (Kult and Vavrik 2001) engineering stress-strain curve

## 9.7 Determination of mesh density

Preliminary results for the selection of mesh density were conducted and are presented in Fig 9-4 below. The computational time and the maximum von Mises stresses according to the number of mesh elements for the straight model at a bend of  $40^\circ$  are presented in Fig 9-4. The mesh density of 5072 elements (Fig 9-5 (b)) has been selected as any further increase of mesh density will provide the same results but a much higher computational time. The meshing of preflexed design is shown in Figure 9-5.

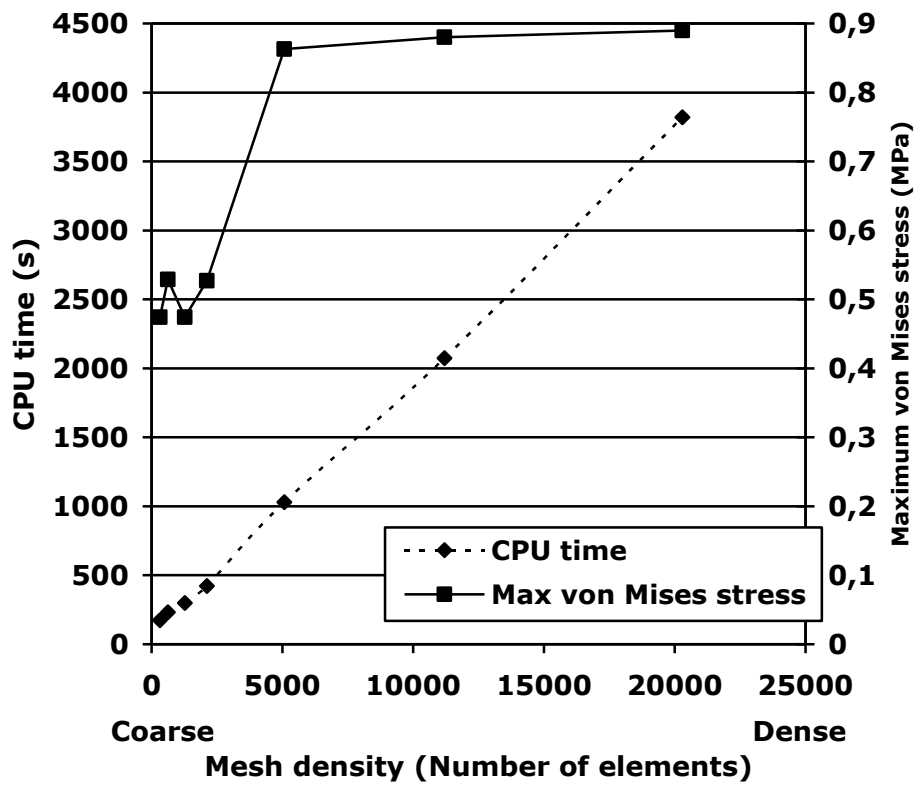


Fig 9-4. Mesh density and computational (CPU) time

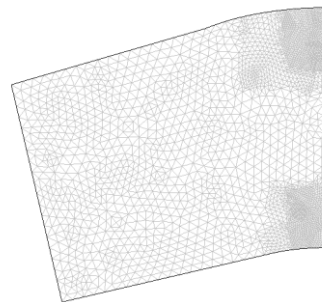
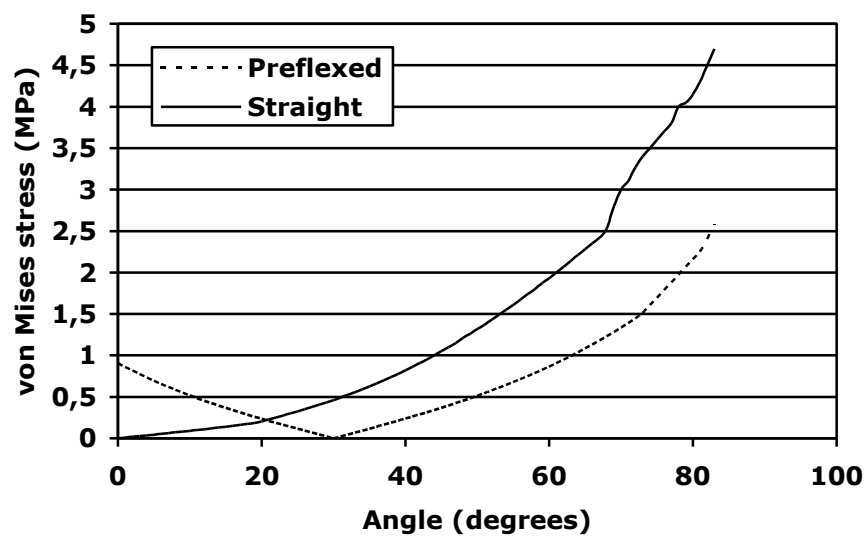


Fig 9-5. Meshing of model used in the analysis

## 9.8 Results

The results show that the maximum von Mises stress occurred at the maximum angle of flexion for both models used. Figure 9-6 shows the von Mises stress against angle of bending for the preflexed design in comparison with the straight design, while in Figure 9-7 the stress distribution while bending is shown. Both models have the minimum stresses at

their neutral position, which is at zero degrees for the straight design and at 30° for the preflexed model. The straight design has higher stresses in comparison with the preflexed design for angles higher than 20°, as it can be seen at Fig 9-6. The maximum stresses were 2.6 MPa and 4.7 MPa at the maximum angle of bending for the preflexed and straight designs, respectively. That means that at 70° of bending the straight design has a von Mises stress 82 % greater than the preflexed design.



**Fig 9-6.** Variation of von Mises stress with angle of flexion for the preflexed and straight designs

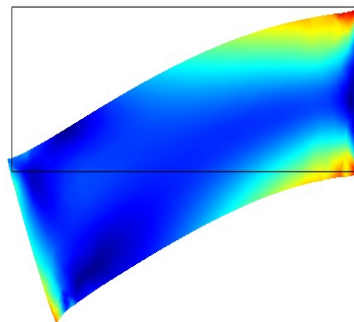


**Fig 9-7.** Stress distribution during deflexion of the FEA Model (Straight design)

## 9.9 Discussion

With the straight design the minimum stress occurs at zero angle of flexion, while the preflexed design has the minimum stress at 30° of flexion, which corresponds to its neutral

position. For the preflexed design the maximum stress was less in comparison with the straight design. That means that when the preflexed design is bent by 20 degrees, the resultant overall bending of the implant will be 50 degrees while the straight design would need to be bent by 50 degrees. The use of a preflexed part in the design proposed in this study will help to lower the stresses.

The maximum strain and tensile strength values, obtained from the literature, for the Swanson design are 300% and 6 MPa, respectively (Kult and Jira 2001). The mode of failure in elastomers is fatigue failure that is connected with strain energy density, maximum stress experienced and crack initiation (Leslie *et al.* 2008b). Reduction of the maximum stress of the design itself is welcomed as this is expected to extend the lifespan of the implant *in vivo*. After a crack has been introduced the crack growth rate is a function of the applied strain to the material (Royo 1992). The crack growth rate of the silicone implants *in vivo* is unknown. Laboratory testing of materials similar to MCP silicone implants at stresses close to the stresses calculated here predict high implant failure (Leslie *et al.* 2008b). While analysis of fracture of silicone implants has shown that crack initiation is the vital point of silicone implant fracture and that could be initiated even with a high impact of the implant *in vivo* (Joyce 2008).

The material properties that have been used are taken from the literature and as the purpose of this analysis was the comparison of the different elastomer part designs the results of this analysis fulfil the purpose of the analysis, assuming that any errors appeared are the same in both models.

## Chapter 10

### Contact stress analysis

#### 10.1 Introduction

A contact stress analysis study of different material combinations is presented in this chapter as the contact stress that the new metacarpophalangeal joint replacement experiences is vital for its success.

#### 10.2 Materials and Methods

##### 10.2.1 Model

The metacarpophalangeal joint replacement was modelled as a ball and socket joint (Fig 10-1) similar to the lubrication analysis presented in Chapter 7. In the model the ball has a radius  $R_1$ , Young's modulus  $E_1$  and Poisson's ratio  $\nu_1$ . The socket has a radius  $R_2$ , with a Young's modulus of  $E_2$ , and Poisson's ratio of  $\nu_2$ . The radial clearance between the ball and socket was defined as  $c$  where

$$c = R_2 - R_1 \quad (10-1)$$

The equivalent radius ( $R$ ) was calculated from:

$$R = \frac{R_1(R_1 + c)}{c} \quad (10-2)$$

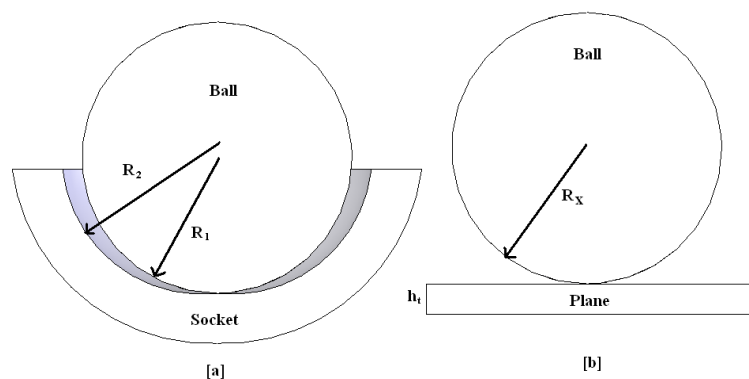


**Fig 10-1.** (a) Ball-and-socket model, (b) equivalent ball-on-plane model

### **10.2.2 Contact stresses**

The contact stress has been calculated for conventional material combinations and soft layer material combinations.

Conventional material combinations refer to:

- Cobalt Chrome molybdenum alloy (CoCr) – on - Ultra High Molecular Weight Polyethylene (UHMWPE) (Metal-on-Polyethylene material combination (MoP)).
- Cobalt Chrome alloy (CoCr) – on - Cobalt Chrome alloy (CoCr) (Metal - on – Metal material combination (MoM)).
- Zirconia - on – Zirconia (Ceramic – on – Ceramic material combination (CoC))

The soft layer material combinations refer to:

- Cobalt Chrome alloy (CoCr) – on - Polyurethane ( Metal – on – Elastomer material combination (MoE))

#### **10.2.2.1 Conventional material combinations**

For conventional material combinations the maximum contact pressure between the ball and socket was determined using Hertzian contact analysis, shown in equation 10-3 (Atkins 1998).

$$P_O = \left[ \frac{6FE_{eq}^2}{\pi^3 R_X^2} \right]^{1/3} \quad (10-3)$$

where  $F$  is the force,  $E_{eq}$  is the equivalent elastic modulus for the two bearing materials and  $R_X$  is the equivalent radius for the radii of the ball and socket. It should be noted that the maximum contact pressure is equal to the maximum contact stress at the surface of the bearing surfaces.

The equivalent elastic modulus ( $E_{eq}$ ) was calculated from:

$$\frac{1}{E_{eq}} = \frac{1 - \nu_1^2}{E_1} + \frac{1 - \nu_2^2}{E_2} \quad (10-4)$$

where  $E_1, E_2$  &  $\nu_1, \nu_2$  are the elastic moduli and Poisson's ratios of the ball and socket, respectively.

### **10.2.2.2 Soft layer material combinations**

The contact stress of the soft layer material combinations could not be described with the use of Hertzian contact theory as the Poisson's ratio approaches incompressibility (Jaffar 1989). Finite element methods and the use of inverse hydrodynamic theory has been used and formulas for the calculation of the peak contact pressure between the bearing surfaces, where one bearing surface is a soft layer, was used for the calculation of contact stresses (Unsworth and Strozzi 1994):

$$p_{max} = \frac{1}{h_t} \left( \frac{9E_2 F^2}{32\pi^2 R_X} \right)^{1/3} \quad (10-5)$$

where  $F$  is the applied load,  $h_t$  is the thickness of the soft layer,  $E_2$  is the Young's modulus of the soft layer and  $R_X$  is the equivalent radius.

### **10.2.3 Parameters**

The parameters that have been used in the contact stress analysis are shown in Table 10-1 and Table 10-2 below. The radius of the metacarpal head has been studied in the range 4 to 10 mm, according to published data on the MCP joint and implant dimensions (Beevers and Seedhom 1999; Joyce 2007b; Unsworth and Alexander 1979).

## Chapter 10

An applied load in the range 2 N to 256 N was used; this is higher than the range that has been used during the lubrication analysis in Chapter 7, as the metacarpophalangeal joint experiences high loads at low mobility (Joyce 2007b; Joyce and Unsworth 2000). At high loads there is no translation so the higher range is needed to study the effect of load in comparison with the material combination.

The radial clearance was varied from 0.08 mm to 3.5 mm going from very constrained to less constrained surfaces (Scholes *et al.* 2005; Swieszkowski *et al.* 2006).

The elastic modulus of the elastomer has been considered in the range of 5 to 25 MPa with a Poisson's ratio of 0.5 (Dowson *et al.* 1991; Quigley *et al.* 2002).

The thickness of the elastomer was varied between 0.5 and 3 mm (Unsworth and Strozzi 1994).

The values of the material parameters have been obtained from similar analysis of small joint synovial joints (Joyce 2007b; Pylios and Shepherd 2004).

**Table 10-1.** Material properties

Material	Elastic modulus (GPa)	References	Poisson's ratio	References
CoCrMo Alloy	210	(Pylios and Shepherd 2004)	0.3	(Pylios and Shepherd 2004)
UHMWPE	1	(Pylios and Shepherd 2004)	0.4	(Pylios and Shepherd 2004)
Zirconia	198	(Joyce 2007b)	0.29	(Pylios and Shepherd 2004)
Polyurethane	5-25	(Quigley <i>et al.</i> 2002)	0.5	(Dowson <i>et al.</i> 1991)

**Table 10-2.** Values of the parameters used in the contact stress analysis

<b>Parameter</b>	<b>Average value</b>	<b>Range</b>
Radius of ball (mm)	7.5	4-10
Radial clearance (mm)		0.08-3.5
Load (N)	14	2-256
Thickness of elastomer (mm)	2	0.5-3
Elastic modulus of elastomer (MPa)		5-25

## **10. 3 Results**

### ***10. 3.1 Contact stresses***

The results of the contact stress analysis are presented in Figures 10-2 to 10-7. Both conventional and soft layer material combinations are presented. Increase in the applied load increases the maximum contact stress as shown in Figures 10-2 to 10-4. In Figure 10-2 the effect of the load in all material combinations is presented, while in Figure 10-3 the effect in the cobalt chrome against UHMWPE material combination in comparison with soft layer material combination is presented as they appear the lower contact stresses according to the results presented in Figure 10-2.

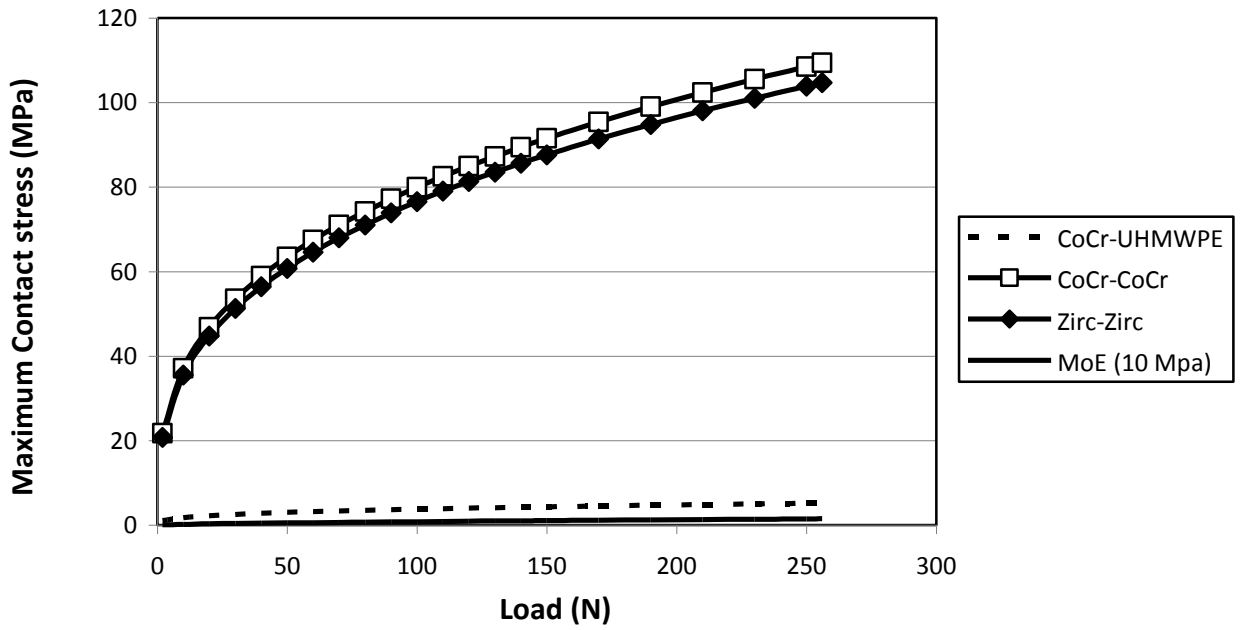


**Fig 10-2.** Effect of load on contact stresses for all material combinations (R1=7.5mm, c=0.08mm, ht=2mm)

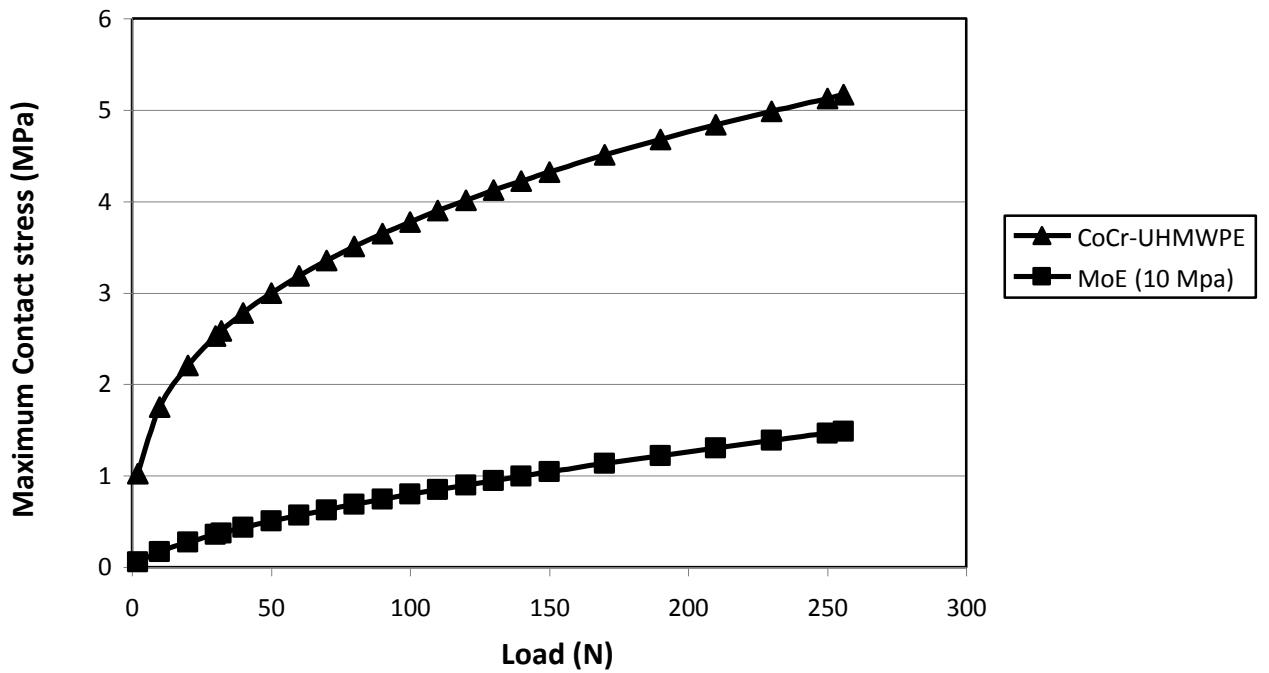


**Fig 10-3.** Effect of load on contact stress for cobalt chrome on polyethylene and metal on elastomer material combinations (R1=7.5 mm, c=0.08mm, ht=2mm)

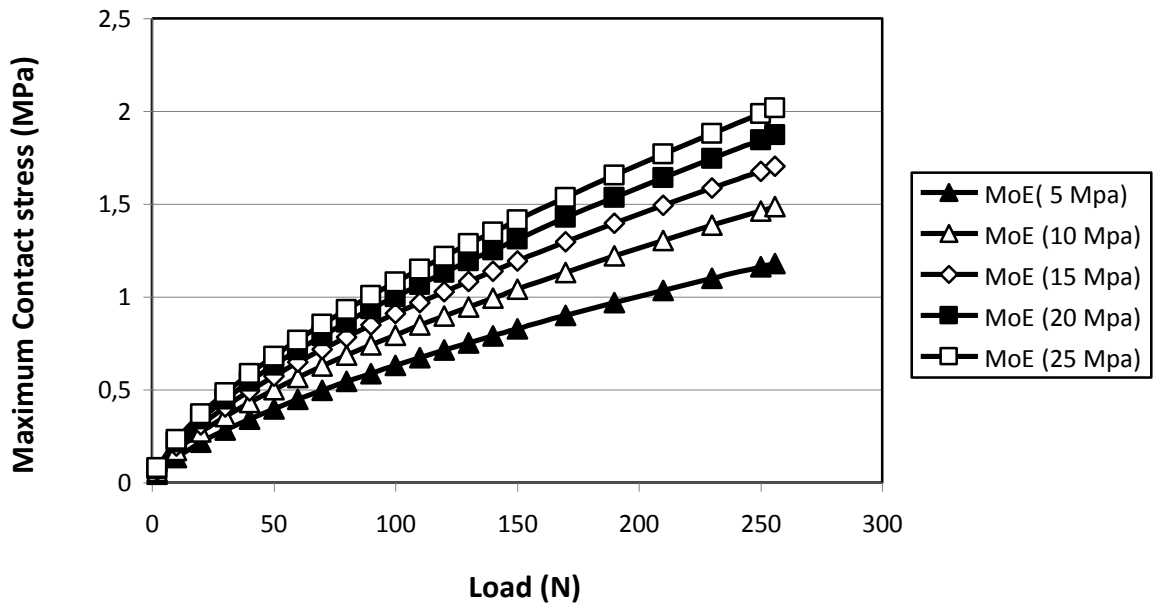


**Fig 10-4.** Effect of load on contact stress for metal on elastomer material combinations over a range of elastomer elastic modulus 5-25 MPa ( $R_1 = 7.5$  mm,  $c = 0.08$  mm,  $h_t = 2$  mm)

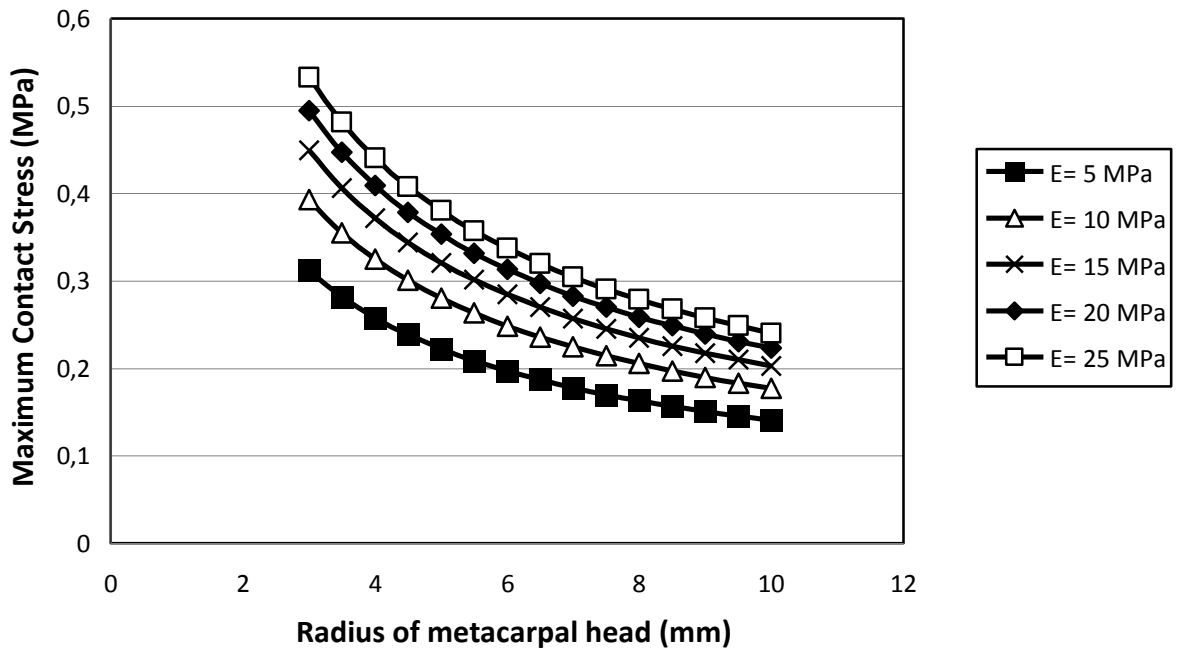


**Fig 10-5.** Effect of radius of metacarpal head on contact stress for soft layer material combinations, with variation in elastic modulus ( $R_1 = 7.5$  mm,  $c = 0.08$  mm, Load = 14 N,  $h_t = 2$  mm)

In Fig 10-4 the effect of the elastic modulus of the soft layer on contact stress with increasing loading is presented. Increase in the elastic modulus of the soft layer increases the maximum contact stresses.

According to Figure 10-5 increase in the radius of the metacarpal head decreases the maximum contact stress. Also decrease of the elastic modulus of the elastomer layer decreases the contact stresses in the soft layer material combinations.

Increase of the soft layer thickness decreases the contact stresses as can be seen in Figure 10-6.

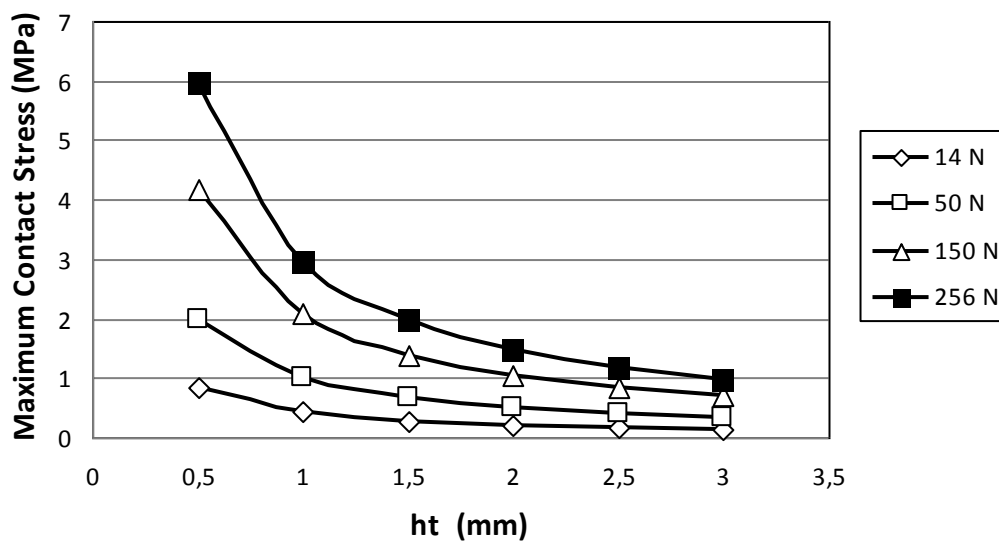


**Fig 10-6.** Effect of soft layer thickness on contact stress for different loading conditions (R1=7.5 mm, c=0.08mm, E=10 MPa)

But as has been described, increase of the thickness of the soft layer increases the shear stress as well (Unsworth and Strozzi 1994).

According to Figure 10-7 increase of the radial clearance increases the contact stresses.

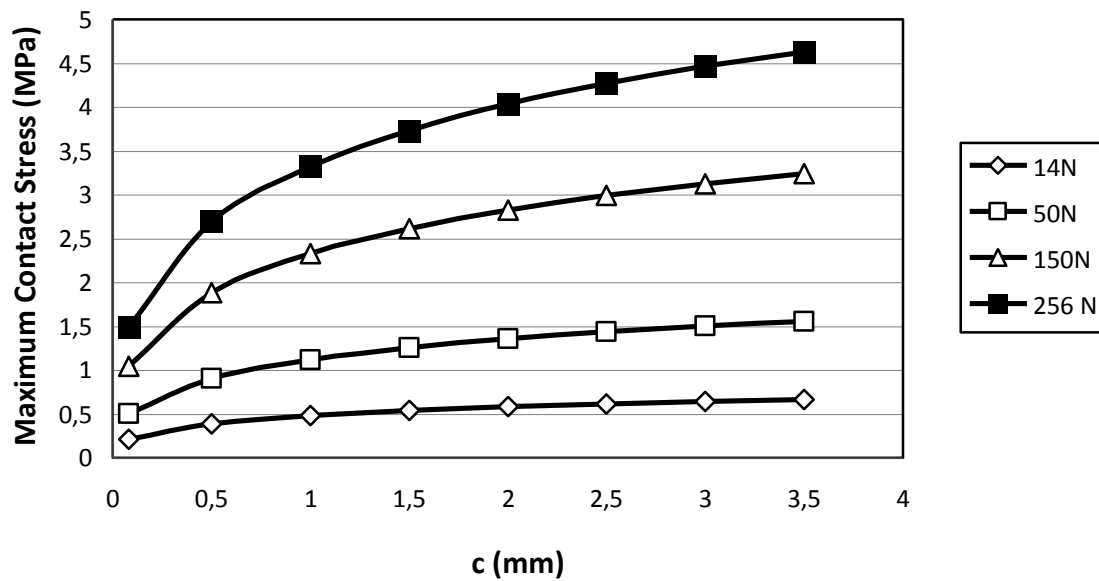


**Fig 10-7.** Effect of radial clearance on contact stress for soft layer material combinations ( $R1=7.5\text{mm}$ ,  $c=0.08\text{ mm}$ ,  $ht=2\text{ mm}$ )

Lower contact stresses can be achieved by:

- decreasing the Young's modulus of the soft layer;
- decreasing the radial clearance;
- increasing the thickness of the soft layer;
- increasing the radius of the ball.

The maximum contact stresses calculated according to Figure 10-2 in ceramic-on-ceramic and metal-on-metal materials combinations in comparison with the metal-on-polyethylene and metal-on-elastomer materials combination are high. At 50 N the calculated stresses for MoM, CoC, MoP and MoE are 64 MPa, 61 MPa, 3 MPa and 0.5 MPa, respectively. While for metal on polyethylene even for the maximum radial clearance of 3.5 mm the contact stress even for higher load of 256 N according to Figure 10-7 was less than 5 MPa.

## 10.4 Discussion

Conventional material combinations typically have bearing articulations of either a metal against a polymer or a metal against a metal. This study has predicted the likely reduction of contact pressures between the bearing surfaces that have a soft layer bearing surface. The use of a soft layer bearing surface for a MCP joint replacement implant has the potential to reduce the contact pressures between the bearing surfaces to below that of a metal against metal or metal against polymer arthroplasty device. The results of this analysis show that the contact stresses that can potentially lead to higher surface contact of the bearing surfaces can be reduced with the use of a soft layer from an elastomer material and this will be used in the novel metacarpophalangeal joint replacement. Metacarpophalangeal joints experience high loads where no motion is presented as has been described in the biomechanics of the metacarpophalangeal joint in Chapter 2 and in the lubrication analysis of the metacarpophalangeal joint prosthesis in Chapter 7. During high loading the stress distribution is vital as it will contribute to stability of the prosthesis as well as the stress distribution of the implant bone interface. Any contribution to the reduction of the stresses in the design is able to help have a longer lasting implant. A layer of low modulus material, like an elastomer, can deform macroscopically and microscopically to enhance the lubrication between the bearing surfaces (Bigsby *et al.* 1998). The squeeze film lubrication present in the cushion joints maintains the fluid film, which remains for a longer period of time in comparison with the hard-on-hard bearing surfaces (Dowson *et al.* 1991; Scholes *et al.* 2005).

## Chapter 11

### Detailed design process

#### 11.1. Introduction

During concept design selection described in Chapter 5, Concept Design 4 was chosen to be developed, as shown in Figure 11-1. In this chapter Concept 4 will be worked up to a final design. Each part will be designed to optimise the size and materials. Information detailed in Chapters 7, 8, 9 and 10 was used to help determine the final geometry and materials for the design. The detailed design process involves the evaluation of a number of different aspects of the final design that need to be revised and re-evaluated in a cyclic process prior to ending up with the final design. This process is known as risk analysis procedure and the final version is presented in Chapter 6. Here the final decisions of the design will be presented.

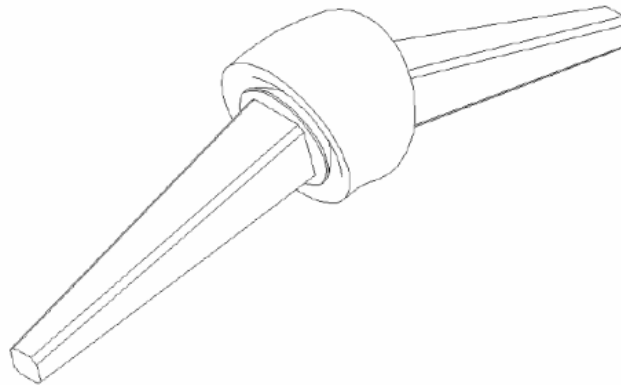


**Fig 11-1.** 3D design of Concept selection 4

Initially the whole concept design has to be divided to smaller parts that need further research for their design aspects and also separate evaluation. The whole design can be divided during the detailed design process into: metacarpal stem, metacarpal ball, middle part, proximal phalangeal ball, proximal phalange stem and the elastomer part. The final

design presented here is to be used in the index finger of the metacarpophalangeal joint, although the metacarpophalangeal joint replacement is designed for the MCP II-V the index finger (MCP II) will be used as the finger model and later the design can be accommodated to the appropriate dimensions to satisfy the other metacarpophalangeal joint sizes as well. The Solidworks CAD software (3DS Daussalt Systemes, Educational Version 2006, Lowell, MA, US) has been used for the design of the new metacarpophalangeal joint replacement.

## **11.2. Selection of model metacarpophalangeal joint for size accommodation**

The index finger has been selected as the initial model joint because the index finger has a history of use as a standard for human metacarpal studies (Barker *et al.* 2005b; Berme *et al.* 1977; Brook *et al.* 1995; Chao and An 1978; Chao *et al.* 1976; Li *et al.* 2003). Moreover the index finger is involved in both the grasp and pinch actions and it is one of the fingers that is more active in power grip (Wise 1975). The deformities of the rheumatoid arthritis are more frequent and more severe in the finger that participate more in the grasp action (Wise 1975) and the osteoarthritis mainly affects the index finger (Nunez and Citron 2005).

## **11.3. Detailed design of the implant parts**

### ***11.3.1 The metacarpal part***

Two specific aspects that should be taken into consideration in the design of the metacarpal part are the stem and the ball.

#### ***11.3.1.1 The stem of the metacarpal part***

The stem of the metacarpal will be inserted inside the medullary cavity of the metacarpal bone. The dimensions of the stem should fit the medullary cavities of the metacarpal bones

with minimal bone removal. The dimensions of the currently available metacarpophalangeal joint replacements have been considered as well together with the data presented in Table 4-1 (Avanta 2008; Swanson 2008). The aim is to minimize the stress at the bone/stem interface. Another important factor is the shape of the stem. A number of available shapes are shown in Figure 11-2 below and regarding the cementless fixation the stems should fit the medullary cavities, accommodate the elastomer part inside, avoid localized stress points, and prevent rotation of the stem inside the metacarpal bone as well. Taking all these aspects into account the design shown in Figure 11-3 has been selected for the metacarpal stem. A rectangular cross section as shown in Figure 11-2(b) has been selected with contoured corners to help the reduction of stress points and provide easier broaching and insertion of the implant's stem into the medullary cavity of the metacarpal bone.

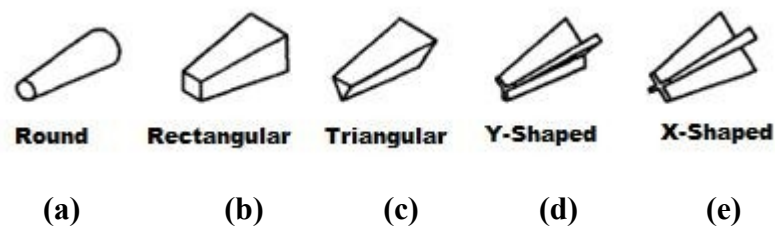


**Fig 11-2.** Stem shapes for metacarpophalangeal joint selection (adopted from (Beevers and Seedhom 1995a) )

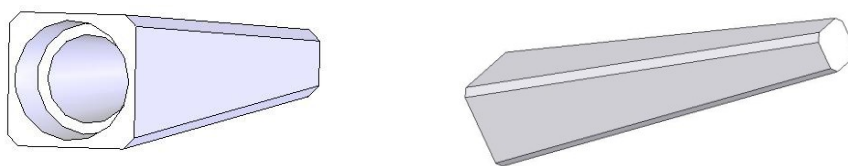


**Fig 11-3 .**Stem of metacarpal

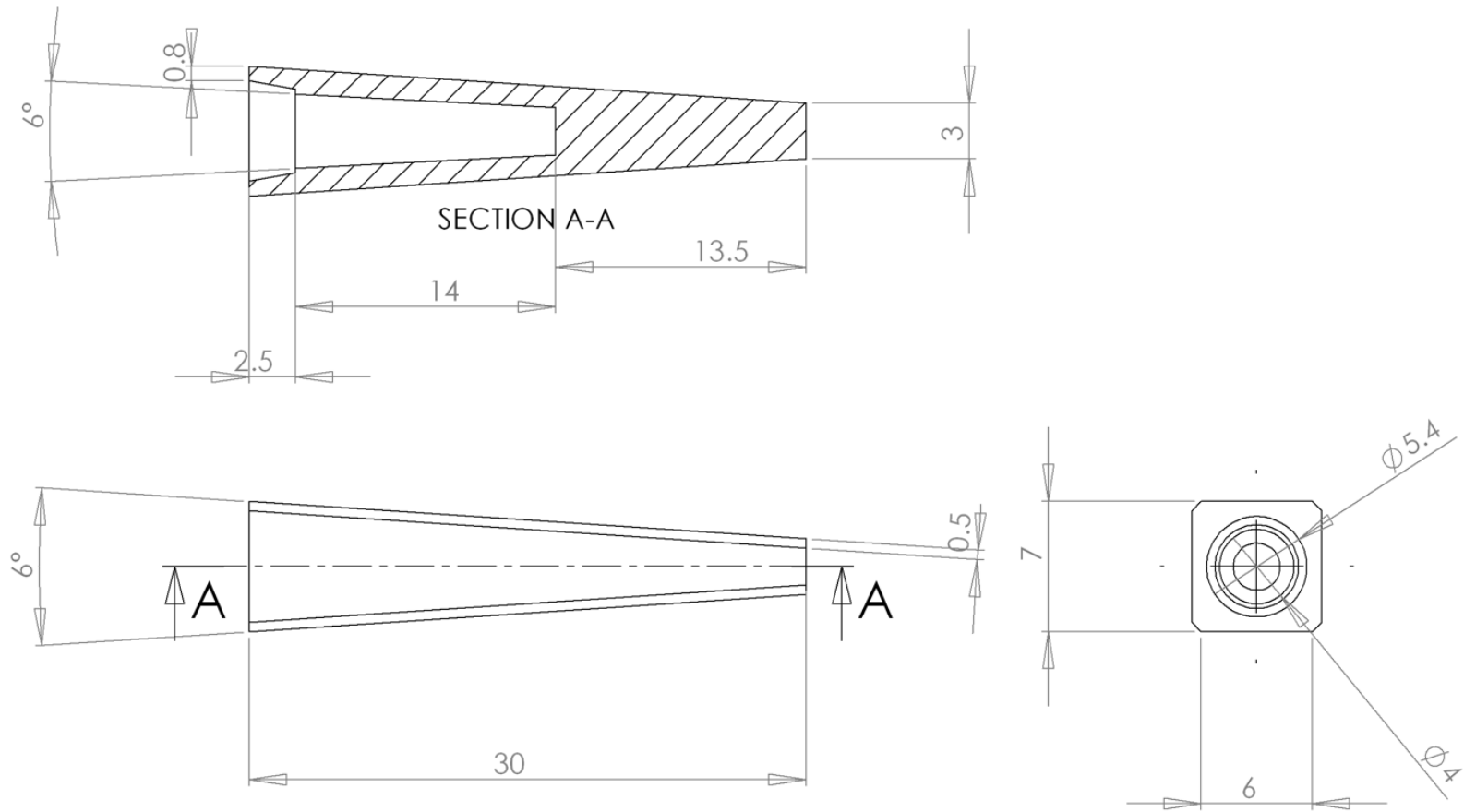
As has been analysed in Chapter 4 cementless fixation is the most appropriate method of fixation in the finger implants as the available bone stock is limited and the necessity to allow for revision surgery for implant removal or any other complication is vital not to sacrifice any additional bone. Therefore, cement is not appropriate for such a joint. Press fit

## Chapter 11

fixation has been selected and UHMWPE seems to be the most appropriate material as it can be shaped easily and it has a low elastic modulus that help stress reduction at the bone implant interface. The stem has a cavity that the elastomer part of the design fits inside. The dimensions of this cavity are larger than the dimensions of the metacarpal part of the elastomer part that will provide free motion of the one-piece inside the cavity. Also, it has a circular hole that the metacarpal head will be fitted.

The engineering drawing of the metacarpal stem is shown in Figure 11-4 with the dimensions of the final design.

Calculations on the adequate wall thickness for the interference fit for the metacarpal and proximal stem are presented in Appendix E.



Material: UHMWPE

Mechanical Engineering  
The University of  
Birmingham

All dimensions in mm

Tolerance unless otherwise stated:  
whole numbers ± 0.25  
one decimal place ± 0.10  
two decimal places ± 0.05

SCALE 3:1

Third angle projection



Drawn by  
Theodoros Pylios

Part name: Metacarpal Stem

Fig 11-4. Drawing of the metacarpal stem

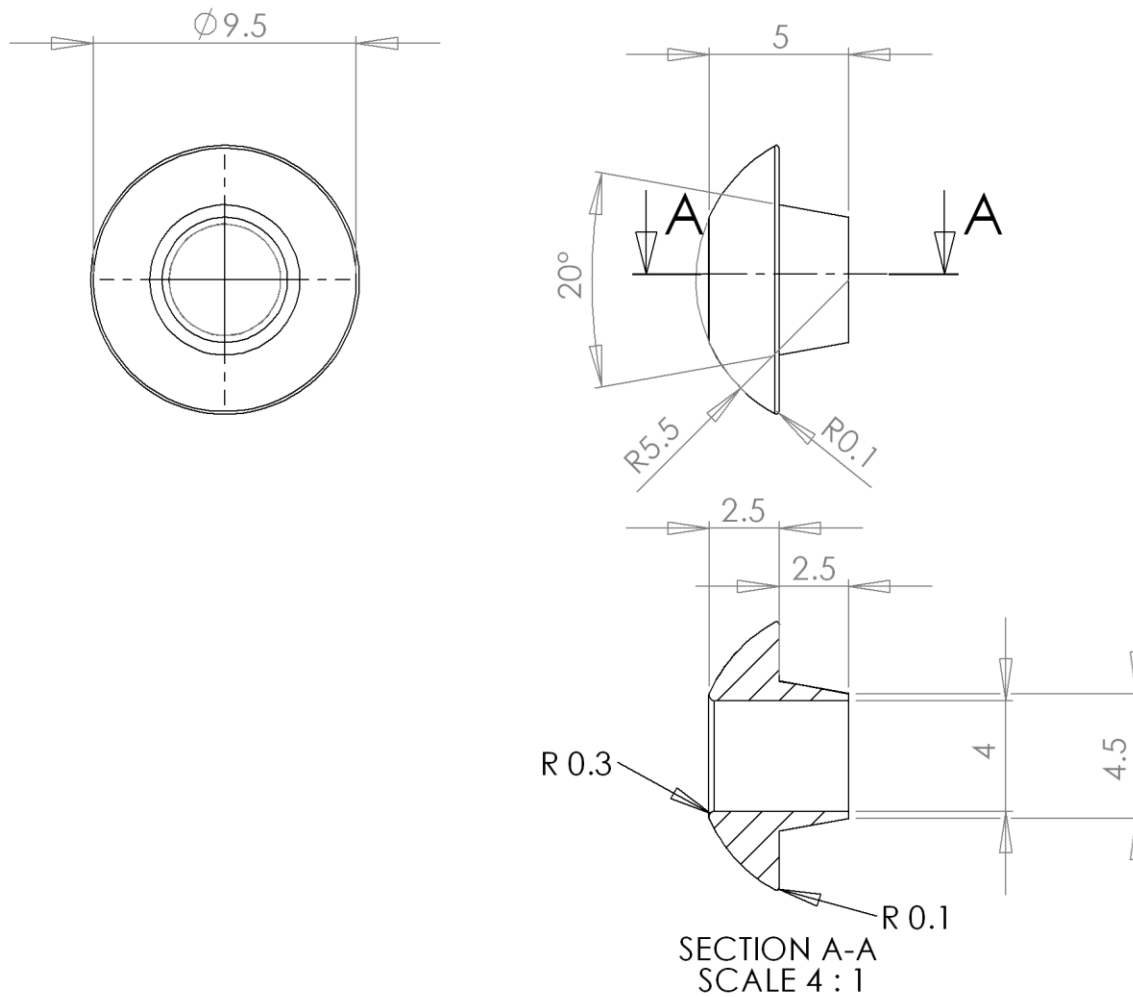
### ***11.3.1.2 The ball of the metacarpal part***

The ball of the metacarpal will be in contact with the corresponding metacarpal socket of the middle part and the reciprocal hole of the metacarpal stem. The radial clearance between the metacarpal head and the socket of the middle part determine the stability of the implant. According to the lubrication analysis and contact stress analysis presented in Chapters 7 & 10, respectively, the soft layer material combination has been found to enhance lubrication and reduce the contact stress in the ball and socket interface. The material that has been chosen for the metacarpal ball is metal and specifically cobalt chrome molybdenum alloy has been chosen as the material combination for the soft layer joints together with polyurethane in many synovial joint replacements (Scholes *et al.* 2005). In Figure 11-5 the 3D design of the ball of the metacarpal head is presented and in Figure 11-6 the engineering drawing of the metacarpal head. The surface finish of the articulating surface for CoCr should be  $0.003 \mu\text{m}$  according to Table 7-2.



**Fig 11-5.** Ball of metacarpal part

Due to the elastomer part, the translation of the metacarpal head towards the socket of the middle part is limited to succeed the functional range of motion. So there is need for the range of motion of the implant to be helped by the design itself.



Material: Cobalt Chrome

<p>Mechanical Engineering The University of Birmingham</p>	<p>All dimensions in mm</p>	<p>Tolerance unless otherwise stated: whole numbers <math>\pm 0.25</math> one decimal place <math>\pm 0.10</math> two decimal places <math>\pm 0.05</math></p>	<p>SCALE 4:1</p>	<p>Third angle projection</p>		<p>Drawn by Theodoros Pyllos</p>	<p>Part name: Metacarpal Head</p>
--	-----------------------------	--	------------------	-------------------------------	--	--------------------------------------	-----------------------------------

Fig 11-6. Drawing of metacarpal head

As the diameter of the elastomer part is smaller than the diameters of the metacarpal and proximal heads the initial degree of flexion of the design will be the result of the translation of the metacarpal head towards the metacarpal socket of the middle part and respectively the translation of the proximal head towards the corresponding socket of the middle part. After this the desired angle of flexion will be provided by bending of the elastomer part until the outer surface of the metacarpal head touches the outer surface of the metacarpal socket or respectively the proximal head the outer surface of the proximal head as can be seen in Figure 11-7 below. In Figure 11.8 the design of the metacarpophalangeal joint replacement can be seen in the extreme conditions of flexion and extension as well as in the neutral position. According to the lubrication analysis and stress analysis, the clearance of the ball and socket of the metacarpal part has to be as small as possible to enhance the lubrication and minimize the stress in the contact interface but a compromise is needed to enable the desirable range of motion the radial clearance between the metacarpal head and middle part socket has to be 3 mm, while the radial clearance between the proximal head and the corresponding middle part socket has to be 2 mm, as with these clearances it is possible for the design to succeed the desired range of motion as shown in Figure 11-7.

The metacarpal head also needs to have a hole to match the diameter with the corresponding inner diameter of the hole of the stem that has been designed to accommodate the elastomer part inside. The hole margin, shown in Figure 11-5, has to have contoured edges to avoid abrasion or scratches produced during the impingement of the elastomer part on the edges of the hole during bending of the design assembly.

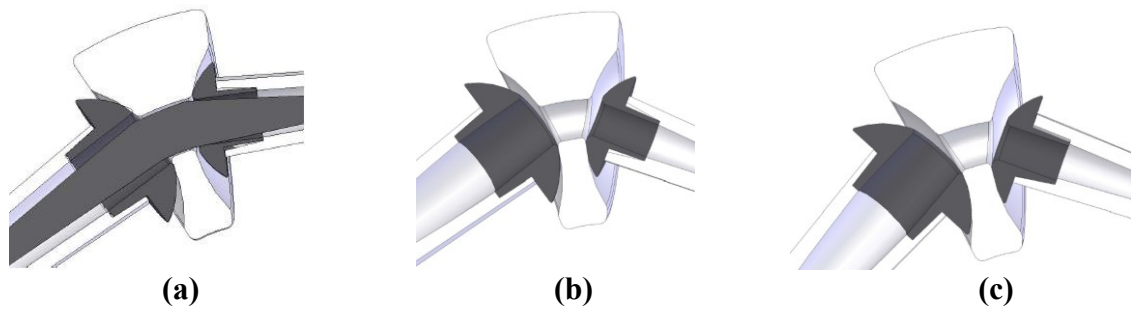


**Fig 11-7.** Section view of the assembly in different position (a) Neutral, (b) flexed, (c) Full flexion (Note: In (b) and (c) the elastomer part has been excluded for better visualisation of the flexed position)

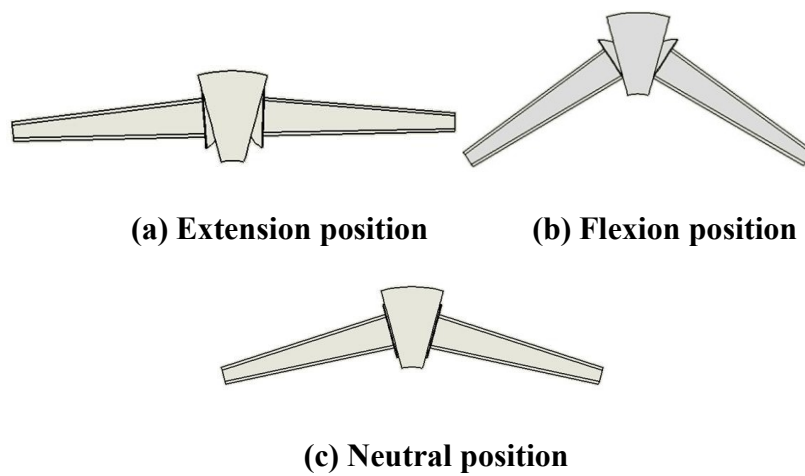


**Fig 11-8.** The MCP prosthesis design in extreme positions of extension (a), of flexion (b) and (c) in neutral position

### ***11.3.1.3 Interfaces in the metacarpal part***

The metacarpal head (ball) and stem is fixed by an interference fit. The main loads in the finger joint are compressive and as the ball will fit the hole of the stem there will be no translation and the two parts will fit in place as can be seen in Figure 11-9.

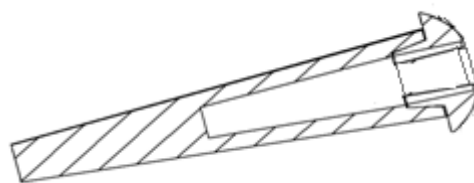


**Fig 11-9.** Cross section of the metacarpal ball stem interface

### ***11.3.2 The Middle part***

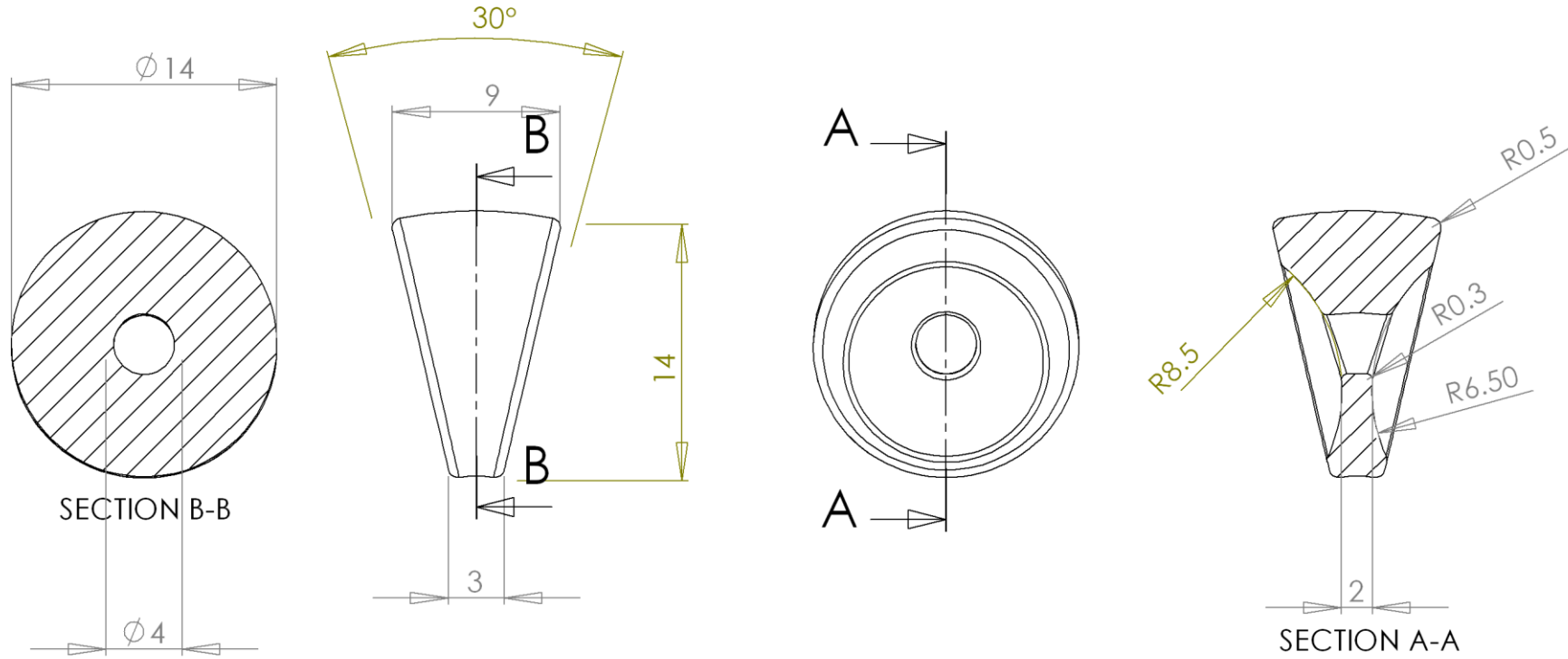
The middle part has two sockets and a hollow; the 3D design is shown in Figure 11-10.

While the engineering drawing is shown in Figure 11-11.



**Fig 11-10.** Middle part 3D design

According to the lubrication analysis in Chapter 7 and stress analysis in Chapter 10 the middle part material has been selected as an elastomer (polyurethane with an elastic modulus of 10 MPa) that represents the soft layer described in the lubrication analysis, contact stress analysis and seems to enhance the lubrication regime and lower the contact stresses (Pyllos and Shepherd 2008a). It will also act as the backing material between the two balls of the design. As can be seen in Figure 11-11 the minimum thickness of the soft layer is 2 mm.



Mechanical Engineering  
The University of  
Birmingham

All dimensions in mm

Tolerance unless otherwise stated:  
 whole numbers  $\pm 0.25$   
 one decimal place  $\pm 0.10$   
 two decimal places  $\pm 0.05$

SCALE 3:1

Third angle  
projection



Drawn by  
Theodoros Pylios

Material: Polyurethane

Part name: Middle Part

Fig 11-11. Drawing of middle part

The middle part, together with the two balls, is designed to match the dimensions of the hinge part of the Neuflex design of corresponding size as shown in Fig 11-12. The resection of the metacarpophalangeal bones will be similar to the technique used for the one-piece implants for maximum preservation of the anatomical entities of the joint.

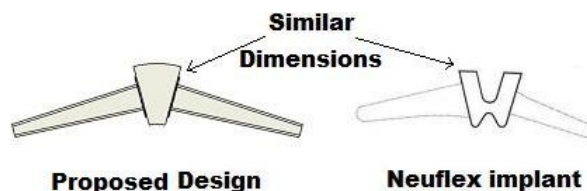


**Fig 11-12.** Comparison of central part of our design in comparison with the commercial available implant Neuflex.

### ***11.3.3 The proximal phalange part***

The proximal phalange part consisted of the proximal phalange stem and the proximal phalange ball.

#### ***11.3.3.1 The stem of the proximal phalange part***

The stem of the proximal phalange part (Fig 11-13) should be inserted inside the medullary cavity of the proximal phalange bone. It will follow the considerations described in section 11.3.1.1 for the metacarpal stem although the dimensions will be restricted to the anatomical specification of the proximal phalange dimensions. The 3D design of the proximal phalange stem is shown in Figure 11-13, while the engineering drawing is shown in Fig 11-14.

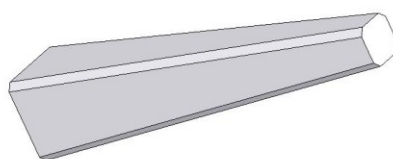


**Fig 11-13.** Proximal phalange stem

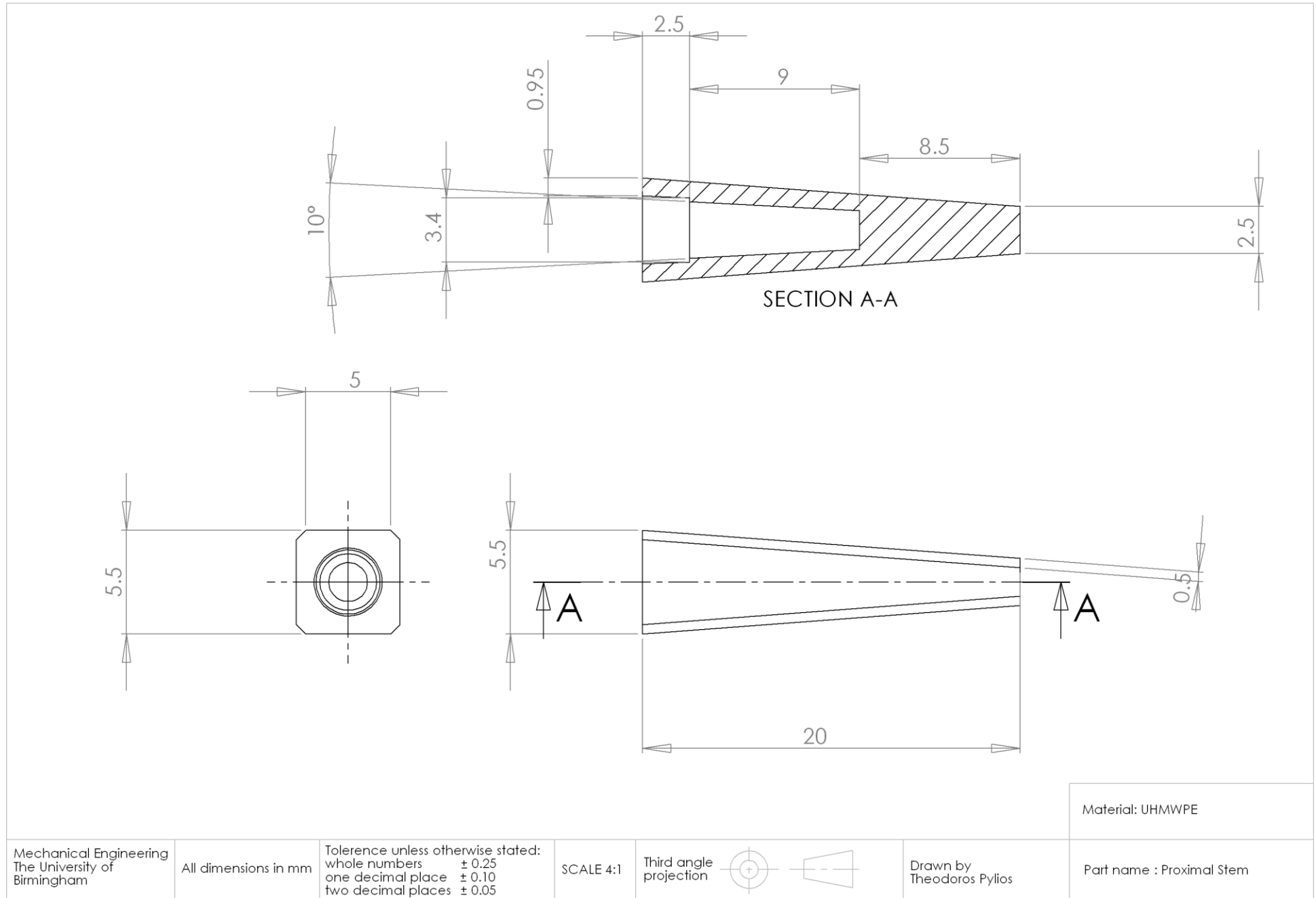


Fig. 11-14 Drawing of proximal phalange stem

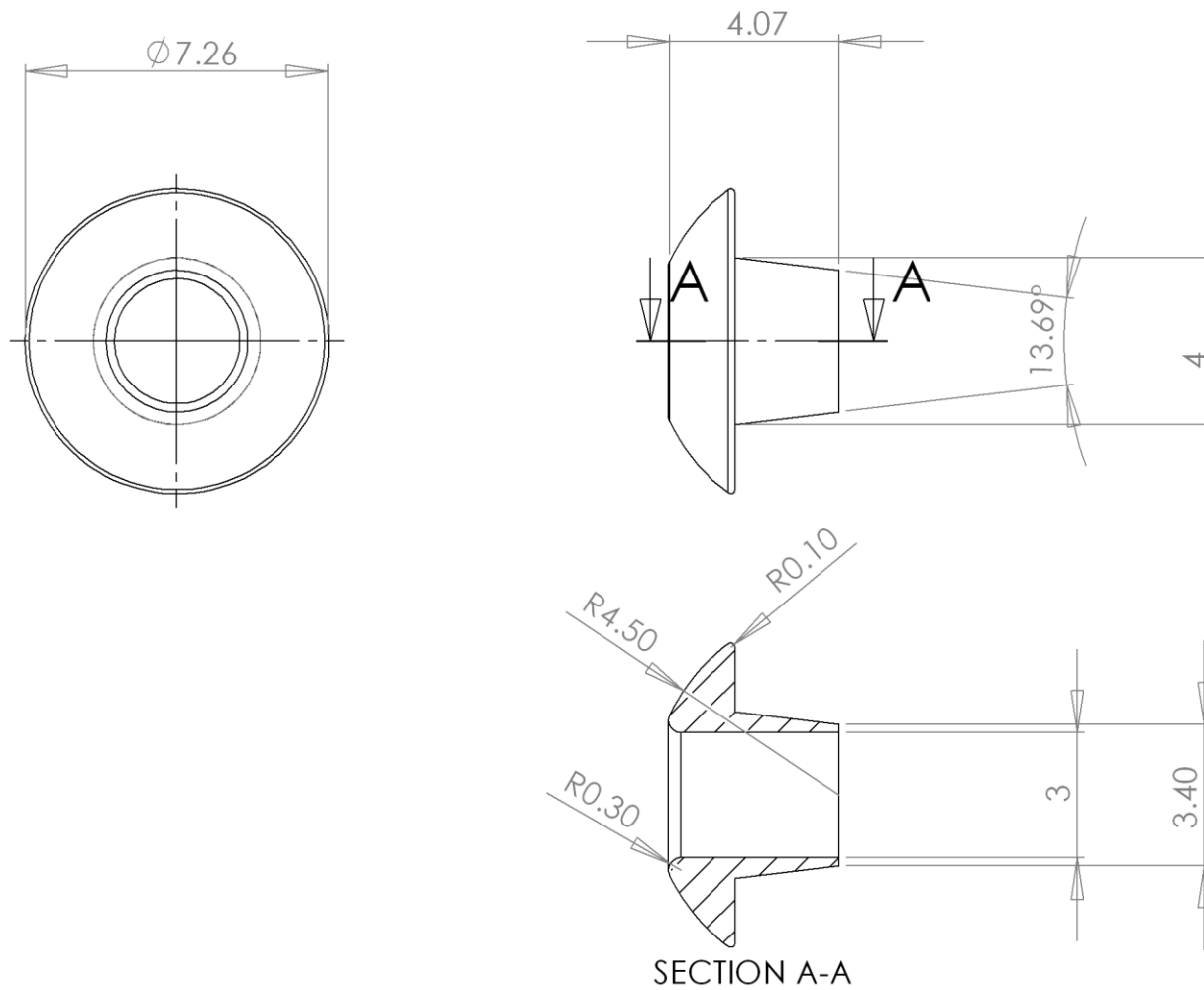
### ***11.3.3.2 The ball of the proximal phalange part***

The ball of the proximal phalange (Fig 11-15) has to be in contact with the corresponding proximal phalange socket of the middle part. It will follow the metacarpal head concept and should be modular for attachment to the proximal stem. The 3D design of the proximal phalange ball is shown in Figure 11-15, while the engineering drawing with the dimensions of the proximal phalange ball are shown in Figure 11-16. It will respectively be a CoCr head with contoured margins in the hole and the inner diameter of the hole will be the same as the inner diameter of the cavity of the corresponding proximal stem. The surface finish of the articulating surface for CoCr should be  $0.003\ \mu\text{m}$  according to Table 7-2 the same as the metacarpal head.



**Fig 11-15.** Proximal phalange head

The material of choice for the metacarpal and proximal head is CoCr although wear tests presented in Chapter 8 were conducted on titanium. That happened as the comparison was to be made between polyethylene and a metal material against silicone rubber. The results show the metal to be the material of choice. According to the lubrication analysis of small joint replacements, titanium and CoCr materials as bearing surfaces against UHMWPE appear similar in terms of minimum film thickness (Pyllos 2002). Also the CoCr has a smoother surface finish than the Titanium surfaces which will result in higher lambda ratios. Also the material combination of CoCr against polyurethane has been already proposed for soft layer joints in larger joints (Scholes *et al.* 2005). The prototype of this design that will be tested in a finger joint simulator will be manufactured by the proposed materials described in this chapter.



Material: Cobalt Chrome
Part name: Proximal Phalange Ball

Mechanical Engineering  
The University of  
Birmingham

All dimensions in mm

Tolerance unless otherwise stated:  
 whole numbers  $\pm 0.25$   
 one decimal place  $\pm 0.10$   
 two decimal places  $\pm 0.05$

SCALE 6:1

Third angle projection

Drawn by  
Theodoros Pyllos

Fig 11-16. Drawing of ball of proximal part

### ***11.3.3.3 Interfaces in the proximal phalange part***

The interfaces between the proximal phalange ball and stem shown in Figure 11.17 follow the pattern of the interfaces of the metacarpal ball and stem respectively that has been already described in section 11.3.1.3.

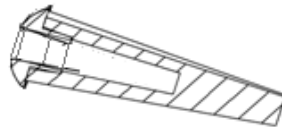


**Fig 11-17.** Cross section of proximal stem and proximal phalange head interface.

### ***11.3.4 The elastomer part***

The elastomer part will act as an internal ligament and will help in the alignment of the other parts of the assembly. It should be capable of pistoning freely inside the corresponding hollows of the stems, balls and middle part. It should, therefore, have smaller dimensions than the available size of the hollow. The drawing is shown in Figure 11-18 while the 3D design of the elastomer part is shown in Figure 11-19.

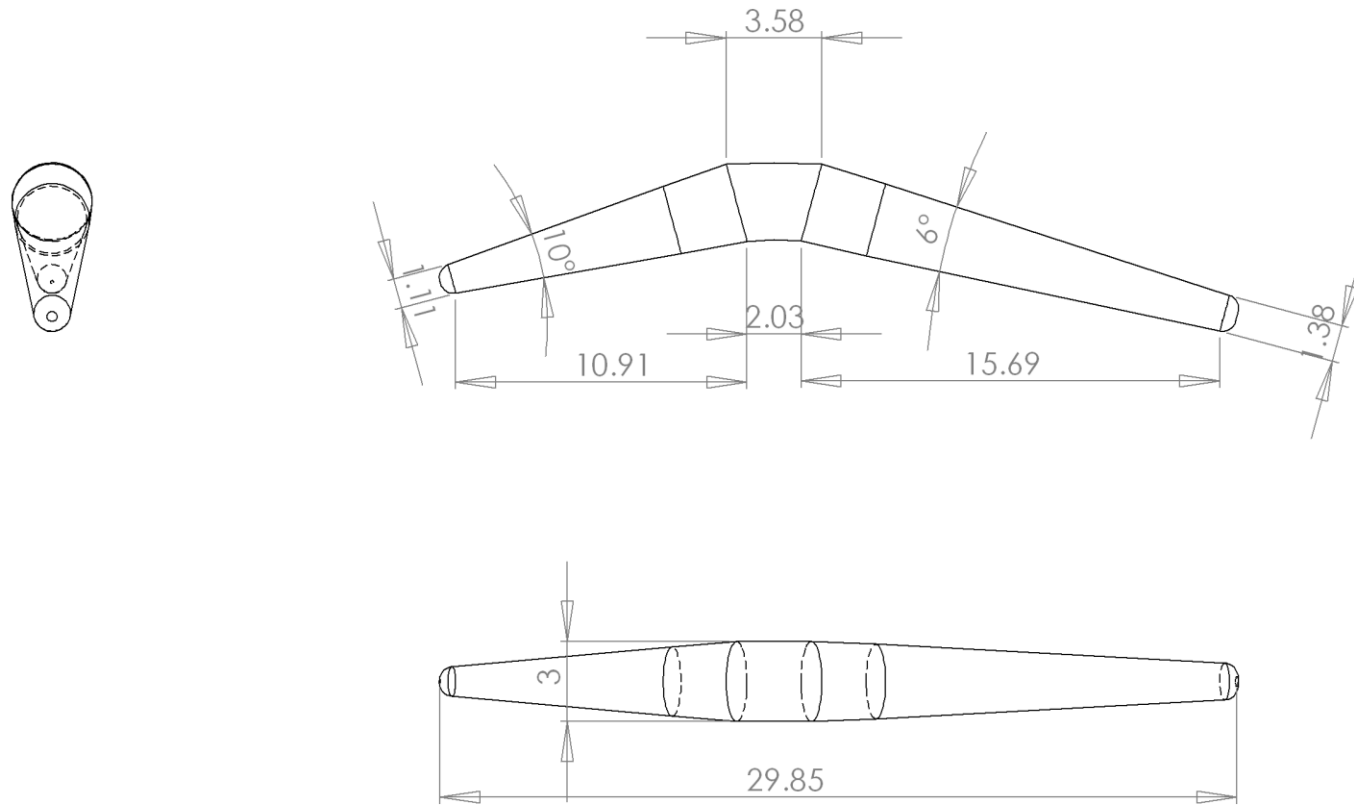
The elastomer part is actually the critical part of the assembly and finite element analysis has been used to find out the best design configuration presented in Chapter 9. Stress and strain reduction on this part will provide a longer serviceable life for the whole design.

There are two main worries about the elastomer part. First is the piston effect of the material inside the cavity of the other parts of the assembly, the wear of the material (silicone rubber or other elastomer) on elastomer, metal and polyethylene. Wear tests have been performed to find out the wear properties of these material combinations and their results are presented in Chapter 8. The elastomer part will mainly bend close to the middle part hole where the

material is CoCr due to the two heads. So according to the findings in Chapter 8 this combination presents the minimum wear between the material combinations that have been tested.

The second problem is the breakage of the elastomer part and the crack growth properties of the material (Hutchinson *et al.* 1997; Leslie *et al.* 2008a; Savory *et al.* 1994). Contoured edges in the interfaces will help prevent the initiation of scratches and also the encapsulation of the elastomer part inside the cavities of the other parts of the assembly will actually stress relief the elastomer in comparison with the one-piece silicone rubber available MCP implants. The one-piece silicone implants sustain all the forces acting on the joint while in the proposed design most of the forces are being transmitted to the ball and middle part interfaces. Also the circular cross section of the elastomer part and the free movement inside the cavities makes high stress points experienced by the past designs as described in their analysis and the sites of failures of this implants to be avoided. Also any rotation of the proximal stem along the longitudinal axis of the implant applies no torsional forces to the elastomer part as shown in Figure 11-20. In current flexible implant designs presented in Chapter 3 the cross-sections of the stems are non-circular, especially the Swanson implant's stems are contoured while the Sutter implant's rectangular leading to concentrated forces while the implant function *in vivo* (Joyce 2007a).

The offset in centrelines of the metacarpal head and proximal phalange described by Unsworth and Alexander has not been incorporated in this design or described in any of the designs reviewed in Chapter 3 as the anatomy and biomechanics of the diseased MCP joint differs from the normal joint and there are no studies describing this offset in the replacement joint (Unsworth and Alexander 1979).



Material: Silicone Rubber

Mechanical Engineering  
The University of  
Birmingham

All dimensions in mm

Tolerance unless otherwise stated:  
whole numbers ± 0.25  
one decimal place ± 0.10  
two decimal places ± 0.05

SCALE 2:1

Third angle projection

Drawn by  
Theodoros Pylios

Part name : Elastomer Part

Fig 11-18. Drawing of elastomer part



**Fig 11-19** .Elastomer part



**Fig 11-20** .Free rotation of the stems and heads towards the elastomer part

The elastomer part is quite well protected against the shear loadings that are present due to the arthritis. In shear loading the balls of the design will be compressed against the polyurethane middle part and the elastomer part will be stress relieved. In the worst case scenario when all the loading is carried by the elastomer part, an analysis had been undertaken, which is detailed in Appendix F.

#### **11.4. The assembly**

The six parts of the assembly are shown in Figure 11-21. An exploded view of the design is shown in Figure 11-22 and all the parts assembled together is shown in Figures 11-23 while the drawing is shown in Figure 11-24.

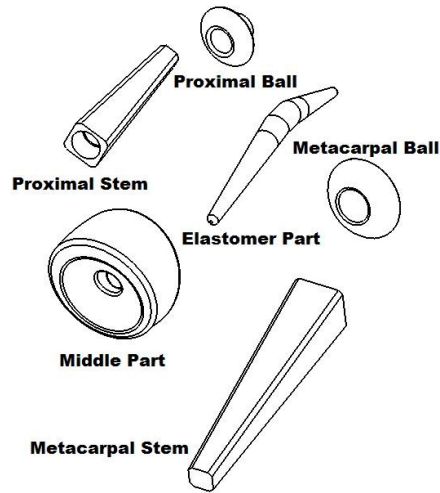


Fig 11-21. Parts of the assembly

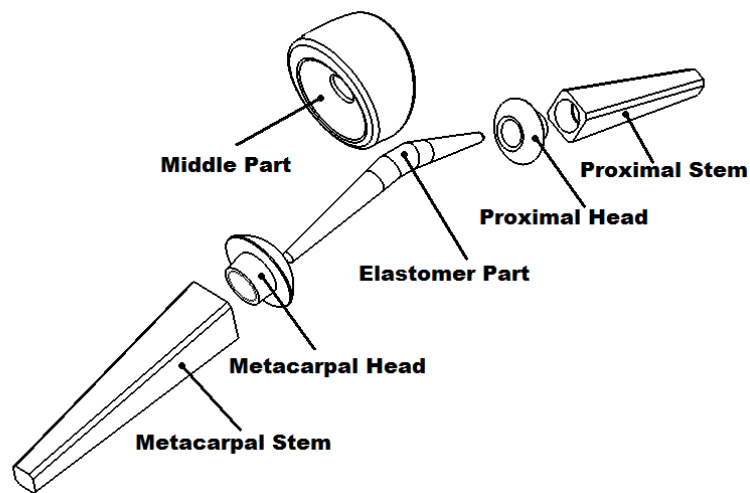


Fig 11-22. Exploded view of the assembly of the metacarpophalangeal design

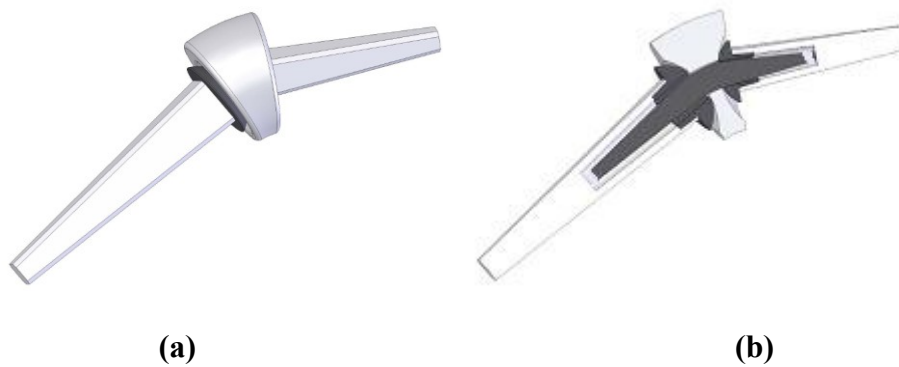


Fig 11-23. Assembly of the metacarpophalangeal final design (a) 3D view, (b) section view

## Chapter 11

The proposed design tries to incorporate a one-piece elastomer implant together with a surface replacement implant. The one-piece flexible implants are susceptible to impingement of the silicone rubber material over the sharp edges of the reamed bones as has been described extensively in this study. The use of titanium grommets by Swanson only protect the impingement of the implant material over the bone edges and give no support to the implant itself during loading (Swanson *et al.* 1997). The encapsulation of the elastomer part in this design protects the impingement of the material over the bones. Also is intended to help the elastomer part to avoid the high loading and the shear forces that the implant will experience *in vivo*.

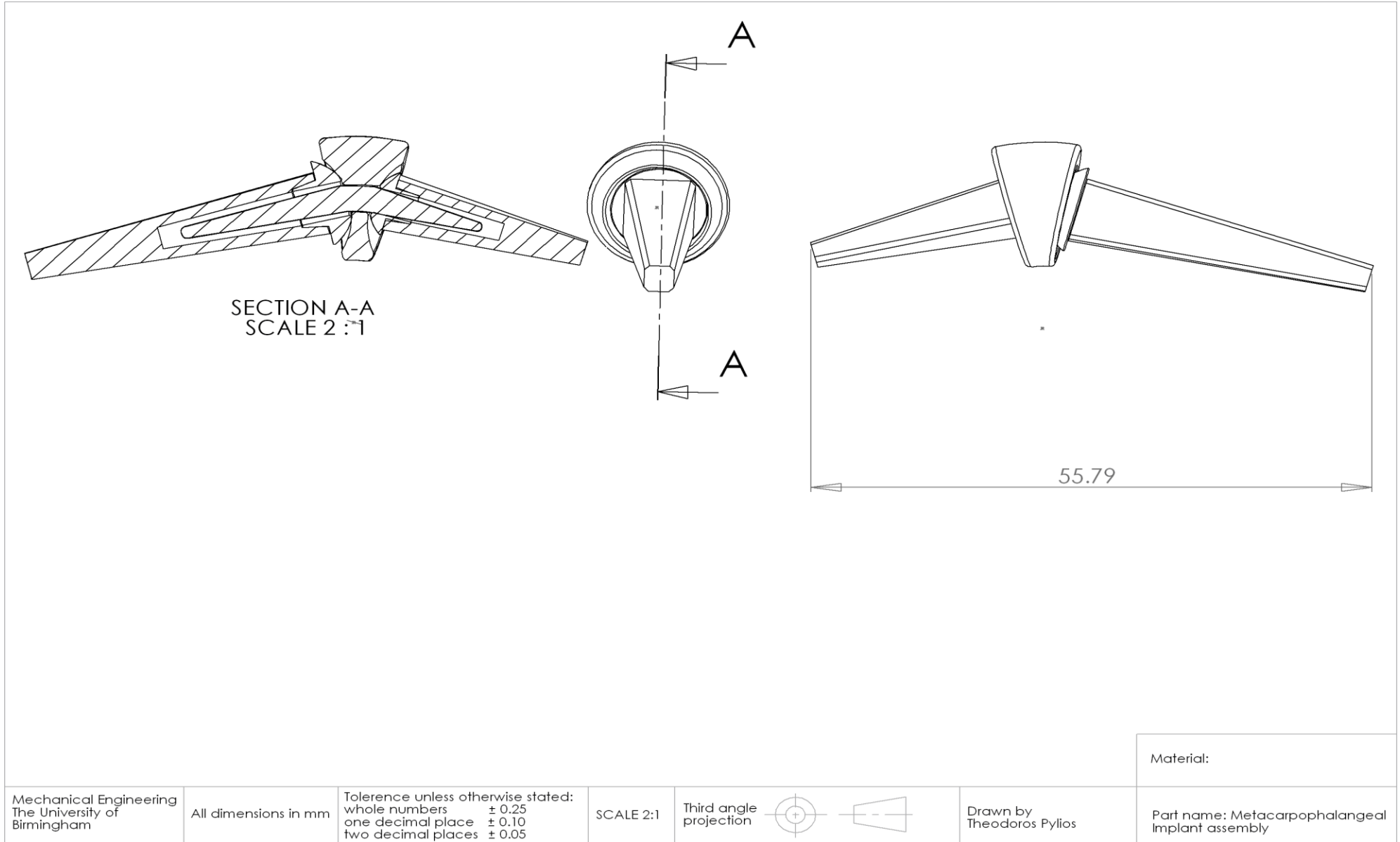


Fig 11-24. Engineering drawing of the assembly.

## **Chapter 12**

### **Overall discussion and evaluation of metacarpophalangeal joint replacement**

#### **12.1 Introduction**

The general discussion of this study will be presented in this chapter. The preclinical testing of metacarpophalangeal prosthesis is vital for their success. Many metacarpophalangeal joint prostheses can be found in the literature, as described in Chapter 3, but for few of them there are results from testing procedures and pre-clinical results available. Evaluation methods that have been used in metacarpophalangeal joint arthroplasty will be also considered.

#### **12.2 General discussion**

Following the development and completion of the new metacarpophalangeal joint replacement which was the ultimate objective of this research project, there are a number of important points of discussion that have been drawn.

Initially the study of the biomechanics of the joint of interested has been presented both in normal and diseased conditions. Both of the conditions should be considered. Initially the functionality of the normal joint that should try to be maintained after joint replacement and secondly the limitations on this functionality due to the progress and process of the disease. The diseased joint is the joint that the metacarpophalangeal joint prosthesis will be intended to replace and the disease process continues after the joint replacement.

## Chapter 12

The study and review of the current and past designs is vital as those can be the base for inspiration and a way to try and validate other designer's ideas. This is especially important when failures and follow up studies are published and their critical consideration and failure analysis could be an advantage in the design progress.

The design considerations and requirements take into account the results of the literature review on the biomechanics of the joint and the current and past designs that have been presented. The concept design procedure follows the design requirements procedure and a scoring method has been used for the selection of the concept for deeper analysis. The risk procedure is a process that helps the designer to help reduce the possible risks that the design is believed to provide.

The validation methods that have been used in this study are in correlation with the initial objectives as the design and construction of a finger simulator was out of the scope of our study. Theoretical analysis that has been proved reliable have been used for lubrication analysis and contact stress analysis to evaluate the possible material combinations that have been proposed for total joint replacement implants and dimensions of the final design.

Wear tests of possible material combinations with the design and construction of the pin-on-disk apparatus has been conducted. Two material combinations have been considered as possible materials for the critical parts of the assembly that is the elastomer part and the middle part.

Finite element analysis has been performed for the optimal shape of the vital part of our design. The design of the elastomer part has been considered and the optimal shape has been decided.

The results of all these validating procedures have been taken into account together with the restrictions and limitations that the new design appears and the compromises that are needed to be done to come up with the final proposed metacarpophalangeal joint replacement implant design. There were made compromises due to the design complexity and the available volume that the design should fit after resection of the diseased metacarpophalangeal joint.

*In-vitro* evaluation of the final design with a prototype tested in a joint simulator has not been performed but as will be described in section 12.3, the testing protocol proposed by Joyce and Unsworth and the Durham testing machine could be used to evaluate the new design as has been proved a well-validated procedure that gives reliable results close to the use of implant *in vivo* (Joyce and Unsworth 2000; Joyce and Unsworth 2002b) .

Further work supplementary to the current study could be done with our proposed metacarpophalangeal joint replacement implant design.

- The manufacturing of a prototype for testing in a finger joint simulator as has been proposed to the discussion session.
- The accommodation of the design to cover all the range of sizes that are needed to cover the human metacarpophalangeal joints.
- Propose implantation method.
- Design of necessary tooling for the surgical procedure.

### **12.3 Evaluation of metacarpophalangeal joint replacements**

Preclinical testing of the device could be divided into material evaluation and implant performance. Material testing regards biocompatibility and wear performance while implant performance regards fixation of the device into the finger bone, testing the entire implant for wear performance, fatigue and stability.

Different ways of testing could be performed in the evaluation procedure including biocompatibility tests, wear tests, finite element analysis of the entire design or critical parts, theoretical analysis of the design under conditions of worst case scenarios as well as clinical trials and follow up studies or retrospective analysis of explanted implants failed *in vivo*.

There is no worldwide accepted testing protocol for metacarpophalangeal implants. The only available ASTM standard for finger implants is the F 1781 – 97 (ASTM 1997) but no information for testing of similar implants could be derived from this. Laboratory simulation of the conditions experienced by the implant *in vivo* is not clearly specified. The force per unit area experienced by the small joints of the hand is thought to be proportionate to those in the larger joints. Ten million cycles through a normal arc of motion at near peak load for an individual joint should simulate the useful lifetime for a middle-aged finger joint. Immersion of the device in calf serum at body temperature simulates physiologic conditions. Adding multiplanar motion makes such laboratory testing difficult to devise, expensive to build, and tedious to perform (Linscheid 2000).

Several simulators for testing finger implants have been described in the literature (Schwarz *et al.* 2001; Stokoe *et al.* 1990; Whalen *et al.* 1993). A testing machine with a range of motion from 0° to 90° is shown in Podnos *et al.* (2006). The most documented finger testing machine together with the proposal of a testing protocol for testing of finger implants and evaluation of the results with retrieved implants is the Durham finger joint simulator (Fig

12-2) (Joyce and Unsworth 2000; Joyce and Unsworth 2002b). The proposed testing cycle by Joyce and Unsworth shown in Fig 12-1 and the proposed testing protocol parameters in Table 12-1 present failures for the Swanson implant similar to failures found *in vivo* from retrieved implants (Joyce and Unsworth 2000; Joyce and Unsworth 2002b).

**Table 12-1.** Proposed testing parameters for finger joint testing (Joyce and Unsworth 2000)

Test parameter	Suggested value
Flexion – extension Load (N)	10-15
Pinch Load (N)	100
Speed (Hz)	1.5
Lubricant	Bovine serum 25% v/v with distilled water
Lubricant temperature (°C)	37
Range of Motion (deg flexion)	0-90°

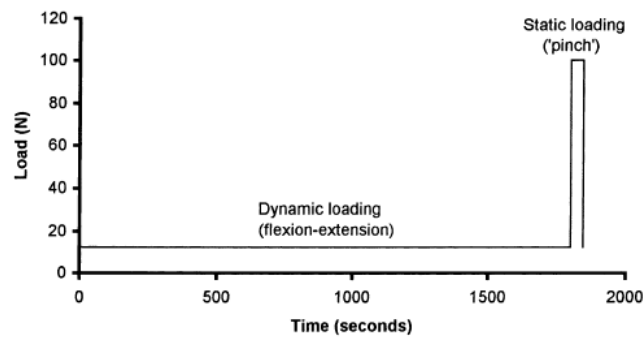


**Fig 12-1.** A typical load cycle proposed for testing finger joints in Durham simulator

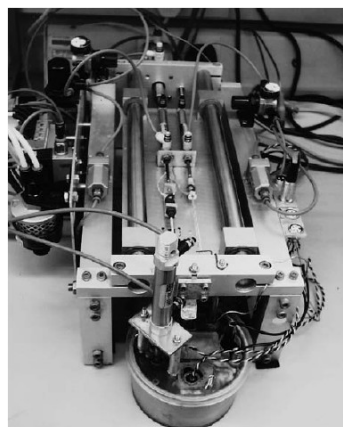


**Fig 12-2.** Durham finger joint simulator

Several studies have been found in the literature that have attempted to model finger implants (Abdul Kadir *et al.* 2008; Biddiss *et al.* 2004; Kult and Jira 2001; Kult and Vavrik

2001; Lewis *et al.* 1998; Penrose *et al.* 1996; Penrose *et al.* 1997; Podnos *et al.* 2006; Williams *et al.* 2000). More information about finite element analysis of finger implants has been presented in Chapter 9. Several studies have concentrated on the evaluation of the material used in metacarpophalangeal joint replacement. Silicone rubber is the material of choice in metacarpophalangeal joint replacement and studies regarding the performance of this material could be found in the literature (Hutchinson *et al.* 1997; Leslie *et al.* 2008b; Leslie *et al.* 2008a; Mahomed *et al.* 2008; Naidu 2007; Naidu 1997; Naidu *et al.* 1997; Savory *et al.* 1994; Swanson and Lebeau 1974). Wear studies of other materials that have been performed for finger implants are polyethylene (Joyce and Unsworth 2004; Joyce *et al.* 1996; Joyce *et al.* 2006; Joyce and Unsworth 1996; Sibly and Unsworth 1991b), ceramic materials (Doi *et al.* 1984), polycarbon materials (Cook *et al.* 1983). Studies regarding the centre of rotation in silicone implants (Weiss *et al.* 2004) as well as biomechanical evaluation of the different designs in laboratory (Gillespie *et al.* 1979). Theoretical evaluation of the different designs have been performed for lubrication analysis (Joyce 2007b) as well as stress distribution and biomechanics (Beevers and Seedhom 1995a; Beevers and Seedhom 1999)

### **12.4 Conclusions**

According to the findings of this study the following conclusions could be presented:

- The proposed implant should be able to withstand the biomechanics of the diseased joint and not try to replicate the normal joint.
- The use of the soft layer concept has been calculated to enhance the lubrication regime of the implant and reduce the contact stresses in comparison with the conventional material combinations.

- The silicone rubber material combined with metal materials provides better wear resistance in comparison with the UHMWPE material.
- A preflexed one-piece elastomer part appears to give lower stresses while succeeding the same bending in comparison with a straight design.
- The encapsulation of the elastomer part protects the elastomer from impingement against the sharp reamed and diseased bones and secondly most of the loading will be carried by the surface replacement part.
- The overall flexion of the implant is the combination of the preflexed design, the sliding of the metacarpal and proximal heads towards the middle part together with the bending of the elastomer part. In that way the elastomer part bends only a proportion of the overall flexion of the implant design.
- A one piece flexible implant has been proven unable to withstand the diseased metacarpophalangeal joint while a surface replacement implant is able to function in diseased joint with minor deformities; a combination of them as has been described in this study could provide a new alternative implant design that could last for longer.

## References

- Abdul Kadir, M.R., Kamsah, N., and Aminullah, M.A. (2008), "Finite element study of Metacarpophalangeal Joint Silicone implants," **4th Kuala Lumpur International Conference On Biomedical Engineering -Kuala Lumpur Malaysia-Springer**, 420-423
- Adams, B. D., Blair, W. F., and Shurr, D. G. (1990), "Schultz metacarpophalangeal arthroplasty: a long-term follow-up study," **Journal of Hand Surgery [Am]**, 15 (4), 641-645
- Aichinson, G. A., Hukins, D. W., Parry, J. J., Shepherd, D. E., and Trotman, S. G. (2009), "A review of the design process for implantable orthopedic medical devices," **The Open Biomedical Engineering Journal**, 3, 21-27
- An, K. N., Chao, E. Y., Cooney, W. P., and Linscheid, R. L. (1985), "Forces in the normal and abnormal hand," **Journal of Orthopaedic Research**, 3 (2), 202-211
- Ash, H. E., Joyce, T. J., and Unsworth, A. (1996), "Biomechanics of the distal upper limb," **Current Orthopaedics**, 10, 25-36
- Ash, H. E. and Unsworth, A. (2000), "Design of a surface replacement prosthesis for the proximal interphalangeal joint," **Proceedings of the Institution of Mechanical Engineers Part H-Journal of Engineering in Medicine**, 214 (2), 151-163
- ASTM (1996), "Standard Test Method for Pin Abrasion Testing ASTM G132-96," **West Conshohocken: American Society for Testing and Materials**
- ASTM (1997), "Standard Specification for Elastomeric Flexible Hinge Finger Total Joint Implants ASTM F-1781-97," **West Conshohocken: American Society for Testing and Materials**
- ASTM (2000), "Standard Test Method for Wear Testing of Polymeric Materials Used in Total joint Prostheses ASTM F372-00," **West Conshohocken: American Society for Testing and Materials**
- Atkins, A. G. (1998), "Stress analysis," in Kempe's Engineers Year-Book, Stephens, J.H., Ed. Tonbridge: Miller Freeman.
- Auger, D. D., Dowson, D., Fisher, J., and Jin, Z. M. (1993), "Friction and lubrication in cushion form bearings for artificial hip joints," **Proceedings of the Institution of Mechanical Engineers Part H-Journal of Engineering in Medicine**, 207 (1), 25-33
- Avanta (2008), "Prosthesis Brochure," 27 November, [http://www.totalsmallbone.com/us/pdfs/SoftSkeletal\\_brochure.pdf](http://www.totalsmallbone.com/us/pdfs/SoftSkeletal_brochure.pdf)
- Barker, D. S., Schultz, C., Krishnan, J., and Hearn, T. C. (2005b), "Bilateral symmetry of the human metacarpal: Implications for sample size calculations," **Clinical Biomechanics**, 20, 846-852

## References

- Bass, R. L., Stern, P. J., and Nairus, J. G. (1996), "High implant fracture incidence with Sutter silicone metacarpophalangeal joint arthroplasty," **Journal of Hand Surgery [Am]**, 21 (5), 813-818
- Beckenbaugh, R. D. (1976), "Reconstructing the crippled arthritic hand," **Geriatrics**, 31 (3), 89-93
- Beckenbaugh, R. D. (1977), "New concepts in arthroplasty of the hand and wrist," **Archives in Surgery**, 112 (9), 1094-1098
- Beckenbaugh, R. D. (2003), "[Arthroplasty of the metacarpophalangeal joint using pyrocarbonate implants]," **Orthopade**, 32 (9), 794-797
- Beckenbaugh, R. D., Dobyns, J. H., Linscheid, R. L., and Bryan, R. S. (1976), "Review and analysis of silicone-rubber metacarpophalangeal implants," **Journal of Bone and Joint Surgery [Am]**, 58 (4), 483-487
- Beevers, D. J. and Seedhom, B. B. (1993), "Metacarpophalangeal joint prostheses: a review of past and current designs," **Proceedings of the Institution of Mechanical Engineers Part H-Journal of Engineering in Medicine**, 207 (4), 195-206
- Beevers, D. J. and Seedhom, B. B. (1995a), "Design of a non-constrained, non-cemented, modular, metacarpophalangeal prosthesis," **Proceedings of the Institution of Mechanical Engineers Part H-Journal of Engineering in Medicine**, 209 (3), 185-195
- Beevers, D. J. and Seedhom, B. B. (1995b), "Metacarpophalangeal joint prostheses. A review of the clinical results of past and current designs," **Journal of Hand Surgery [Br]**, 20 (2), 125-136
- Beevers, D. J. and Seedhom, B. B. (1999), "A new concept for a metacarpophalangeal prosthesis: consequence on joint biomechanics," **Clinical Biomechanics**, 14 (3), 166-176
- Berne, N., Paul, J. P., and Purves, W. K. (1977), "A biomechanical analysis of the metacarpophalangeal joint," **Journal of Biomechanics**, 10 (7), 409-412
- Biddiss, E.A., Bogoch, E. R., and Meguid, S.A. (2004), "Three-dimensional finite element analysis of prosthetic finger joint implants," **International Journal of Mechanics and Materials in Design**, 1, 317-328
- Bieber, E. J., Weiland, A. J., and Volenec-Dowling, S. (1986), "Silicone-rubber implant arthroplasty of the metacarpophalangeal joints for rheumatoid arthritis," **Journal of Bone and Joint Surgery [Am]**, 68 (2), 206-209
- Bigsby, R. J., Auger, D. D., Jin, Z. M., Dowson, D., Hardaker, C. S., and Fisher, J. (1998), "A comparative tribological study of the wear of composite cushion cups in a physiological hip joint simulator," **Journal of Biomechanics**, 31 (4), 363-369
- Blair, S. J., Swanson, A. B., and Swanson, G. D. (1989), "Evaluation of impairment of hand and upper extremity function," **Instructional Course Lectures**, 38, 73-102

## References

- Blair, W. F., Shurr, D. G., and Buckwalter, J. A. (1984), "Metacarpophalangeal joint arthroplasty with a metallic hinged prosthesis," **Clinical Orthopaedics and Related Research** (184), 156-163
- Blazar, P. E. and Bozentka, D. J. (1997), "Metacarpophalangeal arthroplasty," **Seminars in Arthroplasty**, 8 (2), 128-134
- Boast, B. and Coveney, V. A. (1999), Finite element analysis of elastomers: Professional Engineering Publishing.
- Bogoch, E. R. and Judd, M. G. (2002), "The hand: a second face?" **Journal of Rheumatology**, 29 (12), 2477-2483
- Bogoch, E. R. and Moran, E. L. (1999), "Bone abnormalities in the surgical treatment of patients with rheumatoid arthritis," **Clinical Orthopaedics and Related Research** (366), 8-21
- Bono, Edward de (1999), Six thinking hats. London: Penguin Books.
- Branam, B. R., Tuttle, H. G., Stern, P. J., and Levin, L. (2007), "Resurfacing arthroplasty versus silicone arthroplasty for proximal interphalangeal joint osteoarthritis," **Journal of Hand Surgery [Am]**, 32 (6), 775-788
- Brannon, E. W. and Klein, G. (1959), "Experiences with a finger-joint prosthesis," **Journal of Bone and Joint Surgery [Am]**, 41 (1), 87-102
- Brewerton, D. A. (1957), "Hand deformities in rheumatoid disease," **Annals of Rheumatic Diseases**, 16 (2), 183-197
- Brook, N., Mizrahi, J., Shoham, M., and Dayan, J. (1995), "A biomechanical model of index finger dynamics," **Medical Engineering and Physics**, 17 (1), 54-63
- Calnan, J. S. and Reis, N. D. (1968a), "Artificial finger joints in rheumatoid arthritis, I. Development and experimental assessment," **Annals of Rheumatic Diseases**, 27, 207-217
- Calnan, J. S. and Reis, N. D. (1968b), "The development and use of an artificial finger joint," **Bio-Medical Engineering**, 3, 314-319
- Caravia, L., Dowson, D., and Fisher, J. (1993), "Start up and steady state friction of thin polyurethane layers," **Wear**, 160, 191-197
- Caravia, L., Dowson, D., Fisher, J., Corkhill, P. H., and Tighe, B. J. (1995), "Friction of Hydrogel and Polyurethane Elastic Layers When Sliding against Each Other under a Mixed Lubrication Regime," **Wear**, 181, 236-240
- Caravia, L., Dowson, D., Fisher, J., and Jobbins, B. (1990), "The influence of bone and bone cement debris on counterface roughness in sliding wear tests of ultra-high molecular

## References

weight polyethylene on stainless steel," **Proceedings of the Institution of Mechanical Engineers Part H-Journal of Engineering in Medicine**, 204 (1), 65-70

Chao, E. Y. and An, K. N. (1978), "Graphical interpretation of the solution to redundant problem in Biomechanics," **Journal of Biomechanical Engineering**, 100, 159-167

Chao, E. Y., Opgrande, J. D., and Axmear, F. E. (1976), "Three-dimensional force analysis of finger joints in selected isometric hand functions," **Journal of Biomechanics**, 9 (6), 387-396

Charnley, John (1970), *Acrylic Cement in Orthopaedic Surgery*. Edinburgh: E&S Livingstone.

Cole, K. J. and Abbs, J. H. (1986), "Coordination of three-joint digit movements for rapid finger-thumb grasp," **Journal of Neurophysiology**, 55 (6), 1407-1423

Cook, S. D., Beckenbaugh, R. D., Redondo, J., Popich, L. S., Klawitter, J. J., and Linscheid, R. L. (1999), "Long-term follow-up of pyrolytic carbon metacarpophalangeal implants," **Journal of Bone and Joint Surgery [Am]**, 81 (5), 635-648

Cook, S. D., Beckenbaugh, R., Weinstein, A. M., and Klawitter, J. J. (1983), "Pyrolite carbon implants in the metacarpophalangeal joint of baboons," **Orthopedics**, 6 (8), 952-961

Cook, S. D., Thomas, K. A., and Kester, M. A. (1989), "Wear characteristics of the canine acetabulum against different femoral prostheses," **Journal of Bone and Joint Surgery [Br]**, 71 (2), 189-197

Costa, L., Bracco, P., and Brach del Prever, E.M. (2007), "Physicochemical and mechanical properties of UHMWPE a 45 years experience," **Interactive Surgery**, 2 (3-4), 169-173

Cowan, F. S., Allen, J. K., and Mistree, F. (2006), "Functional modelling in engineering design: A pespectual approach featuring living systems theory," **Systems Research and Behavioral Science**, 23, 365-381

Daecke, W., Veyel, K., Wieloch, P., Jung, M., Lorenz, H., and Martini, A-K. (2006), "Osseointegration and Mechanical Stability of Pyrocarbon and Titanium Hand Implants in a Load-Bearing In Vivo Model for Small Joint Arthroplasty," **Journal of Hand Surgery [Am]**, 31 (1), 90-97

Degeorges, R., Laporte, S., Pessis, E., Mitton, D., Goubier, J. N., and Lavaste, F. (2004), "Rotations of three-joint fingers: a radiological study," **Surgical and Radiologic Anatomy**, 26 (5), 392-398

DeHeer, D. H., Owens, S. R., and Swanson, A. B. (1995), "The host response to silicone elastomer implants for small joint arthroplasty," **Journal of Hand Surgery [Am]**, 20 (3 Pt 2), S101-109

## References

Delaney, R., Trail, I. A., and Nuttall, D. (2005), "A comparative study of outcome between the Neuflex and Swanson metacarpophalangeal joint replacements," **Journal of Hand Surgery [Br]**, 30 (1), 3-7

Dellhag, B. and Bjelle, A. (1999), "A five-year followup of hand function and activities of daily living in rheumatoid arthritis patients," **Arthritis Care and Research**, 12 (1), 33-41

Derkash, R. S., Niebauer, J. J., Jr., and Lane, C. S. (1986), "Long-term follow-up of metacarpal phalangeal arthroplasty with silicone Dacron prostheses," **Journal of Hand Surgery [Am]**, 11 (4), 553-558

Devas, M. and Shah, V. (1975), "Link arthroplasty of the metacarpo-phalangeal joints. A preliminary report of a new method," **Journal of Bone and Joint Surgery [Br]**, 57 (1), 72-77

Doi, K., Kuwata, N., and Kawai, S. (1984), "Alumina ceramic finger implants: a preliminary biomaterial and clinical evaluation," **Journal of Hand Surgery [Am]**, 9 (5), 740-749

Dominick, K. L., Jordan, J. M., Renner, J. B., and Kraus, V. B. (2005), "Relationship of radiographic and clinical variables to pinch and grip strength among individuals with osteoarthritis," **Arthritis and Rheumatism**, 52 (5), 1424-1430

Dowson, D., Fisher, J., Jin, Z. M., Auger, D. D., and Jobbins, B. (1991), "Design considerations for cushion form bearings in artificial hip joints," **Proceedings of the Institution of Mechanical Engineers Part H-Journal of Engineering in Medicine**, 205 (2), 59-68

Dowson, D. and Yao, J. Q. (1994), "Elastohydrodynamic lubrication of soft-layered solids at elliptical contacts. Part 2: film thickness analysis," **Proceedings of the Institution of Mechanical Engineers Part J-Journal of Engineering Tribology**, 208, 43-52

Eiken, O. and Hagert, C. G. (1981), "Finger joint replacement," **Recent Advances in Plastic Surgery**, 2, 101-113

EN14971, Medical Devices - Application of Risk Management to Medical Devices (2000), "ISO EN 14971," **European Committee of Standardization**

Erdogan, A. and Weiss, A. P. (2003), "[NeuFlex Silastic implant in metacarpophalangeal joint arthroplasty]," **Orthopade**, 32 (9), 789-793

Ferlic, D. C., Clayton, M. L., and Holloway, M. (1975), "Complications of silicone implant surgery in the metacarpophalangeal joint," **Journal of Bone and Joint Surgery [Am]**, 57 (7), 991-994

Flatt, A. E. (1961), "Restoration of rheumatoid finger joint function," **Journal of Bone and Joint Surgery [Am]**, 43 (5), 753-774

## References

- Flatt, A. E. (1967), "Prosthetic substitution for rheumatoid finger joints," **Plastic and Reconstructive Surgery**, 40 (6), 565-570
- Flatt, A. E. (1973), "Studies in finger joint replacement. A review of the present position," **Archives in Surgery**, 107 (3), 437-443
- Flatt, A. E. (1980), "New joints for old," **Journal of Hand Surgery [Am]**, 5 (6), 525-527
- Flatt, A. E. and Ellison, M. R. (1972), "Restoration of rheumatoid finger joint function. 3. A follow-up note after fourteen years of experience with a metallic-hinge prosthesis," **Journal of Bone and Joint Surgery [Am]**, 54 (6), 1317-1322
- Flatt, A. E. and Fischer, G. W. (1969), "Biomechanical factors in the replacement of rheumatoid finger joints," **Annals of Rheumatic Diseases**, 28 (5), Suppl:36-41
- Fleming, S. G. and Hay, E. L. (1984), "Metacarpophalangeal joint arthroplasty eleven year follow-up study," **Journal of Hand Surgery [Br]**, 9 (3), 300-302
- Foliart, D. E. (1995), "Swanson silicone finger joint implants: a review of the literature regarding long-term complications," **Journal of Hand Surgery [Am]**, 20 (3), 445-449
- Foliart, D. E. (1997), "Synovitis and silicone joint implants: a summary of reported cases," **Plastic and Reconstructive Surgery**, 99 (1), 245-252
- Fowler, N. K. and Nicol, A. C. (2001b), "Long-term measurement of metacarpophalangeal joint motion in the normal and rheumatoid hand," **Proceedings of the Institution of Mechanical Engineers Part H-Journal of Engineering in Medicine**, 215 (6), 549-553
- Fowler, N. K. and Nicol, A. C. (2002), "A biomechanical analysis of the rheumatoid index finger after joint arthroplasty," **Clinical Biomechanics**, 17 (5), 400-405
- Fraser, A., Vallow, J., Preston, A., and Cooper, R. G. (1999), "Predicting 'normal' grip strength for rheumatoid arthritis patients," **Rheumatology (Oxford)**, 38 (6), 521-528
- Gillespie, T. E., Flatt, A. E., Youm, Y., and Sprague, B. L. (1979), "Biomechanical evaluation of metacarpophalangeal joint prosthesis designs," **Journal of Hand Surgery [Am]**, 4 (6), 508-521
- Gold, R. H., Bassett, L. W., and Seeger, L.L. (1988), "The other arthritides," **Radiologic Clinics of North America**, 26 (6), 1195-1212
- Goldfarb, C. A. and Stern, P. J. (2003), "Metacarpophalangeal joint arthroplasty in rheumatoid arthritis. A long-term assessment," **Journal of Bone and Joint Surgery [Am]**, 85 (10), 1869-1878
- Goldner, J. L., Gould, J. S., Urbaniak, J. R., and McCollum, D. E. (1977), "Metacarpophalangeal joint arthroplasty with silicone-Dacron prostheses (Niebauer type): six and a half years' experience," **Journal of Hand Surgery [Am]**, 2 (3), 200-211

## References

- Griffiths, R. W. and Nicolle, F. V. (1975), "Three years' experience of metacarpophalangeal joint replacement in the rheumatoid hand," **Hand**, 7 (3), 275-283
- Hagena, F. W. and Mayer, B. (2005), "Destruction of metacarpophalangeal joints in rheumatoid arthritis. Indications and results with the ELOGENICS™ MCP prosthesis," **Aktuelle Rheumatologie**, 30, 125-133
- Hagert, C. G. (1975a), "Metacarpophalangeal joint implants. II. Roentgenographic study of the Niebauer--Cutter Metacarpophalangeal Joint Prosthesis," **Scandinavian Journal of Plastic and Reconstructive Surgery**, 9 (2), 158-164
- Hagert, C. G. (1975b), "Metacarpophalangeal joint implants. III. Roentgenographic study of the in vivo function," **Scandinavian Journal of Plastic and Reconstructive Surgery**, 9 (3), 216-226
- Hagert, C. G. (1975c), "Implants designed for finger joints. A roentgenographic study and a study of implant wear and tear," **Scandinavian Journal of Plastic and Reconstructive Surgery**, 9 (1), 53-63
- Hagert, C. G. (1978), "Advances in hand surgery: finger joint implants," **Surgery Annual**, 10, 253-275
- Hagert, C. G., Branemark, P. I., Albrektsson, T., Strid, K. G., and Irstam, L. (1986), "Metacarpophalangeal joint replacement with osseointegrated endoprostheses," **Scandinavian Journal of Plastic and Reconstructive Surgery and Hand Surgery**, 20 (2), 207-218
- Hagert, C. G., Eiken, O., Ohlsson, N. M., Aschan, W., and Movin, A. (1975), "Metacarpophalangeal joint implants. I. Roentgenographic study on the silastic finger joint implant, swanson design," **Scandinavian Journal of Plastic and Reconstructive Surgery**, 9 (2), 147-157
- Hall, R. M., Unsworth, A., Siney, P., and Wroblewski, B. M. (1996), "Wear in retrieved Charnley acetabular sockets," **Proceedings of the Institution of Mechanical Engineers Part H-Journal of Engineering in Medicine**, 210 (3), 197-207
- Hamrock, B. J. (1994), *Fundamentals of fluid film lubrication*. New York: McGraw-Hill Companies.
- Hamrock, B. J. and Dowson, D. (1978), "Elastohydrodynamic Lubrication of Elliptical Contacts for Materials of Low Elastic-Modulus I - Fully Flooded Conjunction," **Journal of Lubrication Technology-Transactions of the Asme**, 100 (2), 236-245
- Harkonen, R., Piirtomaa, M., and Alaranta, H. (1993), "Grip strength and hand position of the dynamometer in 204 Finnish adults," **Journal of Hand Surgery [Br]**, 18 (1), 129-132
- Harris, D. and Dias, J. J. (2003), "Five-year results of a new total replacement prosthesis for the finger metacarpo-phalangeal joints," **Journal of Hand Surgery [Br]**, 28 (5), 432-438

## References

- Helliwell, P. S., Howe, A., and Wright, V. (1988), "An evaluation of the dynamic qualities of isometric grip strength," **Annals of Rheumatic Diseases**, 47 (11), 934-939
- Herren, D. B., Schindele, S., Goldhahn, J., and Simmen, B. R. (2006), "Problematic bone fixation with pyrocarbon implants in proximal interphalangeal joint replacement: short-term results," **Journal of Hand Surgery [Br]**, 31 (6), 643-651
- Hill, David (1998), Design engineering of biomaterials for medical devices. Chichester: John Wiley & Sons.
- Hills, B. A. (2000), "Boundary lubrication in vivo," **Proceedings of the Institution of Mechanical Engineers Part H-Journal of Engineering in Medicine**, 214 (1), 83-94
- Hirakawa, K., Bauer, T. W., Culver, J. E., and Wilde, A. H. (1996), "Isolation and quantitation of debris particles around failed silicone orthopedic implants," **Journal of Hand Surgery [Am]**, 21 (5), 819-827
- Haupt, P. (2000), "Cemented and non-cemented biological fixation and osseointegration: design and clinical behaviour," in Hand Arthroplasties, Simmen, B. R., Allieu, Y., Luch, A., Stanley, J., Eds. London: Martin Dunitz Ltd.
- Hume, M. C., Gellman, H., McKellop, H., and Brumfield, R. H., Jr. (1990), "Functional range of motion of the joints of the hand," **Journal of Hand Surgery [Am]**, 15 (2), 240-243
- Hutchinson, D. T., Savory, K. M., and Bachus, K. N. (1997), "Crack-growth properties of various elastomers with potential application in small joint prostheses," **Journal of Biomedical Materials Research**, 37 (1), 94-99
- Ibrahim, Talal and Taylor, Grahame John Saint Clair (2004), "The new press-fit ceramic Moje metatarsophalangeal joint replacement: short-term outcomes," **The Foot**, 14 (3), 124
- Ishikawa, H., Murasawa, A., and Hanyu, T. (2002), "The effect of activity and type of rheumatoid arthritis on the flexible implant arthroplasty of the metacarpophalangeal joint," **Journal of Hand Surgery [Br]**, 27 (2), 180-183
- Jaffar, M. J. (1989), "Asymptotic behaviour of thin elastic layers bonded and unbonded to a rigid foundation," **International Journal of Mechanical Sciences**, 31 (3), 229-235
- Jagatia, M. and Jin, Z. M. (2002), "Analysis of elastohydrodynamic lubrication in a novel metal-on-metal hip joint replacement," **Proceedings of the Institution of Mechanical Engineers Part H-Journal of Engineering in Medicine**, 216 (3), 185-193
- Jalali-Vahid, D., Jagatia, N., Jin, Z. M., and Dowson, D. (2001), "Prediction of lubricating film thickness in a ball-in-socket model with a soft lining representing human natural and artificial hip joints," **Proceedings of the Institution of Mechanical Engineers Part J-Journal of Engineering Tribology**, 215 (J4), 363-372

## References

- Jin, Z. M. (2002), "Analysis of mixed lubrication mechanism in metal-on-metal hip joint replacements," **Proceedings of the Institution of Mechanical Engineers Part H-Journal of Engineering in Medicine**, 216 (1), 85-89
- Jin, Z. M., Dowson, D., and Fisher, J. (1993), "Wear and friction of medical grade polyurethane sliding on smooth metal counterfaces," **Wear**, 162-164, 627-630
- Jin, Z. M., Stone, M., Ingham, E., and Fisher, J. (2006), "(v) Biotribology," **Current Orthopaedics**, 20 (1), 32-40
- Johnson, K. L., Greenwood, J. A., and Poon, S. Y. (1972), "A simple theory of asperity contact in elastohydro-dynamic lubrication," **Wear**, 19 (1), 91-108
- Jones, A. R., Unsworth, A., and Haslock, I. (1985), "A microcomputer controlled hand assessment system used for clinical measurement," **Engineering in Medicine**, 14 (4), 191-198
- Joyce, T. J. (2003), "Snapping the fingers," **Journal of Hand Surgery [Br]**, 28 (6), 566-567
- Joyce, T. J. (2004), "Currently available metacarpophalangeal prostheses: their designs and prospective considerations," **Expert Review of Medical Devices**, 1 (2), 193-204
- Joyce, T. J. (2007a), "Letter to the Editor," **Journal of Hand Surgery [Br]**, 32 (2), 236
- Joyce, T. J. (2007b), "Prediction of lubrication regimes in two-piece metacarpophalangeal prostheses," **Medical Engineering and Physics**, 29 (1), 87-92
- Joyce, T. J. (2008), "Analysis of the mechanism of fracture of silicone metacarpophalangeal prostheses," **Journal of Hand Surgery [Eur Vol]**, Corrected proof - In press
- Joyce, T. J. (2009), "Analysis of the mechanism of fracture of silicone metacarpophalangeal prostheses," **J Hand Surg Eur Vol**, 34 (1), 18-24
- Joyce, T. J., Ash, H. E., and Unsworth, A. (1996), "The wear of cross-linked polyethylene against itself," **Proceedings of the Institution of Mechanical Engineers Part H-Journal of Engineering in Medicine**, 210 (1), 11-16
- Joyce, T. J., Milner, R. H., and Unsworth, A. (2003), "A comparison of ex vivo and in vitro Sutter metacarpophalangeal prostheses," **Journal of Hand Surgery [Br]**, 28 (1), 86-91
- Joyce, T. J., Rieker, C., and Unsworth, A. (2006), "Comparative in vitro wear testing of PEEK and UHMWPE capped metacarpophalangeal prostheses," **Bio-Medical Materials and Engineering**, 16 (1), 1-10
- Joyce, T. J. and Unsworth, A. (1996), "A comparison of the wear of cross-linked polyethylene against itself with the wear of ultra-high molecular weight polyethylene against itself," **Proceedings of the Institution of Mechanical Engineers Part H-Journal of Engineering in Medicine**, 210 (4), 297-300

## References

- Joyce, T. J. and Unsworth, A. (2000), "The design of a finger wear simulator and preliminary results," **Proceedings of the Institution of Mechanical Engineers Part H-Journal of Engineering in Medicine**, 214 (5), 519-526
- Joyce, T. J. and Unsworth, A. (2001), "The wear of artificial finger joints using different lubricants in a new finger wear simulator," **Wear**, 250, 199-205
- Joyce, T. J. and Unsworth, A. (2002a), "A literature review of "failures" of the Swanson finger prosthesis in the metacarpophalangeal joint," **Hand Surgery**, 7 (1), 139-146
- Joyce, T. J. and Unsworth, A. (2002b), "A test procedure for artificial finger joints," **Proceedings of the Institution of Mechanical Engineers Part H-Journal of Engineering in Medicine**, 216 (2), 105-110
- Joyce, T. J. and Unsworth, A. (2005), "NeuFlex metacarpophalangeal prostheses tested in vitro," **Proceedings of the Institution of Mechanical Engineers Part H-Journal of Engineering in Medicine**, 219 (2), 105-110
- Joyce, T. and Unsworth, A. (2004), "Wear studies of all UHMWPE couples under various bio-tribological conditions," **Journal of Applied Biomaterials & Biomechanics**, 2, 29-34
- Kay, A. G., Jeffs, J. V., and Scott, J. T. (1978), "Experience with Silastic prostheses in the rheumatoid hand. A 5-year follow-up," **Annals of Rheumatic Diseases**, 37 (3), 255-258
- Kessler, I. (1974), "A new silicone implant for replacement of destroyed metacarpal heads," **Hand**, 6 (3), 308-310
- Khoo, C. T. (1993), "Silicone synovitis. The current role of silicone elastomer implants in joint reconstruction," **Journal of Hand Surgery [Br]**, 18 (6), 679-686
- Khoo, C. T., Davison, J. A., and Ali, M. (2004), "Tissue reaction to titanium debris following Swanson arthroplasty in the hand: a report of two cases," **Journal of Hand Surgery [Br]**, 29 (2), 152-154
- Kimani, B. M., Trail, I. A., Hearnden, A., Delaney, R., and Nuttall, D. (2009), "Survivorship of the Neuflex silicone implant in MCP joint replacement," **J Hand Surg Eur Vol**, 34 (1), 25-28
- Kimball, H. L., Terrono, A. L., Feldon, P., and Zelouf, D. S. (2003), "Metacarpophalangeal joint arthroplasty in rheumatoid arthritis," **Instructional Course Lectures**, 52, 163-174
- King, P. H. and Fries, R. C. (2003), *Design of Biomedical device and Systems*. New York: Marcel Dekker.
- Kirschenbaum, D., Schneider, L. H., Adams, D. C., and Cody, R. P. (1993), "Arthroplasty of the metacarpophalangeal joints with use of silicone-rubber implants in patients who have rheumatoid arthritis. Long-term results," **Journal of Bone and Joint Surgery [Am]**, 75 (1), 3-12

## References

- Knutson, J. S., Kilgore, K. L., Mansour, J. M., and Crago, P. E. (2000), "Intrinsic and extrinsic contributions to the passive moment at the metacarpophalangeal joint," **Journal of Biomechanics**, 33 (12), 1675-1681
- Koh, S., Buford, W. L., Jr., Andersen, C. R., and Viegas, S. F. (2006), "Intrinsic muscle contribution to the metacarpophalangeal joint flexion moment of the middle, ring, and small fingers," **Journal of Hand Surgery [Am]**, 31 (7), 1111-1117
- Kujala, S., Bongiorno, V., Leppilahti, J., Kaarela, O., and Ryhanen, J. (2006), "Pyrolytic carbon MCP arthroplasty: A report of seven prostheses implanted in two patients," **Journal of Orthopaedics and Traumatology**, 7 (1), 12
- Kult, J. and Jira, J. (2001), "Computational model of Swanson's PIP joint implant," **Computer Methods in Biomechanical & Biomedical Engineering** 4
- Kult, J. and Vavrik, D. (2001), "Experimental methods used for verification of the computational model of silicon rubber implant," **39th International conference-Experimental Stress Analysis**
- Kung, P. L., Chou, P., Linscheid, R. L., Berglund, L. J., Cooney, W. P., 3rd, and An, K. N. (2003), "Intrinsic stability of an unconstrained metacarpophalangeal joint implant," **Clinical Biomechanics**, 18 (2), 119-125
- Labi, M. L., Gresham, G. E., and Rathey, U. K. (1982), "Hand function in osteoarthritis," **Archives of Physical Medicine and Rehabilitation**, 63 (9), 438-440
- Lanzetta, M., Herbert, T. J., and Conolly, W. B. (1994), "Silicone synovitis. A perspective," **Journal of Hand Surgery [Br]**, 19 (4), 479-484
- Lazar, G. and Schuller-Ellis, F. P. (1980), "Intramedullary structure of human metacarpals," **Journal of Hand Surgery [Am]**, 5 (5), 477-481
- Leslie, L. J., Jenkins, M. J., Shepherd, D. E., and Kukureka, S. N. (2008a), "The effect of the environment on the mechanical properties of medical grade silicones," **J Biomed Mater Res B Appl Biomater**, 86B (2), 460-465
- Leslie, L., Kukureka, S., and Shepherd, D. E. (2008b), "Crack growth of medical-grade silicone using pure shear tests," **Proceedings of the Institution of Mechanical Engineers Part H-Journal of Engineering in Medicine**, 222 (6), 977-982
- Levack, B., Stewart, H. D., Flierenga, H., and Helal, B. (1987), "Metacarpo-phalangeal joint replacement with a new prosthesis: description and preliminary results of treatment with the Helal flap joint," **Journal of Hand Surgery [Br]**, 12 (3), 377-381
- Lewis, G., Jonathan, V., and Kambhampati, S. (1998), "Effect of material property representation on stresses in endoprostheses," **Bio-Medical Materials and Engineering**, 8 (1), 11-23

## References

- Li, Z-M., Pfaeffle, H. J., Sotereanos, D. G., Goitz, R. J., and Woo, S. L-Y. (2003), "Multi-directional strength and force envelope of the index finger," **Clinical Biomechanics**, 18, 908-915
- Li, Z. M. (2002), "The influence of wrist position on individual finger forces during forceful grip," **Journal of Hand Surgery [Am]**, 27 (5), 886-896
- Li, Z. M., Zatsiorsky, V. M., and Latash, M. L. (2000), "Contribution of the extrinsic and intrinsic hand muscles to the moments in finger joints," **Clinical Biomechanics**, 15 (3), 203-211
- Li, Z. M., Zatsiorsky, V. M., and Latash, M. L. (2001), "The effect of finger extensor mechanism on the flexor force during isometric tasks," **Journal of Biomechanics**, 34 (8), 1097-1102
- Linscheid, R. L. (2000), "Implant arthroplasty of the hand: retrospective and prospective considerations," **Journal of Hand Surgery [Am]**, 25 (5), 796-816
- Linscheid, R. L. and Chao, E. Y. (1973), "Biomechanical assessment of finger function in prosthetic joint design," **Orthopedic Clinics of North America**, 4 (2), 317-330
- Linscheid, R. L. and Dobyns, J. H. (1979), "Total joint arthroplasty. The hand," **Mayo Clinic Proceedings**, 54 (8), 516-526
- Lundborg, G., Besjakov, J., and Branemark, P. I. (2007), "Osseointegrated wrist-joint prostheses: a 15-year follow-up with focus on bony fixation," **Scandinavian Journal of Plastic and Reconstructive Surgery and Hand Surgery**, 41 (3), 130-137
- Lundborg, G. and Branemark, P. I. (2001), "Osseointegrated silicone implants for joint reconstruction after septic arthritis of the metacarpophalangeal joint: a 10-year follow-up," **Scandinavian Journal of Plastic and Reconstructive Surgery and Hand Surgery**, 35 (3), 311-315
- Lundborg, G., Branemark, P. I., and Carlsson, I. (1993), "Metacarpophalangeal joint arthroplasty based on the osseointegration concept," **Journal of Hand Surgery [Br]**, 18 (6), 693-703
- Madhav, T. J. and Stern, P. J. (2007), "Current opinions in orthopaedics: Advances in joint replacement in the hand and wrist," **Current Opinion in Orthopaedics**, 18 (4), 352
- Mahomed, A., Chidi, N. M., Hukins, D. W., Kukureka, S. N., and Shepherd, D. E. (2008), "Frequency dependence of viscoelastic properties of medical grade silicones," **Journal of Biomedical Materials Research - Part B Applied Biomaterials**, Corrected Proof - in press DOI 10.1002/jbm.b.31208
- Mandl, L. A., Galvin, D. H., Bosch, J. P., George, C. C., Simmons, B. P., Axt, T. S., Fossel, A. H., and Katz, J. N. (2002), "Metacarpophalangeal arthroplasty in rheumatoid arthritis: what determines satisfaction with surgery?" **Journal of Rheumatology**, 29 (12), 2488-2491

## References

- Mannerfelt, L. and Andersson, K. (1975), "Silastic arthroplasty of the metacarpophalangeal joints in rheumatoid arthritis," **Journal of Bone and Joint Surgery [Am]**, 57 (4), 484-489
- Massy-Westropp, N. and Krishnan, J. (2003), "Postoperative therapy after metacarpophalangeal arthroplasty," **Journal of Hand Therapy**, 16 (4), 311-314
- Massy-Westropp, N., Massy-Westropp, M., Rankin, W., and Krishnan, J. (2003), "Metacarpophalangeal arthroplasty from the patient's perspective," **Journal of Hand Therapy**, 16 (4), 315-319
- Massy-Westropp, N., Rankin, W., Ahern, M., Krishnan, J., and Hearn, T. C. (2004), "Measuring grip strength in normal adults: reference ranges and a comparison of electronic and hydraulic instruments," **Journal of Hand Surgery [Am]**, 29 (3), 514-519
- Mathiowetz, V., Kashman, N., Volland, G., Weber, K., Dowe, M., and Rogers, S. (1985), "Grip and pinch strength: normative data for adults," **Archives of Physical Medicine and Rehabilitation**, 66 (2), 69-74
- Matthewson, M. J. (1981), "Axi-symmetric contact on thin compliant coatings," **Journal of the Mechanics and Physics of Solids**, 29 (2), 89
- Mayer, B. and Hagen, F. W. (2005), "[Results after arthroplasty of the metacarpophalangeal joints with uncemented, unconstrained HM prosthesis in rheumatoid patients]," **Handchirurgie Mikrochirurgie Plastische Chirurgie**, 37 (1), 18-25
- McArthur, P. A., Cutts, A., Milner, R. H., and Johnson, G. R. (1998), "A study of the dimensions and taper angles of the medullary canals of the proximal and middle phalanges," **Journal of Hand Surgery [Br]**, 23 (1), 24-27
- McArthur, P. A. and Milner, R. H. (1998), "A prospective randomized comparison of Sutter and Swanson silastic spacers," **Journal of Hand Surgery [Br]**, 23 (5), 574-577
- MDD, Directive 98/79/EC of the European Parliament and of the Council of 27 October 1998 on in vitro diagnostic medical devices (1998), **Official Journal of European Communities**, L331, 1-37
- Minami, M., Yamazaki, J., Kato, S., and Ishii, S. (1988), "Alumina ceramic prosthesis arthroplasty of the metacarpophalangeal joint in the rheumatoid hand. A 2-4-year follow-up study," **Journal of Arthroplasty**, 3 (2), 157-166
- Minamikawa, Y., Peimer, C. A., Ogawa, R., Fujimoto, K., Sherwin, F. S., and Howard, C. (1994a), "In vivo experimental analysis of silicone implants used with titanium grommets," **Journal of Hand Surgery [Am]**, 19 (4), 567-574
- Minamikawa, Y., Peimer, C. A., Ogawa, R., Howard, C., and Sherwin, F. S. (1994b), "In vivo experimental analysis of silicone implants on bone and soft tissue," **Journal of Hand Surgery [Am]**, 19 (4), 575-583

## References

- Moller, K., Geijer, M., Sollerman, C., and Lundborg, G. (2004), "Radiographic evaluation of osseointegration and loosening of titanium implants in the MCP and PIP joints," **Journal of Hand Surgery [Am]**, 29 (1), 32-38
- Moller, K., Sollerman, C., Geijer, M., and Branemark, P. I. (1999a), "Osseointegrated silicone implants. 18 patients with 57 MCP joints followed for 2 years," **Acta Orthopaedica Scandinavica**, 70 (2), 109-115
- Moller, K., Sollerman, C., Geijer, M., and Branemark, P. I. (1999b), "Early results with osseointegrated proximal interphalangeal joint prostheses," **Journal of Hand Surgery [Am]**, 24 (2), 267-274
- Moller, K., Sollerman, C., Geijer, M., Kopylov, P., and Tagil, M. (2005), "Avanta versus Swanson silicone implants in the MCP joint--a prospective, randomized comparison of 30 patients followed for 2 years," **Journal of Hand Surgery [Br]**, 30 (1), 8-13
- Morgan, D. B., Spiers, F. W., Pulvertaft, C. N., and Fourman, P. (1967), "The amount of bone in the metacarpal and the phalanx according to age and sex," **Clinical Radiology**, 18 (1), 101-108
- Morrison, C., Macnair, R., MacDonald, C., Wykman, A., Goldie, I., and Grant, M. H. (1995), "In vitro biocompatibility testing of polymers for orthopaedic implants using cultured fibroblasts and osteoblasts," **Biomaterials**, 16 (13), 987-992
- Murray, P. M. (2003), "New-generation implant arthroplasties of the finger joints," **Journal of the American Academy of Orthopaedic Surgeons**, 11 (5), 295-301
- Murray, P. M. (2007), "Surface replacement arthroplasty of the proximal interphalangeal joint," **Journal of Hand Surgery [Am]**, 32 (6), 899-904
- Naidu, S. H. (1997), "Silicone Elastomers and Silicone synovitis: Materials and Basic science," **Seminars in Arthroplasty**, 8 (2), 191-197
- Naidu, S. H., Graham, J., and Laird, C. (1997), "Pre- and postimplantation dynamic mechanical properties of silastic HP-100 finger joints," **Journal of Hand Surgery [Am]**, 22 (2), 299-301
- Naidu, Sanjiv H. (2007), "Oxidation of Silicone Elastomer Finger Joints," **Journal of Hand Surgery [Am]**, 32 (2), 190
- Nalebuff, E. A. (1984), "The rheumatoid hand. Reflections on metacarpophalangeal arthroplasty," **Clinical Orthopaedics and Related Research** (182), 150-159
- Napier, J. R. (1956), "The prehensile movements of the human hand," **Journal of Bone and Joint Surgery [Br]**, 38 (4), 902-913
- Netscher, D., Eladoumikdachi, F., and Gao, Y. H. (2000), "Resurfacing arthroplasty for metacarpophalangeal joint osteoarthritis: a good option using either perichondrium or extensor retinaculum," **Plastic and Reconstructive Surgery**, 106 (6), 1430-1433

## References

- Neumann, D. A. (1999), "Joint deformity and dysfunction: a basic review of underlying mechanisms," **Arthritis Care and Research**, 12 (2), 139-151
- Nicolle, F. V. and Calnan, J. S. (1972), "A new design of finger joint prosthesis for the rheumatoid hand," **Hand**, 4 (2), 135-146
- Nicolle, F. V. and Gilbert, S. (1979), "Assessment of past results and current practice in the treatment of rheumatoid metacarpophalangeal joints. Five year review," **Hand**, 11 (2), 151-156
- Niebauer, J. J. and Landry, R. M. (1971), "Dacron--silicone prosthesis for the metacarpophalangeal and interphalangeal joints," **Hand**, 3 (1), 55-61
- Niebauer, J. J., Shaw, J. L., and Doren, W. W. (1969), "Silicone-dacron hinge prosthesis. Design, evaluation, and application," **Annals of Rheumatic Diseases**, 28 (5), Suppl:56-58
- Nikas, George K. and Sayles, Richard S. (2004), "Nonlinear elasticity of rectangular elastomeric seals and its effect on elastohydrodynamic numerical analysis," **Tribology International**, 37 (8), 651-660
- Nordenskiold, U. M. and Grimby, G. (1993), "Grip force in patients with rheumatoid arthritis and fibromyalgia and in healthy subjects. A study with the Grippit instrument," **Scandinavian Journal of Rheumatology**, 22 (1), 14-19
- Nunez, V. A. and Citron, N. D. (2005), "Short-term results of the Ascension pyrolytic carbon metacarpophalangeal joint replacement arthroplasty for osteoarthritis," **Chirurgie de la Main**, 24 (3-4), 161-164
- Opitz, J. L. and Linscheid, R. L. (1978), "Hand function after metacarpophalangeal joint replacement in rheumatoid arthritis," **Archives of Physical Medicine and Rehabilitation**, 59 (4), 160-165
- Pagowski, S. and Piekarski, K. (1977), "Biomechanics of metacarpophalangeal joint," **Journal of Biomechanics**, 10 (3), 205-209
- Park, J. B. (1992), "Orthopedic prosthesis fixation," **Annals of Biomedical Engineering**, 20 (6), 583-594
- Parkkila, T. J., Belt, E. A., Hakala, M., Kautiainen, H., and Leppilahti, J. (2005), "Comparison of Swanson and Sutter Metacarpophalangeal Arthroplasties in Patients With Rheumatoid Arthritis: A Prospective and Randomized Trial," **Journal of Hand Surgery [Am]**, 30 (6), 1276-1281
- Pavier, Julian (2005), "A catastrophic failure of a first MTP joint ceramic implant," **The Foot**, 15 (1), 47-49
- Peimer, C. A. (1989), "Arthroplasty of the hand and wrist: complications and failures," **Instructional Course Lectures**, 38, 15-30

## References

- Peimer, C. A., Medige, J., Eckert, B. S., Wright, J. R., and Howard, C. S. (1986), "Reactive synovitis after silicone arthroplasty," **Journal of Hand Surgery [Am]**, 11 (5), 624-638
- Penrose, J. M., Williams, N. W., Hose, D. R., and Trowbridge, E. A. (1996), "An examination of one-piece metacarpophalangeal joint implants using finite element analysis," **Journal of Medical Engineering and Technology**, 20 (4-5), 145-150
- Penrose, J. M., Williams, N. W., Hose, D. R., and Trowbridge, E. A. (1997), "In-situ simulation of one-piece metacarpophalangeal joint implants using finite element analysis," **Medical Engineering and Physics**, 19 (4), 303-307
- Pereira, J. A. and Belcher, H. J. (2001), "A comparison of metacarpophalangeal joint silastic arthroplasty with or without crossed intrinsic transfer," **Journal of Hand Surgery [Br]**, 26 (3), 229-234
- Petrolati, M., Abbiati, G., Delaria, G., Soffiatti, R., Robotti, P., and Guerriero, C. (1999), "A new prosthesis for the metacarpophalangeal joint. Study of materials and biomechanics," **Journal of Hand Surgery [Br]**, 24 (1), 59-63
- Pettersson, K., Wagnsjo, P., and Hulin, E. (2006a), "NeuFlex compared with Sutter prostheses: A blind, prospective, randomised comparison of Silastic metacarpophalangeal joint prostheses," **Scandinavian Journal of Plastic and Reconstructive Surgery and Hand Surgery**, 40 (5), 284-290
- Pettersson, K., Wagnsjo, P., and Hulin, E. (2006b), "Replacement of proximal interphalangeal joints with new ceramic arthroplasty: A prospective series of 20 proximal interphalangeal joint replacements," **Scandinavian Journal of Plastic and Reconstructive Surgery and Hand Surgery**, 40 (5), 291-296
- Podnos, E., Becker, E., Klawitter, J., and Strzepa, P. (2006), "FEA analysis of silicone MCP implant," **Journal of Biomechanics**, 39 (7), 1217-1226
- Pylios, T. (2002), "Theoretical prediction of lubrication regimes in wrist implants," University of Aberdeen.
- Pylios, T. and Shepherd, D. E. (2004), "Prediction of lubrication regimes in wrist implants with spherical bearing surfaces," **Journal of Biomechanics**, 37 (3), 405-411
- Pylios, T. and Shepherd, D. E. (2007), "Biomechanics of the normal and diseased metacarpophalangeal joint: implications on the design of joint replacement implants," **Journal of Mechanics in Medicine and Biology**, 7 (2), 163-174
- Pylios, T. and Shepherd, D. E. (2008a), "Soft layered concept in the design of metacarpophalangeal joint replacement implants," **Bio-Medical Materials and Engineering**, 18 (2), 73-82

## References

- Pylios, T. and Shepherd, D. E. (2008b), "Wear of medical grade silicone rubber against titanium and ultrahigh molecular weight polyethylene," **Journal of Biomedical Materials Research - Part B Applied Biomaterials**, 84 (2), 520-523
- Quigley, F. P., Buggy, M., and Birkinshaw, C. (2002), "Selection of elastomeric materials for compliant-layered total hip arthroplasty," **Proceedings of the Institution of Mechanical Engineers Part H-Journal of Engineering in Medicine**, 216 (1), 77-83
- Radmer, S., Andresen, R., and Sparmann, M. (2003), "Poor experience with a hinged endoprosthesis (WEKO) for the metacarpophalangeal joints: all 28 prostheses removed within 2 years in 8 patients having rheumatoid arthritis," **Acta Orthopaedica Scandinavica**, 74 (5), 586-590
- Rand, D. T. and Nicol, A. C. (1993), "An instrumented glove for monitoring MCP joint motion," **Proceedings of the Institution of Mechanical Engineers Part H-Journal of Engineering in Medicine**, 207 (4), 207-210
- Reis, N. D. and Calnan, J. S. (1969), "Integral hinge joint," **Annals of Rheumatic Diseases**, 28 (5), Suppl:59-62
- Rettig, L. A., Luca, L., and Murphy, M. S. (2005), "Silicone implant arthroplasty in patients with idiopathic osteoarthritis of the metacarpophalangeal joint," **Journal of Hand Surgery [Am]**, 30 (4), 667-672
- Rieker, C. B., Joyce, T., Unsworth, A., Hagena, F. W., and Meuli, C. (2003), "[Tribologic investigation of a metacarpophalangeal prosthesis]," **Orthopade**, 32 (9), 784-788
- Rittmeister, M., Porsch, M., Starker, M., and Kerschbaumer, F. (1999), "Metacarpophalangeal joint arthroplasty in rheumatoid arthritis: results of Swanson implants and digital joint operative arthroplasty," **Archives of Orthopaedic and Trauma Surgery**, 119 (3-4), 190-194
- Rosen, A. and Weiland, A. J. (1998), "Rheumatoid arthritis of the wrist and hand," **Rheumatic Diseases Clinics of North America**, 24 (1), 101-128
- Royo, J. (1992), "Fatigue testing of rubber materials and articles," **Polymer Testing**, 11 (5), 325-344
- Savio, J. A., 3rd, Overcamp, L. M., and Black, J. (1994), "Size and shape of biomaterial wear debris," **Clinical Materials**, 15 (2), 101-147
- Savory, K. M., Hutchinson, D. T., and Bloebaum, R. (1994), "Materials testing protocol for small joint prostheses," **Journal of Biomedical Materials Research**, 28 (10), 1209-1219
- Sawae, Y., Murakami, T., Higaki, H., and Moriyama, S. (1996), "Lubrication property of total knee prostheses with PV A hydrogel layer as artificial cartilage," **JSME International Journal, Series C: Dynamics, Control, Robotics, Design and Manufacturing**, 39 (2), 356-364

## References

- Schettrumpf, J. (1975), "A new metacarpophalangeal joint prosthesis," **Hand**, 7 (1), 75-77
- Schmidt, K., Willburger, R. E., Miehke, R. K., and Witt, K. (1999b), "Ten-year follow-up of silicone arthroplasty of the metacarpophalangeal joints in rheumatoid hands," **Scandinavian Journal of Plastic and Reconstructive Surgery and Hand Surgery**, 33 (4), 433-438
- Schmidt, K., Willburger, R., Ossowski, A., and Miehke, R. K. (1999a), "The effect of the additional use of grommets in silicone implant arthroplasty of the metacarpophalangeal joints," **Journal of Hand Surgery [Br]**, 24 (5), 561-564
- Scholes, S. C., Smith, S. L., Ash, H. E., and Unsworth, A. (2002), "The lubrication and friction of conventional UHMWPE, novel compliant layer, and hard bearing surfaces for use in total hip prostheses," **Friction, Lubrication, and Wear of Artificial Joints Ed. I.M. Hutchings, Institute of Mechanical Engineers Press**, 59-74
- Scholes, S. C., Unsworth, A., Blamey, J. M., Burgess, I. C., Jones, E., and Smith, N. (2005), "Design aspects of compliant, soft layer bearings for an experimental hip prosthesis," **Proceedings of the Institution of Mechanical Engineers Part H-Journal of Engineering in Medicine**, 219 (2), 79-87
- Schulter-Ellis, F. P. and Lazar, G. T. (1984), "Internal morphology of human phalanges," **Journal of Hand Surgery [Am]**, 9 (4), 490-495
- Schultz, R. J., Johnston, A. D., and Krishnamurthy, S. (1987b), "Thermal effects of polymerization of methyl-methacrylate on small tubular bones," **International Orthopaedics**, 11 (3), 277-282
- Schwartz, Christian J. and Bahadur, Shyam (2006), "Development and testing of a novel joint wear simulator and investigation of the viability of an elastomeric polyurethane for total-joint arthroplasty devices," **Wear**, In Press, Corrected Proof
- Schwarz, M. L. R., Bouman, H. W., Bayer, M., and Feinle, P. (2001), "Design and construction of a simulator for testing finger joint replacements," **Biomedizinische Technik**, 46 (6), 176-180
- Shapiro, P. S. (1999), "Operative and non-operative management of arthritis of the hand and wrist," **Current Opinion in Orthopedics**, 10, 277-281
- Shepherd, D. E. (2002), "Risk analysis for a radio-carpal joint replacement," **Proceedings of the Institution of Mechanical Engineers Part H-Journal of Engineering in Medicine**, 216 (1), 23-29
- Shepherd, D. E. and Johnstone, A. (2005), "A new design concept for wrist arthroplasty," **Proceedings of the Institution of Mechanical Engineers Part H-Journal of Engineering in Medicine**, 219 (1), 43-52

## References

Sibly, T. F. and Unsworth, A. (1991a), "Fixation of a surface replacement endoprosthesis of the metacarpophalangeal joint," **Proceedings of the Institution of Mechanical Engineers Part H-Journal of Engineering in Medicine**, 205 (4), 227-232

Sibly, T. F. and Unsworth, A. (1991b), "Wear of cross-linked polyethylene against itself: a material suitable for surface replacement of the finger joint," **Journal of Biomedical Engineering**, 13 (3), 217-220

Skie, M., Gove, N., and Ciocanel, D. (2007), "Intraoperative fracture of a pyrocarbon PIP total joint - A case report," **Hand**, 2 (3), 90-93

Smith, E. M., Juvinall, R. C., Bender, L. F., and Pearson, J. R. (1964), "Role Of The Finger Flexors In Rheumatoid Deformities Of The Metacarpophalangeal Joints," **Arthritis and Rheumatism**, 19, 467-480

Stephens, J.H. (1998), *Kempe's Engineers Year Book*. Tonbridge UK: Miller Freeman.

Stewart, T., Jin, Z. M., and Fisher, J. (1997), "Friction of composite cushion bearings for total knee joint replacements under adverse lubrication conditions," **Proceedings of the Institution of Mechanical Engineers Part H-Journal of Engineering in Medicine**, 211 (6), 451-465

Stewart, T., Jin, Z. M., and Fisher, J. (1998), "Analysis of contact mechanics for composite cushion knee joint replacements," **Proceedings of the Institution of Mechanical Engineers Part H-Journal of Engineering in Medicine**, 212 (1), 1-10

Stirrat, C. R. (1996), "Metacarpophalangeal joints in rheumatoid arthritis of the hand," **Hand Clinics**, 12 (3), 515-529

Stokoe, S. M., Unsworth, A., Viva, C., and Haslock, I. (1990), "A finger function simulator and the laboratory testing of joint replacements," **Proceedings of the Institution of Mechanical Engineers Part H-Journal of Engineering in Medicine**, 204 (4), 233-240

Storace, A. and Wolf, B. (1979), "Functional analysis of the role of the finger tendons," **Journal of Biomechanics**, 12 (8), 575-578

Swanson (2008), "Prosthesis Brochure," Accessed 27 November), <http://www.wmt.com/Downloads/Techniques/SOSTU003%020R005.006%020Swanson%020Flex%020Finger%020ST.pdf>

Swanson, A. B. (1969), "Finger joint replacement by silicone rubber implants and the concept of implant fixation by encapsulation," **Annals of Rheumatic Diseases**, 28 (5), Suppl:47-55

Swanson, A. B. (1972), "Flexible implant arthroplasty for arthritic finger joints: rationale, technique, and results of treatment," **Journal of Bone and Joint Surgery [Am]**, 54 (3), 435-455

## References

- Swanson, A. B., de Groot Swanson, G., and Ishikawa, H. (1997), "Use of grommets for flexible implant resection arthroplasty of the metacarpophalangeal joint," **Clinical Orthopaedics and Related Research** (342), 22-33
- Swanson, A. B., Poitevin, L. A., de Groot Swanson, G., and Kearney, J. (1986), "Bone remodeling phenomena in flexible implant arthroplasty in the metacarpophalangeal joints. Long-term study," **Clinical Orthopaedics and Related Research** (205), 254-267
- Swanson, J. W. and Lebeau, J. E. (1974), "The effect of implantation on the physical properties of silicone rubber," **Journal of Biomedical Materials Research**, 8 (6), 357-367
- Swieszkowski, W., Ku, D. N., Bersee, H. E., and Kurzydowski, K. J. (2006), "An elastic material for cartilage replacement in an arthritic shoulder joint," **Biomaterials**, 27 (8), 1534-1541
- Synnott, K., Mullett, H., Faull, H., and Kelly, E. P. (2000), "Outcome measures following metacarpophalangeal joint replacement," **Journal of Hand Surgery [Br]**, 25 (6), 601-603
- Tamai, K., Ryu, J., An, K. N., Linscheid, R. L., Cooney, W. P., and Chao, E. Y. (1988), "Three-dimensional geometric analysis of the metacarpophalangeal joint," **Journal of Hand Surgery [Am]**, 13 (4), 521-529
- Tan, A. L., Tanner, S. F., Conaghan, P. G., Radjenovic, A., O'Connor, P., Brown, A. K., Emery, P., and McGonagle, D. (2003), "Role of metacarpophalangeal joint anatomic factors in the distribution of synovitis and bone erosion in early rheumatoid arthritis," **Arthritis and Rheumatism**, 48 (5), 1214-1222
- Tan, V., Bozentka, D. J., and Osterman, A. L. (2000), "Metacarpophalangeal joint in rheumatoid arthritis," **Seminars in Arthroplasty**, 11 (2), 107-114
- Trail, I. A. (2005), "Metacarpophalangeal Joint Silicone Implant Arthroplasty," **Journal of the American Society for Surgery of the Hand**, 5 (4), 201-208
- Trail, I. A. (2006), "Silastic metacarpophalangeal joint arthroplasty," **International Congress Series**, 1295, 129-143
- Trail, I. A., Martin, J. A., Nuttall, D., and Stanley, J. K. (2004), "Seventeen-year survivorship analysis of silastic metacarpophalangeal joint replacement," **Journal of Bone and Joint Surgery [Br]**, 86 (7), 1002-1006
- Unsworth, A. and Alexander, W. J. (1979), "Dimensions of the metacarpophalangeal joint with particular reference to joint prostheses," **Engineering in Medicine**, 8 (2), 75-80
- Unsworth, A., Dowson, D., and Wright, V. (1971), "'Cracking joints'. A bioengineering study of cavitation in the metacarpophalangeal joint," **Annals of Rheumatic Diseases**, 30 (4), 348-358

## References

- Unsworth, A., Pearcy, M., White, E. F., and White, G. (1987), "Soft layer lubrication of artificial hip joints," **Proc Inst Mech Eng - International Conference on tribology-friction, lubrication and wear, fifty years on, London**, 715-724
- Unsworth, A., Roberts, B., and Thompson, J.C (1981), "The application of soft-layered to hip prostheses," **Journal of Bone and Joint Surgery [Br]**, 63 (2), 297
- Unsworth, A. and Strozzi, A. (1994), "Axisymmetric finite element analysis of hip replacements possessing an elastomeric layer: the effects of layer thickness," **Proceedings of the Institution of Mechanical Engineers Part H-Journal of Engineering in Medicine**, 208 (1), 139-149
- Varma, S. K. and Milward, T. M. (1991), "The Nicolle finger joint prosthesis: a reappraisal," **Journal of Hand Surgery [Br]**, 16 (2), 187-190
- Vasenius, J., Patiala, H., Santavirta, N., Santavirta, S., and Konittinen, Y. (2000), "Swanson arthroplasty of the rheumatoid metacarpophalangeal joints," **Current Orthopaedics**, 14, 284-289
- Vermeiren, J. A., Dapper, M. M., Schoonhoven, L. A., and Merx, P. W. (1994), "Isoelastic arthroplasty of the metacarpophalangeal joints in rheumatoid arthritis: a preliminary report," **Journal of Hand Surgery [Am]**, 19 (2), 319-324
- Viceconti, M., Affatato, S., Baleani, M., Bordini, B., Cristofolini, L., and Taddei, F. (2009), "Pre-clinical validation of joint prostheses: A systematic approach," **Journal of the Mechanical Behavior of Biomedical Materials**, 2 (1), 120-127
- Walker, P. S. and Erkman, M. J. (1975), "Laboratory evaluation of a metal-plastic type of metacarpophalangeal joint prosthesis," **Clinical Orthopaedics and Related Research (112)**, 349-356
- Weightman, B. and Amis, A. A. (1982), "Finger joint force predictions related to design of joint replacements," **Journal of Biomedical Engineering**, 4 (3), 197-205
- Weightman, B., Evans, D. M., and Light, D. (1983), "The laboratory development of a new metacarpophalangeal prosthesis," **Hand**, 15 (1), 57-69
- Weiss, A. P. (2000), "Neuflex prostheses," in *Hand Arthroplasties*, Simmen, B. R., Allieu, Y., Lluch, A., Stanley, J., Eds. London: Martin Dunitz Ltd.
- Weiss, A. P., Moore, D. C., Infantolino, C., Crisco, J. J., Akelman, E., and McGovern, R. D. (2004), "Metacarpophalangeal joint mechanics after 3 different silicone arthroplasties," **Journal of Hand Surgery [Am]**, 29 (5), 796-803
- Werner, D., Kozin, S. H., Brozovich, M., Porter, S. T., Junkin, D., and Seigler, S. (2003), "The biomechanical properties of the finger metacarpophalangeal joints to varus and valgus stress," **Journal of Hand Surgery [Am]**, 28 (6), 1044-1051

## References

- Wessels, K. D. (2005), "[The WEKO finger joint prosthesis]," **Handchirurgie Mikrochirurgie Plastische Chirurgie**, 37 (1), 7-12
- Whalen, R. L., Bowen, M. A., Sarrasin, M. J., Fukumura, F., and Harasaki, H. (1993), "A new finger joint prosthesis," **ASAIO Journal**, 39 (3), M 480- M 485
- Williams, N. W., Penrose, J. M., and Hose, D. R. (2000), "Computer model analysis of the Swanson and Sutter metacarpophalangeal joint implants," **Journal of Hand Surgery [Br]**, 25 (2), 212-220
- Wilson, R. L. and Carlblom, E. R. (1989), "The rheumatoid metacarpophalangeal joint," **Hand Clinics**, 5 (2), 223-237
- Wilson, Y. G., Sykes, P. J., and Niranjani, N. S. (1993), "Long-term follow-up of Swanson's silastic arthroplasty of the metacarpophalangeal joints in rheumatoid arthritis," **Journal of Hand Surgery [Br]**, 18 (1), 81-91
- Wise, K. S. (1975), "The anatomy of the metacarpo-phalangeal joints, with observations of the aetiology of ulnar drift," **Journal of Bone and Joint Surgery [Br]**, 57 (4), 485-490
- Yao, J. Q., Parry, T. V., Unsworth, A., and Cunningham, J. L. (1994), "Contact mechanics of soft layer artificial hip joints. Part 2: application to joint design," **Proceedings of the Institution of Mechanical Engineers Part H-Journal of Engineering in Medicine**, 208, 206-215
- Youm, Y., Gillespie, T. E., Flatt, A. E., and Sprague, B. L. (1978), "Kinematic investigation of normal MCP joint," **Journal of Biomechanics**, 11 (3), 109-118
- Zangger, P., Keystone, E. C., and Bogoch, E. R. (2005), "Asymmetry of small joint involvement in rheumatoid arthritis: prevalence and tendency towards symmetry over time," **Joint Bone Spine**, 72 (3), 241-247
- Zheng-Qiu, G., Jiu-Mei, X., and Xiang-Hong, Z. (1998), "The development of artificial articular cartilage - PVA-hydrogel," **Bio-Medical Materials and Engineering**, 8 (2), 75-81

## **Appendices**

### **Appendix A**

Engineering drawings of the pin-on-disk apparatus

That consists of the:

1. Disk plate
2. Pin holder
3. Security disk plate ring
4. Test pin holder

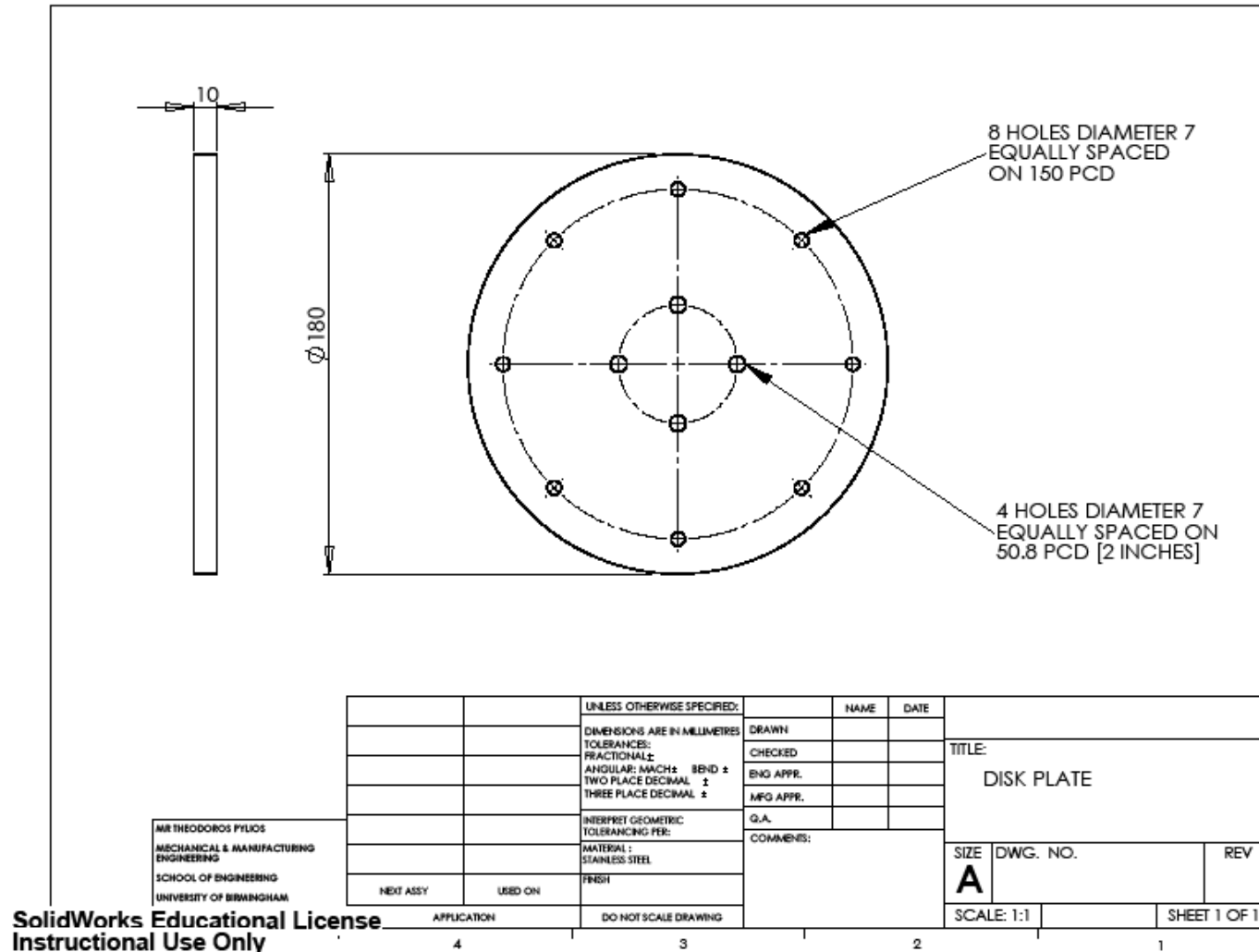


Fig ApA-1. Disk plate of the pin-on-disk apparatus

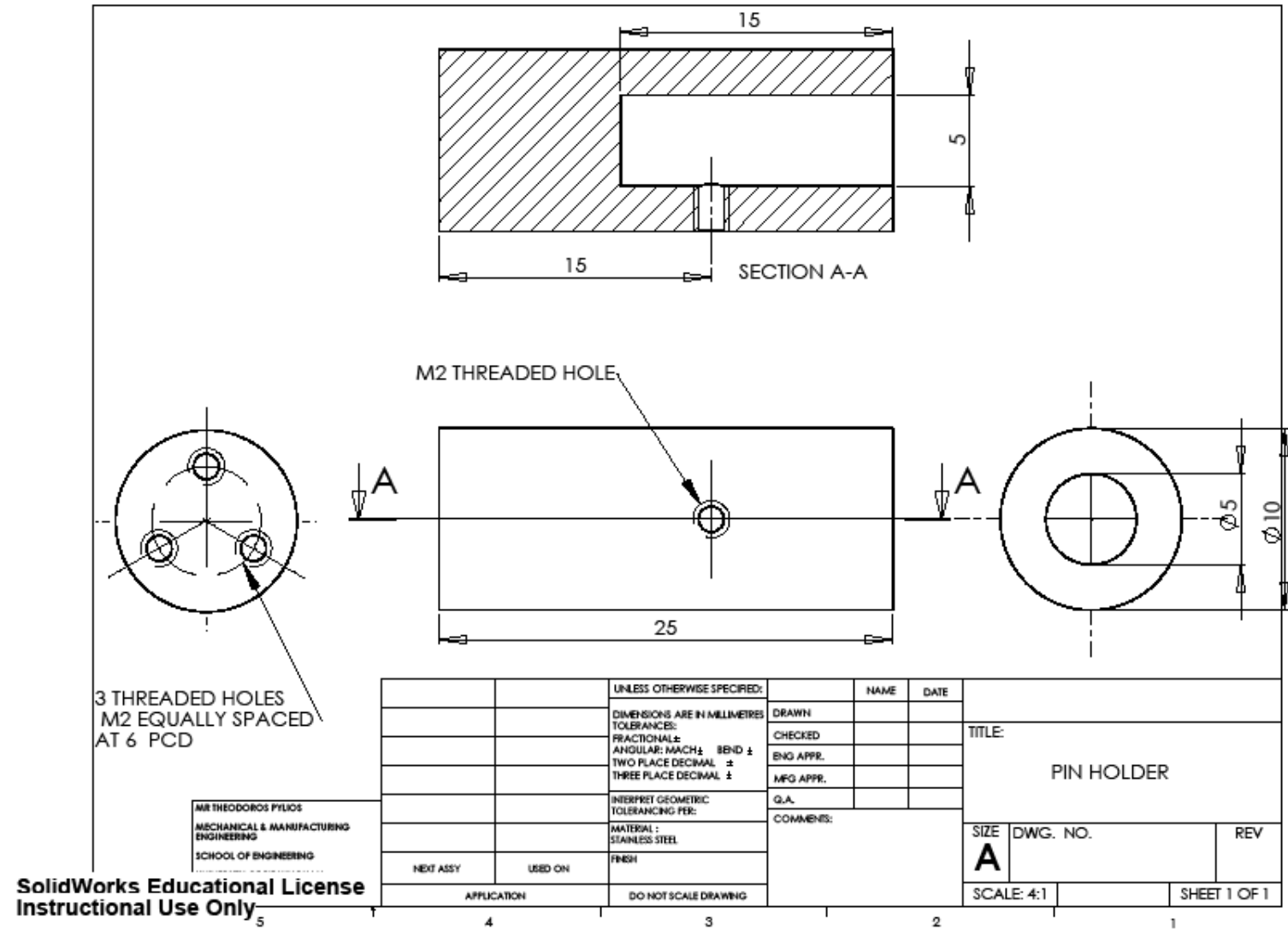


Fig ApA-2. Pin holder of the pin-on-disk apparatus

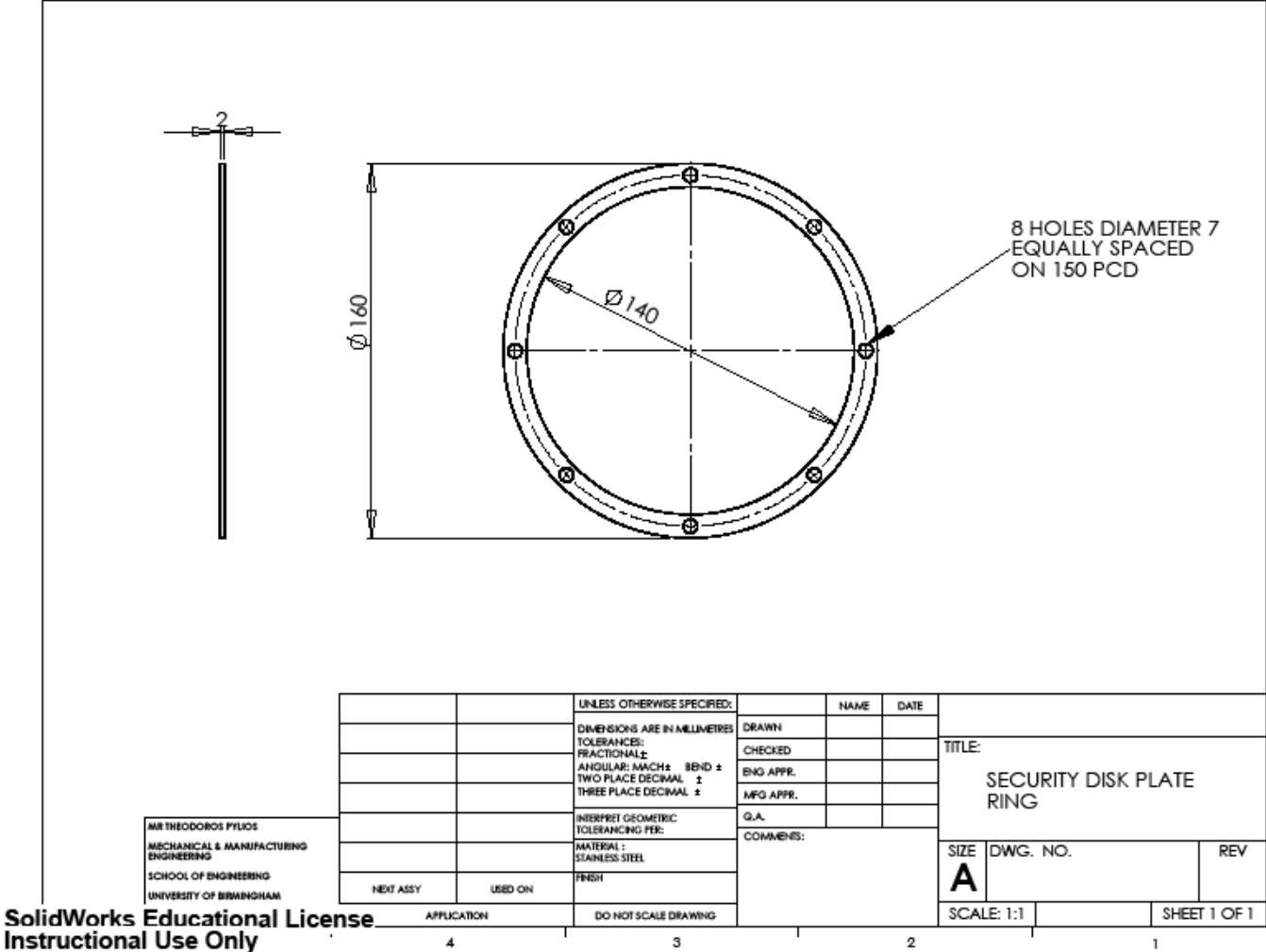


Fig ApA-3. Security disk plate ring of the pin-on-disk apparatus

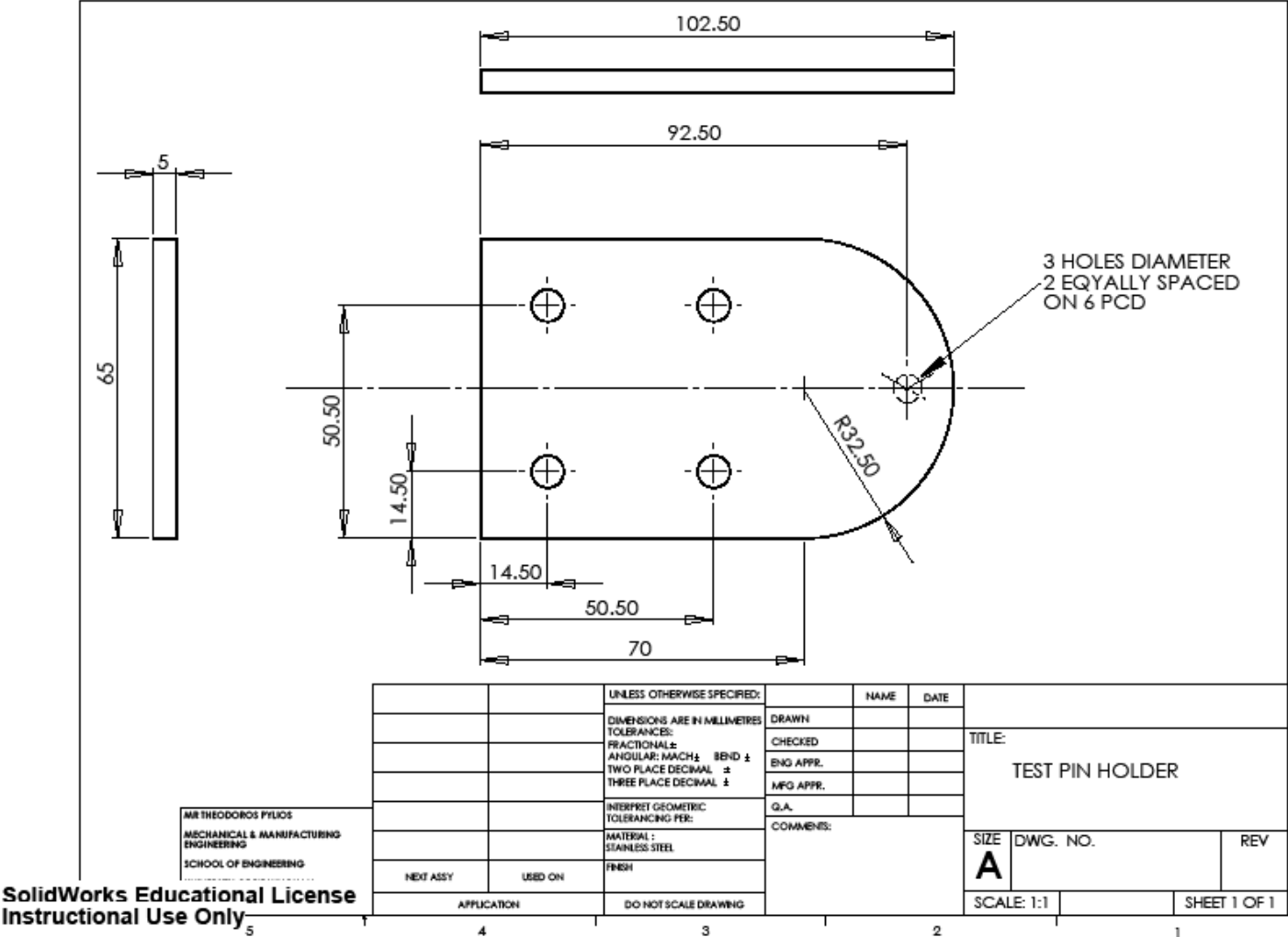


Fig ApA-4. Test pin holder of the pin-on-disk apparatus

## Appendix B

**Table ApB-1** .Materials properties of Medical grade silicone rubber MED-71 and HP-100 Swanson implant silicone rubber.

<b>Manufacturer</b>	<b>Material</b>	<b>Durometer (Shore A)</b>	<b>Tensile Strength (psi)</b>	<b>% Elongation at Failure</b>	<b>Tear Die B ASTM D624</b>	<b>Reference</b>
Dow Corning	HP-100 (Swanson flexible implant)	55	1400	600	300	(Hutchinson <i>et al.</i> 1997; Savory <i>et al.</i> 1994)
CS Hyde Company	MED-71	50.5	1200	600	150	Manufacturer Material Sheet

## Appendix C

Lab – sheet forms used for the materials in the wear tests

### Wear Measurements - Sample ID

Sample name	
Material	

Start time	No of cycles	Duration	Sliding distance (m)	Number measurement	Mass (mg)	Notes
	0		0	1		Initial mass
				2		
				3		
				1		
				2		
				3		Final mass

## Appendix D

Matlab script for calculation of coefficients of Mooney-Rivlin hyperelastic model.

```
% Uniaxial strain test
% Use Least Squares Fit Analysis to match C01 and C10 to the data above.
engStrain = [0, .075, .103, .15, .174, .2004, .25, .305, .351, .37];
engStressExp = [0, 4.9e5, 8.67e5, 1.36e6, 1.55e6, 1.71e6, 1.95e6, 2.10e6,
2.17e6, 2.21e6];
lam1 = 1 + engStrain;
lam1=lam1';
CoeffMatrix = zeros(length(engStrain),2);

CoeffMatrix(:,1) = 2./lam1.*(lam1.^2-1./lam1);
CoeffMatrix(:,2) = 2./(lam1.^2).*(lam1.^2-1./lam1);
C10C01=CoeffMatrix\engStressExp';
% Calculate stress from this data
engStressMRML = CoeffMatrix*C10C01;
%Plot
plot(engStrain, engStressExp);
hold on
plot(engStrain, engStressMRML);
```

## Appendix E

### Stress analysis of UHMWPE section of the implant

The stress analysis of the metacarpal stem is calculated according to the worst case scenario by the following equations (Fig ApE-1) (Stephens 1998).

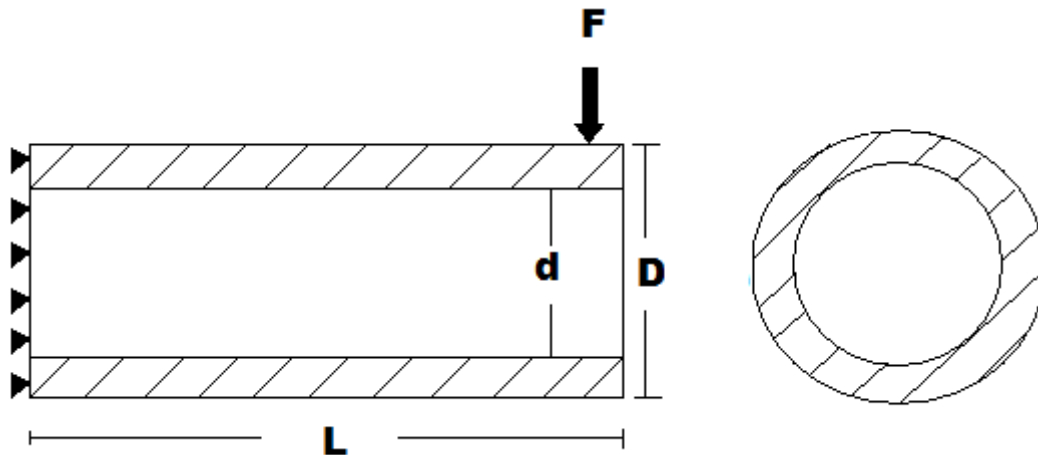


Fig ApE-1. Model of stem for stress calculation

$$\text{stress} = \frac{My}{I} \quad (\text{ApE-1})$$

Where  $M$  is moment,  $y$  is perpendicular distance from neutral axis and  $I$  is the moment of inertia.

$M$  is calculated by equation (ApE-2)

$$M = FL \quad (\text{ApE-2})$$

Where  $F$  is the applied Load and  $L$  is the length of the beam.

$y$  is calculated by equation ApE-3

$$y = \frac{D}{2} \quad (\text{ApE-3})$$

Where  $D$  is the outer diameter of the beam.

The  $I$  moment of inertia is calculated by equation ApE-4.

## Appendices

$$I = \frac{\pi D^3 t}{8} \quad (\text{ApE-4})$$

Where  $\pi$  is 3.14,  $D$  is the outer diameter of the beam and  $t$  is the thickness of the beam and is given by equation ApE-5.

$$t = \frac{D - d}{2} \quad (\text{ApE-5})$$

Applying equations ApE-2 to ApE-5 to equation ApE-1 equation ApE-6 is given.

$$\text{stress} = \frac{8FL}{\pi D^2 (D - d)} \quad (\text{ApE-6})$$

Applying equation ApE-6 for the dimensions of the metacarpal and proximal phalange stems the following results are calculated.

### **Metacarpal stem**

F=100 N, L= 2.5 mm, D=7 mm, d=5.4 mm

According to the previous parameters the calculated stress of metacarpal stem using equation ApE-6 is:

**Stress Metacarpal = 8.12 MPa**

### **Proximal stem**

F=100 N, L= 2.5 mm, D=5.5 mm, d=3.4 mm

According to the previous parameters the calculated stress of proximal stem using equation ApE-6 is:

**Stress Proximal = 10.02 MPa**

Both of the calculated stresses are below the ultimate and yield tensile stress of the UHMWPE that are 27 and 19 MPa respectively (Costa *et al.* 2007).

## Appendix F

### Shear stress analysis of elastomer part

The model that has been used in Chapter 9 for the finite element analysis has been used for the shear stress analysis of the elastomer part. Instead of displacement loading this time force loading has been used to simulate the event of the loading due to the subluxing shear forces that the implant will experience in vivo. Loading up to 100 N has been applied to the model that is a normal load for subluxing force according to the analysis in Chapter 2. The preflexed model only has been used for this analysis as this is the model of selection in the detailed design process in Chapter 11. The results are shown in Fig ApF-1.

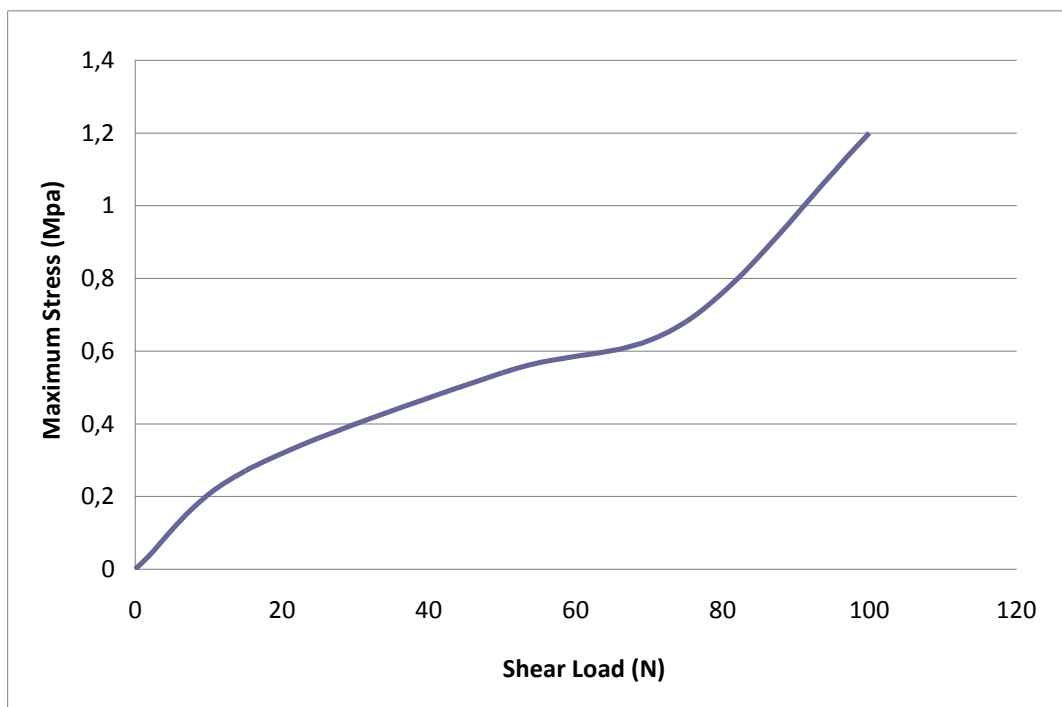


**Fig ApF-1.** Maximum stress against shear load for elastomer part.

Compared the results with the results from Chapter 9 where the elastomer part was subjected to bending it can be seen that the maximum stress in shear loading is almost 50% the maximum stress in bending for the preflexed model. The literature has shown that the

## Appendices

initiation of the scratches in the elastomer surface is the case of failure of the implants and the concept of this design is the protection of the elastomer part from direct contact with the finger bones. The shear loading of the elastomer due to the design is possible but most of the times the balls of the design will be compressed against the polyurethane middle part. The balls of the design and the middle part have contoured edges to avoid sharp edges, a site of possible impingement of the elastomer *in vivo*.

## Appendix G

### List of Publications for current work

#### Refereed Journals

- **T.Pylios, D.E.T. Shepherd, 2007.**“*Biomechanics of the normal and diseased metacarpophalangeal joint: implications on the design of joint replacement implants*”, ***Journal of Mechanics in Medicine and Biology***, Vol 7, Issue 2, pages 163-174
- **T.Pylios, D.E.T. Shepherd, 2008.**” *Wear of medical grade silicone rubber on titanium and UHMWPE*”, ***Journal of Biomedical Materials Research: Part B- Applied Biomaterials***, Vol 84B, Issue 2, pages 520-523
- **T.Pylios, D.E.T. Shepherd, 2008.**“*Soft layered concept in the design of metacarpophalangeal joint replacement implants*”, ***Bio-Medical Materials & Engineering***, Vol 18, Issue 2, Pages 73-82

#### Refereed Conference Papers

- **T.Pylios, D.E.T Shepherd, 2006,** *Cushion joint concept in metacarpophalangeal joint arthroplasty, Royal Academy of Engineering Futures Meeting on Musculoskeletal mechanics, Durham 13-15 September 2006, p 29.*
- **T.Pylios, D.E.T Shepherd, 2007,** *A new metacarpophalangeal metacarpophalangeal prosthesis, World Congress on Engineering, International Conference of Systems Biology and Bioengineering, London 2-4 July 2007,Imperial College,WCE 2007 Proceedings, Vol II, pages1443-1445 .*